Title
Retrograde signaling by endogenous cannabinoids at hippocampal synapses

Author
Wilson, Rachel I.

Publication Date
2001

Peer reviewed|Thesis/dissertation

Retrograde signaling by endogenous cannabinoids at hippocampal synapses

by

Rachel I. Wilson

DISSERTATION

Submitted in partial satisfaction of the requirements for the degree of

DOCTOR OF PHILOSOPHY

in

Neuroscience

in the

GRADUATE DIVISION

of the

UNIVERSITY OF CALIFORNIA SAN FRANCISCO

Date University Librarian

Degree Conferred: .....

for Dr. and Mr. Wilson

Acknowledgments

The work presented in this thesis would not have been possible without the generous help of many individuals. I would like to acknowledge Robert Zucker (UC Berkeley) for technical assistance in the calcium uncaging experiments, and Richard Scheller and Yu Chen (Stanford) for the gift of recombinant BoTxE light chain and SNAP-25. Particular thanks is due to George Kunos (NIAAA/NIH) for cheerfully giving us $CB1^{-/-}$ mice and littermates from the colony which he maintained and genotyped, and for sharing his ideas on endocannabinoids. Finally, thanks to Andreas Zimmer (now at the University of Bonn) for giving to the Kunos lab the $CB1^{-/-}$ mouse strain which he developed.

The outlines of the work described in Chapter 3 were developed with the help of my qualifying exam committee, namely David Copenhagen, Robert Edwards, Lily Jan, Peter Sargent, and Mark von Zastrow. Without their advice, the early stages of this project would have been much less informative. I am also indebted to David Bredt for helpful early conversations on calcium-dependent, membrane-permeant signaling molecules.

I am grateful to my thesis committee for frank criticism, useful suggestions, words of encouragement, comments on the manuscripts, and "life advice". David Copenhagen, Robert Edwards, and Michael Stryker, and Shaul Hestrin (Stanford) all contribute in different and complementary ways to my committee, and I am lucky to be their advisee.

My fellow "Nicolleans" are irreplaceable resources and friends whom I will sorely miss. I am particularly grateful to Kaspar Vogt for helping me set up my rig and

teaching me how to patch, Steven Gomperts for first suggesting that I work on DSI, Christian Lüscher for encouraging me to undertake the calcium uncaging experiments, Eric Schnell for first suggesting that cannabinoids might mediate DSI and assisting me in conducting the blind study with $CB1^{-/-}$ mice, Dietmar Schmitz for guiding my reading on hippocampal interneurons and encouraging me to do the paired recordings, Jack Mellor for scrutinizing my figures, Lu Chen for advice on juggling experiments and postdoc applications, and, last but not least, Matthew Frerking for advice and criticism in all phases of the project. I am also grateful to Carl Petersen, Min-Yi Xiao, Qiang Zhou, and Greg Hjelmstad for their contributions in informal conversations. Finally, I owe a special acknowledgement to (former Nicollean) Jeff Isaacson, who independently came to the realization that cannabinoids might mediate DSI, and whose suggestions played an important role in initiating the critical experiments of the study.

I owe the greatest debt to my advisor, Roger Nicoll. Luck has been on my side throughout these past four years, but to have been Roger's student was the luckiest stroke of all. His unflagging enthusiasm for this project, and his obvious pleasure in seeing any kind of raw data, carried me though many a dark period. I am grateful for his compassionate supervision, gentle criticism, and committed advocacy on my behalf. Largely by his own example, he tried to teach me a few lessons of science—how to choose an engaging question, how to find a kernel of interest in the results of the first forays, how to design informative and elegant experiments to follow up these early hints, and how to communicate the results in the clearest and fairest manner possible. I hope to continue to practice the lessons he has assigned me.

Advisor's Statement

Most of the material presented here has been or will be published elsewhere:

Chapter 2, Sections 1-8	Wilson, R.I. and **Nicoll, R.A.**: Endogenous cannabinoids mediate retrograde signalling at hippocampal synapses. Nature 410: 588-592 (2001).
Chapter 2, Sections 9 and 10:	in submission.
Chapters 3 and 4:	Wilson, R.I. and **Nicoll, R.A.**: Endogenous cannabinoids mediate retrograde signalling at hippocampal synapses. Nature 410: 588-592 (2001).
Chapter 5:	in submission.

Rachel conceived of the vast majority of the experiments contained in this thesis. All of the experiments were carried out exclusively by Rachel. In chapter 5 Rachel carried out a series of experiments on CB1 knockout mice. These mice were provided by Dr. George Kunos and the genotyping of these mice was carried out in his lab.

Roger A. Nicoll
Professor
Department of Cellular and Molecular Pharmacology
University of California, San Francisco

Abstract

Although more than a decade has elapsed since the discovery of cannabinoid receptors and endogenous cannabinoid ligands in the brain, the function of these neural modulators remains mysterious. We have found that endocannabinoids function as retrograde synaptic messengers that are initially released from depolarized hippocampal pyramidal neurons and then travel backwards across synapses to suppress GABA release from inhibitory interneurons. Our results imply that this mechanism accounts for the phenomenon of "depolarization-induced suppression of inhibition" (DSI), which has been previously described by other investigators but not fully understood at the molecular level. We have found that DSI is blocked by antagonists of cannabinoid receptor-1 (CB1). Furthermore, DSI is completely absent in $CB1^{-/-}$ mice. A CB1 agonist mimics and occludes DSI, and DSI is also occluded by blocking removal of endocannabinoids from the extracellular space. DSI is associated with an increase in the paired-pulse ratio and a decrease in the frequency of Ca^{2+}-dependent miniature IPSCs, consistent with the previously published conclusion that CB1 inhibits GABA release by inhibiting presynaptic Ca^{2+} channels. We suggest on the basis of pharmacological and kinetic evidence that CB1 activation inhibits Ca^{2+} influx by a direct, membrane-delimited pathway. Consistent with the conclusion that the retrograde messenger in DSI is an endocannabinoid, we have found that this messenger is diffusible, and is likely to be synthesized in response to Ca^{2+} influx and released from the postsynaptic cell by simple diffusion or passive transport.

We have also used paired recordings of single interneuron-pyramidal cell connections to investigate whether endocannabinoids selectively target a class of GABAergic synapses with distinctive physiological properties. We find that unitary GABAergic connections are either extremely sensitive to DSI or else completely insensitive. DSI-sensitive connections have fast synaptic kinetics and large synaptic conductances. Consistent with the morphological identification of CB1-positive interneurons as basket cells, DSI-sensitive interneurons have moderate spiking rates and small after-hyperpolarizations. Together, these results suggest that endocannabinoids selectively suppress inhibitory synapses localized to the somata and proximal dendrites of pyramidal neurons, synapses which are thought to be responsible for gamma-range oscillations in synchronous pyramidal cell spiking. Finally, we have found that DSI-sensitive interneurons use only N-type Ca^{2+} channels for GABA release. Since N-type channels are more sensitive to G-protein-mediated inhibition than P/Q-type channels, this unusual presynaptic specialization may account for why CB1 activation suppresses GABA release so profoundly at these synapses.

Table of Contents

List of Figures

CHAPTER 1: General Introduction

Retrograde synaptic signaling

> "The transmission of the nervous impulse is always from the dendritic branches and the cell body to the axon..."
> —Revista de Ciencas médicas de Barcelona, núms. 22-23

It was in these terms that, in 1891, Ramon y Cajal formulated his "principle of dynamical polarization". This idea—that information transfer within neurons and between neurons is unidirectional—was not completely new. However, it had not been stated so boldly before. Cajal's principle of one-way traffic challenged contemporary ideas that nerve impulses might "spread in all directions, like sound and light", or, (as Golgi maintained) that the shorter processes of neurons might serve a purely nutritional function. Remarked one skeptical contemporary, "To admit [Cajal's] hypothesis... it would be necessary to change completely our idea of the dendrites." (Ramon y Cajal, 1937).

The mechanism by which this one-way communication is enforced—the transfer of electrical impulses by unidirectional chemical secretion—was finally established in the mid-1950s. In the decades since, neurophysiology has established that unidirectional synaptic communication is a general rule in the CNS. Yet, at the same time, evidence has accumulated to suggest that postsynaptic dendrites and somata can also send signals backwards across the synapse to influence the form and function of axons. It seems that, now as then, we must "change completely our idea of dendrites".

Retrograde synaptic signaling can be conceptually divided into two types. First, there are many examples of slow, long-term regulation of presynaptic axons by postsynaptic signals. Target-derived factors influence the guidance of afferent axons

during neural development (Tessier-Lavigne and Goodman, 1996) and the survival of presynaptic neurons once connections have been formed (Barde, 1989). Retrograde signals also control the phenotype of presynaptic neurons, a phenomenon that has been called "synaptic matching" (Davis and Murphey, 1994a). Target derived factors can control presynaptic neurotransmitter phenotype (Schotzinger et al., 1994) and the properties of presynaptic vesicular release (Davis and Murphey, 1994b; Davis and Murphey, 1994a). Recent examples in the literature include synaptic matching at the *Drosophila* NMJ ion (Davis et al., 1998) and at glutamatergic synapses of the hippocampus and cortex (Tóth and McBain, 2000). Synaptic matching is thought to occur slowly (on the timescale of nervous system development, i.e. hours-weeks, rather than the timescale of electrical information transfer, i.e. milliseconds-minutes) and to have long-term effects on presynaptic function that normally persist throughout the lifetime of the organism. The molecular basis of synaptic matching is the subject of ongoing research (Davis and Goodman, 1998).

A very different type of retrograde signaling has also been proposed to occur at synapses. In this case, specific patterns of postsynaptic activity are thought to trigger the synthesis or release of a postsynaptic molecule which then acutely regulates synaptic strength. This sort of retrograde signaling is conceptually distinct from synaptic matching in that it is rapidly induced (in seconds), and that its effects on synaptic strength are highly reversible. Fast, reversible retrograde signaling has been proposed to play an important role in information processing and storage by the mature nervous system (Alger and Pitler, 1995; Fitzsimonds and Poo, 1998).

Fast retrograde signaling has been proposed to occur in many contexts; the four examples reviewed in this section are supported by at least some physiological data and are the focus of current research.

Glutamatergic synapses in CA1

First, and most famously, fast retrograde signaling was postulated as a requirement for long-term potentiation (LTP) and long-term depression (LTD) of glutamatergic transmission in the CA1 region of the hippocampus. This was based on the universally-accepted conclusion that LTP/LTD are induced postsynaptically, and on the controversial conclusion that expression of LTP/LTD are presynaptic. The evidence for and against a presynaptic locus of expression in LTP/LTD is still accumulating and has been extensively reviewed elsewhere (Bliss and Collingridge, 1993; Nicoll and Malenka, 1999). Molecules that have been proposed as the retrograde signal in LTP and/or LTD include lipids (arachidonic and/or its lipoxygenase metabolites, platelet activating factor), neutral gaseous molecules (nitric oxide, carbon monoxide), and secreted protein growth factors (NGF, EGF, BDNF, NT-3). The effects of these molecules (if any) on synaptic transmission, the mechanisms of those effects, and their relationship to LTP/LTD are still the topic of research and debate (Williams, 1996).

Xenopus neuromuscular junction

Second, fast retrograde signaling has been proposed to mediate LTD at the *Xenopus* NMJ. In *Xenopus* motoneuron-myocyte co-cultures, cytoplasmic Ca^{2+} spikes in

a myocyte cause a persistent decrease in cholinergic miniature end-plate currents (mEPCs) recorded in that cell (Lo and Poo, 1991; Dan and Poo, 1992; Cash et al., 1996a). During LTD, there is no change in currents elicited by acetylcholine iontophoresis (Dan and Poo, 1992) and no change in mEPC amplitude (Dan and Poo, 1992; Cash et al., 1996a), suggesting a presynaptic locus of expression. LTD appears to spread to synapses made by the same presynaptic motoneuron onto other myocytes. Rapid perfusion of culture medium over the myocyte where the depression was initially induced did not affect LTD in that myocyte or the propagation of LTD to other myocyes (Cash et al., 1996b). This suggested that the initial retrograde signal might be a direct, physical interaction between transmembrane proteins. This local signal would then initiate a wave of second messengers inside the presynaptic axon; this in turn would propagate the depression through that axon to other synapses. The initial retrograde signal in this process remains unknown, as do the factors responsible for LTD propagation (Fitzsimonds and Poo, 1998).

Cortical synapses

Two recent studies of short-term cortical plasticity suggest a role for fast retrograde messengers. The first study (Zilberter et al., 1999) examined unitary glutamatergic connections from layer 2/3 cortical pyramidal cells onto bitufted interneurons using paired recordings. Trains of action potentials in a bitufted interneuron transiently depressed the amplitude of unitary excitatory postsynaptic potentials (EPSPs) recorded in that cell. Postsynaptic BAPTA or GDP-β-S blocked the depression, indicating a postsynaptic requirement for Ca^{2+} and GTP. A presynaptic locus of

expression was indicated by an increase in the paired-pulse ratio and an increase in EPSP failures. As the depression was blocked by a GABA-B antagonist, the authors hypothesized that GABA released from the dendrites of the bitufted cell acted on presynaptic GABA-B receptors to inhibit glutamate release.

A mirror image of this phenomenon has recently been reported by the same investigator (Zilberter, 2000) using paired recordings of GABAergic connections from fast spiking interneurons to pyramidal cells. In this case, trains of action potentials in the pyramidal cell transiently depressed the amplitude of unitary inhibitory postsynaptic potentials (IPSPs) recorded in that cell. This depression was also blocked by postsynaptic BAPTA or GDP-β-S, and associated with an increase in the paired pulse ratio and an increase in IPSP failures. Furthermore, the depression of IPSPs was blocked by a cocktail of metabotropic glutamate receptor antagonists. This suggested that glutamate released from pyramidal cell somata and/or dendrites was acting on presynaptic mGluRs to inhibit GABA release. This phenomenon was also blocked by postsynaptic botulinum toxin D light chain, which cleaves the SNARE protein VAMP2, implicating postsynaptic vesicular release.

Both these phenomena are intriguing, but will require further investigation to verify a role for retrograde signaling. Interestingly, both types of depression appeared only after several minutes of repetitive postsynaptic spiking, and also required several minutes to reverse, suggesting a global accumulation of some molecule in a large extracellular space, rather than a fast and focal retrograde signal. Experiments of this type are confounded by the fact that in the cortex many of these connections are reciprocal—i.e., interneurons often make synapses onto and receive synapses from the

same pyramidal cells. It would be informative to repeat these experiments in voltage clamp mode while postsynaptic action potentials are blocked (using the internal Na^+ channel blocker QX-314) and/or while the reciprocal synapses are blocked with antagonists of ionotropic GABA/glutamate receptors. This would eliminate any possibility that repetitive spiking of the postsynaptic cell could influence the presynaptic cell via the direct reciprocal synapse from post to pre.

GABAergic synapses in the cerebellum and hippocampus (DSI)

In cerebellar slices, depolarizing a Purkinje cell in voltage-clamp mode results in a transient depression of pharmacologically-isolated GABAergic IPSCs (Llano et al., 1991). This phenomenon, dubbed "depolarization-induced suppression of inhibition" (DSI) is blocked by postsynaptic BAPTA. A presynaptic locus for cerebellar DSI is indicated by the observation that currents evoked by GABA iontophoresis are unchanged or are even transiently potentiated during DSI. Furthermore, DSI is accompanied by a decrease in the frequency of miniature IPSCs (mIPSCs), putatively quantal events corresponding to the release of single vesicles which are observed in the presence of TTX. By contrast, mIPSC amplitude is unchanged during DSI, implying that postsynaptic sensitivity to GABA is not altered (Llano et al., 1991).

Curiously, depolarizing a single Purkinje cell can cause DSI in a nearby, nondepolarized cell only when a high proportion of spontaneous IPSCs in the two cells are coincident (Vincent and Marty, 1993). This was interpreted as representing a requirement for common presynaptic inputs. According to this hypothesis, DSI is somehow propagated inside presynaptic axons to spread the depression.

The search for a retrograde signal in cerebellar DSI has ruled out participation by adenosine, GABA, arachidonic acid, carbon dioxide, and nitric oxide (Glitsch et al., 1996). Based on the observation that cerebellar DSI is reduced (by about 40%) by the mGluR antagonist L-AP3, it was concluded that glutamate is the retrograde signal in cerebellar DSI (Glitsch et al., 1996). However, L-AP3 also increased sIPSC frequency and directly depolarized Purkinje cells in these experiments. This raises the possibility that the effects of L-AP3 on cerebellar DSI could be nonspecific, which is consistent with the finding that the more specific mGluR antagonist MCPG had no effect on cerebellar DSI (Glitsch et al., 1996).

A very similar phenomenon, termed hippocampal DSI, has been independently described at GABAergic synapses in the hippocampal CA1 region. Depolarization of a CA1 pyramidal cell causes a transient depression in spontaneous or evoked GABAergic synaptic responses. This depression is similar in its kinetics and average magnitude to cerebellar DSI. Depolarization may be supplied by either trains of postsynaptic action potentials recorded in current-clamp mode, or brief depolarizations in voltage-clamp mode (Pitler and Alger, 1992; Pitler and Alger, 1994). A presynaptic locus for hippocampal DSI is indicated by the following results:

1. DSI does not affect the current elicited by GABA iontophoresis (Pitler and Alger, 1992).
2. DSI does not affect mIPSCs amplitude (Pitler and Alger, 1994; Alger et al., 1996).
3. DSI increases the coefficient of variation of IPSCs and increases the failure rate (Alger et al., 1996), consistent with a decrease in either the number of release sites (n) and/or the probability of release (p).

4. When extracellular Ca^{2+} is replaced by Sr^{2+}, DSI decreases the frequency of the asynchronous, quantal IPSCs elicited by extracellular stimulation (Morishita and Alger, 1997), again consistent with a decrease in *n* and/or *p*. The amplitude of evoked quanta in Sr^{2+} is not changed.
5. Veratridine, which increases Na^+ channel open times, decreases DSI when postsynaptic Na^+ channels are completely blocked by internal QX-314 (Alger et al., 1996).

In light of these data, hippocampal DSI may reasonably be considered the neurophysiological phenomenon demonstrating the strongest evidence in favor of fast retrograde signaling.

The presynaptic mechanism of hippocampal DSI has been harder to describe conclusively. One study found that DSI did not change the paired-pulse ratio (PPR), the ratio of IPSC amplitudes elicited by two closedly-spaced stimuli ($PPR = amp_2/amp_1$) (Alger et al., 1996). In general, PPR is determined by the sum of several simultaneous processes, including facilitation (caused by residual presynaptic cytoplasmic Ca^{2+}) and depression (probably caused by transient depletion of "primed" or otherwise readily releasable vesicles) (Zucker, 1989). In simplified terms, PPR is generally high when *p* is low, and vice versa, since depression/depletion contributes less prominently to total PPR when $p<<1$ (Dobrunz and Stevens, 1997). Therefore, a failure to detect a change in PPR was interpreted by Alger et al. as meaning that DSI does not affect *p*. Another study, however, has reported that DSI at single connections between cultured hippocampal interneurons and pyramidal cells is accompanied by a pronounced increase in PPR, suggesting a decrease in *p* (Ohno-Shosaku et al., 1998). One explanation for these

conflicting results is that dissociated, cultured neurons may exhibit certain phenomena which are an artifact of culture conditions and have no relevance to acute slices or to *in vivo* brain function. An alternative explanation is that DSI may selectively affect some GABAergic synapses but not others; this is consistent with the finding that some individual connections among cultured neurons show no DSI whatsoever (Ohno-Shosaku et al., 1998). Similarly, monosynaptic evoked IPSCs in acute slices sometimes exhibit multiple components with clearly different latencies, presumably originating from different axons; these components also show clear heterogeneity in their DSI sensitivity, with some components evidently insensitive to DSI (Alger et al., 1996). In this scenario, DSI might decrease p at a subpopulation of synapses, which would then contribute little to the total evoked IPSC during DSI; a change in PPR that affected only these (now-small) synaptic responses could easily be undetectable. In paired recordings among cultured neurons, however, a unitary connection that is sensitive to DSI is sampled without contamination by DSI-insensitive connections, and a change in PPR may be more noticeable.

Another measure of p, mIPSC frequency, was examined during DSI in two studies from the same laboratory. The first study detected a very small (12%) but statistically significant decrease in mIPSC frequency during DSI (Pitler and Alger, 1994). In a second study, no change in mIPSC frequency was detected (Alger et al., 1996), suggesting no change in p. Under ordinary recording conditions, presynaptic voltage-dependent calcium channels (VDCCs) are closed and mIPSCs are not dependent on extracellular Ca^{2+} (Scanziani et al., 1992; Doze et al., 1995). This means that a retrograde signal that decreases p by decreasing Ca^{2+} influx would not be expected to

affect mIPSCs under these conditions. Therefore these authors then recorded mIPSCs under depolarizing conditions (high external K^+) where a majority of mIPSCs are sensitive to the VDCC blocker Cd^{2+}. They found that DSI also did not affect these Ca^{2+}-dependent mIPSCs (Alger et al., 1996), suggesting that the retrograde signal does not affect Ca^{2+} influx or a Ca^{2+}-dependent step in release. Based on these experiments, along with the negative results in PPR measurements, Alger et al. concluded that DSI probably represented axonal conduction failures in the presynaptic interneuron. However, mIPSCs under depolarizing conditions are largely dependent on only one subtype of presynaptic VDCC (Doze et al., 1995), and so may not reflect the sensitivity of all VDCCs that participate in GABA release. Therefore, the evidence on this point remains inconclusive.

Based on reports of glutamate's involvement in cerebellar DSI, glutamate has also been investigated as a candidate retrograde messenger in hippocampal DSI. (S)-MCPG was reported to reduce hippocampal DSI by 50-60% at high doses (5 mM) (Morishita et al., 1998; Morishita and Alger, 1999). DSI was not blocked by specific antagonists of group II and group III mGluRs, suggesting that if an mGluR is the presynaptic target in DSI, it is probably a group I receptor (mGluR1 or mGluR5). The mGluR hypothesis is consistent with the conclusion that presynaptic G-protein coupled receptors seem to be involved, as DSI is blocked by pertussis toxin but not by postsynaptic GTPγS (Pitler and Alger, 1994). However, in a recent study by the same authors, a mGluR antagonist was reported not to affect DSI in the CA3 region of the hippocampus (Morishita and Alger, 2000). The retrograde signal in both hippocampal and cerebellar DSI has therefore been considered to be glutamate (or a related molecule), but the evidence on this point has not been conclusive.

Cannabinoid receptors and ligands

Cannabinoid receptors in the CNS

Marijuana, hashish, and other deriatives of the hemp plant *Cannabis sativa* have been used for medicinal and recreational purposes for thousands of years (Snyder, 1971). The primary psychoactive ingredient in these preparations, Δ^9-THC, was isolated in 1964 (Gaoni and Mechoulam, 1964). Δ^9-THC is extremely hydrophobic, and by one estimate the amount of labeled Δ^9-THC that intercalates into membranes is 10^6-fold greater than that which binds to receptors (Devane et al., 1988). Therefore, it was proposed initially that general membrane perturbation is the mechanism by which cannabinoids affect neural function (Lawrence and Gill, 1975).

In 1986 the "non-classical" cannabinoid agonist CP-55940 was synthesized. This drug reproduces behavioral effects of Δ^9-THC in animals, but is more potent and less lipophilic than Δ^9-THC (Johnson and Melvin, 1986). CP-55940 was found to inhibit adenylate cyclase in a stereoselective manner, and this inhibition required G_i. The behavioral effects of CP-55940 showed the same stereoselectivity (Howlett and Fleming, 1984). Furthermore, [^{3}H]CP-55940 bound to a high affinity, stereoselective site in brain tissue, implicating a specific receptor for cannabinoids (Devane et al., 1988). The brain cannabinoid receptor (CB1) was cloned in 1990, and found to represent a seven transmembrane-domain, G protein-coupled receptor (Matsuda et al., 1990). Surprisingly, CB1 is one of the most abundant neuromodulatory receptors in the brain; it is expressed at higher levels than most other G-protein coupled receptors, and is 10-fold more abundant than the μ-opioid receptor (Sim et al., 1996). CB1 mRNA and protein

generally parallels [^{3}H]CP-55940 binding, with high CB1 levels in the hippocampus, basal ganglia, and cerebellum, and moderately high levels in the cortex (Herkenham et al., 1990; Herkenham et al., 1991; Matsuda et al., 1993; Tsou et al., 1998; Egertová and Elphick, 2000). This expression pattern presumably accounts for the striking effects of Δ^9-THC on memory, cognition, and psychomotor behavior (Snyder, 1971). The only obvious mismatch occurs in the olfactory bulb, where [^{3}H]CP-55940 binding and CB1 protein is high, but CB1 mRNA is low or absent; this pattern is plausibly explained by the suggestion that CB1 is present only on the axons of centrifugal inputs to the bulb (Matsuda et al., 1993).

CB1 is expressed at much lower levels in various other organs (Galiègue et al., 1995). A second cannabinoid receptor (CB2) was subsequently cloned, and found to be present at high levels in spleen, but completely absent from the brain and spinal cord (Munro et al., 1993). All CNS effects of of Δ^9-THC (catalepsy, analgesia, hypolocomotion) are absent in CB1$^{-/-}$ mice, with the exception of reflexive spinal responses to noxious heat (tail flick test) (Ledent et al., 1999; Zimmer et al., 1999). This suggests that all the major effects of cannabinoids on the brain may be mediated by CB1.

Identification of endocannabinoids in the CNS

Based, in part, on the identification of opioid receptors (Pert and Snyder, 1973) and the subsequent purification of endogenous opioids (Hughes et al., 1975), specific [^{3}H]CP-55940 binding sites suggested the presence of endogenous cannabinoids in the brain. Early work found that depolarization caused the Ca^{2+}-dependent efflux of a substance from brain that could displace [^{3}H]CP-55940 from brain tissue in a dose-

dependent fashion (Evans et al., 1992). Cannabinoid receptor binding activity was increased by peptidase inhibitors, suggesting that endogenous cannabinoids (like the endogenous opioids) might be peptides stored in synaptic vesicles (Evans et al., 1994).

Reasoning that endogenous cannabinoids, like Δ^9-THC, are likely to be lipophilic, Mechoulam and colleagues instead focused on chloroform/methanol extracts of brain, and selected purification techniques based on the assumption that the endogenous cannabinoid would be a lipid. They purified a compound they called anandamide which competitively inhibited [^{3}H]CP-55940 binding to brain tissue, and showed cannabimimetic activity *in vivo* (Devane et al., 1988). Subsequent experiments showed that anandamide binds specifically to CB1 and acts as an agonist, inhibiting adenylate cyclase in a pertussis toxin-sensitive mechanism (Felder et al., 1993; Vogel et al., 1993).

A second endocannabinoid, 2-arachidonylglycerol (2-AG) was subsequently isolated from gut (Mechoulam et al., 1995). 2-AG binds both CB1 and CB2 (Mechoulam et al., 1995), and is present in brain (Sugiura et al., 1995). 2-AG is released by hippocampal slices in response to electrical stimulation in an action potential-dependent, Ca^{2+}-dependent manner (Stella et al., 1997).

It is likely that there are also other endocannabinoids related to anandamide and 2-AG (Devane et al., 1988; Walter et al., 2000). Furthermore, the existence of structurally dissimilar endocannabinoids, including peptides and other hydrophilic compounds, is still considered a possibility (Childers and Breivogel, 1998).

Biosynthesis, uptake, and degradation of endocannabinoids

Although anandamide was initially thought to form via the condensation of arachidonic acid with ethanolamine (Deutsch and Chin, 1993), it is now clear that the most physiologically plausible synthetic pathway is Ca^{2+}-dependent N-transacylation of phosphatidylethanolamide with arachidonic acid donated from di-arachidonoylphosphatidylcholine, followed by Ca^{2+}-dependent hydrolysis by a phospholipase D to form arachidonylethanolamide (anandamide) (Di Marzo et al., 1994; Sugiura et al., 1996). The biosynthetic pathways that produce 2-AG are less well characterized, and at least two Ca^{2+}-dependent pathways are plausible (Bisogno et al., 1997).

Both anandamide and 2-AG are degraded by a single enzyme, fatty acid amide hydrolase (FAAH). This enzyme converts anandamide to arachidonic acid and ethanolamine, and converts 2-AG to arachidonic acid and glycerol (Deutsch and Chin, 1993; Di Marzo et al., 1994; Bisogno et al., 1997; Goparaju et al., 1998). FAAH has been cloned (Cravatt et al., 1996), and was found to be present in every brain region tested, with the highest expression in hippocampus, cortex, cerebellum, striatum, and amygdala, regions where CB1 expression is also high (Thomas et al., 1997; Egertová et al., 1998). Sequence analysis suggests that FAAH is intracellular (Cravatt et al., 1996), and immunocytochemistry shows FAAH localized to the somata and dendrites of cerebellar Purkinje neurons and hippocampal/cortical pyramidal neurons (Egertová et al., 1998). Astrocytes also participate in the hydrolysis of endocannabinoids (Di Marzo et al., 1994).

The lipophilicity of anandamide and 2-AG suggests that these molecules might diffuse rather freely though cell membranes. However, specific transport systems are also known to escort some lipids across membranes. Both long chain fatty acids (Schaffer and Lodish, 1994) and prostaglandins (Kanai et al., 1995) are carried across plasma membranes by Na^+-independent, passive, specific transport proteins. Similarly, there is now evidence that cannabinoids are also substrates for specific transporters. Exogenous [^{3}H]anandamide is cleared from the medium of neuronal cultures in a rapid, temperature-dependent, saturable manner, suggestive of carrier-mediated uptake (Di Marzo et al., 1994). This transporter is more selective for anandamide and 2-AG than is FAAH, which hydrolyzes a wide range of fatty acid amides and esters (Maurelli et al., 1995; Cravatt et al., 1996; Di Marzo et al., 1998a; Goparaju et al., 1998; Piomelli et al., 1999). A specific antagonist of the anandamide/2-AG transporter, AM404, potentiates the effect of anandamide on CB1-mediated adenylate cyclase inhibition in cultured neurons (Beltramo et al., 1997). *In vivo*, AM404 similarly potentiates the effects of anandamide on blood pressure (Calignano et al., 1997) and increases circulating levels of anandamide in plasma (Giuffrida et al., 2000). These data suggest that anandamide and 2-AG may not be able to enter cells by diffusion and may require transporters to deliver them to intracellular FAAH.

Functional neuroanatomy and electrophysiology of cannabinoids

Fifteen years ago, a review of cannabinoids remarked that "it is disconcerting that they seem to exert some alteration in almost every biological system that has been studied" (Martin, 1986). A comprehensive review of cannabinoid physiology is no more

possible now than then. A confounding element in any review of this literature is that high concentrations of Δ^9-THC *in vitro* have direct effects on membranes, receptors, and enzymes (Martin, 1986) that may not be relevant to marijuana's major CNS actions, as $CB1^{-/-}$ mice lack all observable supra-spinal CNS reactions to Δ^9-THC (Ledent et al., 1999; Zimmer et al., 1999). These diverse *in vitro* effects elicited by high Δ^9-THC concentrations probably have even less relevance to endocannabinoids. The remainder of this introduction will therefore focus on the effects of selective, "nonclassical", synthetic CB1 agonists (WIN55212-2, CP-55940) and endocannabinoids (anandamide, 2-AG). Although cannabinoids clearly affect synaptic transmission in many brain regions (including the amygdala, striatum, spinal cord, and retina), this review will focus on the hippocampus and cerebellum, where the mechanisms of these effects have been studied in greatest detail, and where retrograde signaling is of particular interest.

Hippocampus

Clues to the functional consequences of CB1 activation lie in the cellular and subcellular localization of CB1 protein. In the hippocampus, glutamatergic neurons (pyramidal neurons and dentate granule cells) are CB1-negative (Tsou et al., 1998; Tsou et al., 1999; Katona et al., 1999; Egertová and Elphick, 2000; Hajos et al., 2000; Katona et al., 2000). Very low levels of CB1 mRNA are, however, detectable in hippocampal pyramidal cells (Mailleux and Vanderhaeghen, 1992; Matsuda et al., 1993; Marsicano and Lutz, 1999), although extended exposures are required to observe this signal (Mailleux and Vanderhaeghen, 1992). It is possible, therefore, that CB1 protein may be present at undetectable levels in glutamatergic neurons. By contrast, other neurons in the

hippocampus show extremely high levels of CB1 mRNA and protein. These scattered cells are interneurons, since they also express the GABA synthetic enzyme GAD65, along with other interneuron markers (Mailleux and Vanderhaeghen, 1992; Matsuda et al., 1993; Marsicano and Lutz, 1999; Tsou et al., 1998; Tsou et al., 1999; Katona et al., 1999; Egertová and Elphick, 2000; Hajos et al., 2000; Katona et al., 2000). These CB1-positive cells represent only a subset of hippocampal interneurons, identified as cholecystokinin-positive, parvalbumin-negative basket cells (Marsicano and Lutz, 1999; Tsou et al., 1999; Katona et al., 1999). Immunogold electron microscopy reveals that CB1 is targeted selectively to the presynaptic boutons of these interneurons. Heavy CB1 labeling decorates the presynaptic boutons at symmetric (GABAergic) synapses in hippocampal sections, but no gold particles are detected on postsynaptic dendrites. At asymmetric (glutamatergic) synapses, presynaptic boutons are always CB1-negative (Katona et al., 1999; Katona et al., 2000).

These anatomical findings suggest that cannabinoids regulate GABA release in the hippocampus. Accordingly, the CB1 agonist WIN55212-2 reduces [^{3}H]GABA release from electrically stimulated hippocampal slices. This reduction is not affected by ionotropic glutamate receptor antagonists, implying that WIN55212-2 is not acting on glutamatergic transmission. Finally, the specific CB1 antagonist SR141716 blocks the effect of WIN55212-2 on [^{3}H]GABA efflux (Katona et al., 1999). WIN55212-2 also depresses evoked IPSCs recorded in CA1 pyramidal cells (Hoffman and Lupica, 2000; Hajos et al., 2000). Presumptive single GABAergic fibers in CA1 can be either very sensitive or completely insensitive to the CB1 agonist CP-55940 (Hajos et al., 2000), consistent with the restricted expression of CB1 in a subset of basket cells.

WIN55212-2 also depresses eIPSCs recorded in hippocampal dentate granule cells (Hajos et al., 2000). This is consistent with intense expression of CB1 by presumptive basket cells in the subgranular zone of the dentate gyrus (Matsuda et al., 1993). Importantly, this effect of WIN55212-2 is completely absent in $CB1^{-/-}$ mice (Hajos et al., 2000).

An informative series of experiments by Hoffman and Lupica (2000) recently described the mechanism by which WIN55212-2 inhibits GABA release. Recording from CA1 pyramidal cells in hippocampal slices, these authors found that WIN55212-2 decreased evoked IPSC amplitude, and decreased the frequency and amplitude of spontaneous IPSCs. Ca^{2+}-independent mIPSCs were insensitive to WIN55212-2, suggesting that CB1 activation does not affect the presynaptic release machinery *per se*. However, WIN55212-2 did depress the frequency of Ca^{2+}-dependent mIPSCs recorded in high external K^+. This implies that WIN55212-2 inhibits a Ca^{2+}-dependent step in GABA release, and suggested that CB1 activation might inhibit VDCCs in the presynaptic terminal. These authors also reported that the effect of WIN55212-2 could still be observed in the presence of barium or 4-AP, demonstrating that presynaptic K^+ channels are not directly involved, as has been suggested for CB1 activation in other contexts (see below). The conclusion that WIN55212-2 inhibits GABA release by blocking presynaptic Ca^{2+} channels agrees with previous observations in other systems. CB1 activation in neural cell lines inhibits N-type VDCCs by a membrane-delimited pathway whereby $G\beta\gamma$ interacts directly with the channel (Mackie and Hille, 1992; Pan et al., 1996).

In addition to its effects on GABAergic transmission, WIN55212-2 also inhibits electrically evoked [^{14}C]acetylcholine efflux from hippocampal slices (Gifford and

Ashby, 1996). This effect was reversed by SR141716, implying that CB1 is required. Moderate levels of CB1 mRNA are present in the medial septum and diagonal band of Broca, where cholinergic afferents to the hippocampus originate (Mailleux and Vanderhaeghen, 1992).

A large literature documents the effects of cannabinoids on cultured hippocampal neurons. Unlike pyramidal neurons in acute slices, pyramidal neurons in dissociated culture reportedly express high levels of CB1 protein (Twitchell et al., 1997). In these cells, WIN55212-2 decreases whole-cell Ca^{2+} currents (Twitchell et al., 1997; Shen and Thayer, 1998), decreases the I_A K^+ current via downregulation of PKA (Mu et al., 2000), and inhibits glutamate release (Shen et al., 1996; Sullivan, 1999; Kim and Thayer, 2000). Interestingly, WIN55212-2 had no effect on GABAergic connections in these cultures (Shen et al., 1996). This implies that CB1 may be expressed on pyramidal cells but not interneurons in these cultures, which would be the reverse of the situation in slices. This phenotypic switch is consistent with the general observation that hippocampal neurons in dissociated cultures can undergo dramatic morphological and physiological changes *in vitro* (E. Schnell, personal communication). The switch in CB1 expression seems to depend on culture conditions, since another study reported that virtually all CB1-immunopositive cells in dissociated culture are GABAergic (Irving et al., 2000).

Finally, although hippocampal pyramidal neurons appear to lack detectable CB1 protein, some studies have described effects of cannabinoids on glutamatergic transmission in CA1. WIN55212-2 reportedly depresses evoked EPSCs in whole-cell recordings, as well as field EPSPs (Misner and Sullivan, 1999). Identical results were obtained in the presence and absence of picrotoxin, suggesting that WIN55212-2 was not

acting indirectly by modulating GABAergic transmission. Although moderately high concentrations of agonist (5 μM) were used in this study, its effect was blocked by SR141716, implying a specific effect on cannabinoid receptors, and was not mimicked by the inactive enantiomer of WIN55212-2. This suggests that the non-specific effects of high WIN5512-2 concentrations (Shen and Thayer, 1998) cannot account for these results. However, another study found that 5 μM WIN55212-2 did not affect field EPSPs, but did increase the size of the field potential population spike, suggesting a decrease in GABAergic inhibition (Paton et al., 1998).

Misner and Sullivan (1999) also found that WIN55212-2 blocked LTP in CA1, which could easily be explained by a presynaptic inhibition of glutamate release. A previous study (Terranova et al., 1995) had also reported that WIN55212-2 blocked the tetanus-induced potentiation of the CA1 population spike; population spike potentiation indicates either LTP of EPSPs, or LTD of GABAergic inhibition, or some long-term increase in intrinsic excitability. However, Terranova et al. found no effect of WIN55212-2 on basal population spikes, suggesting no effect on basal EPSPs. This appears to be inconsistent with Misner et al. (1999) and consistent with Paton et al. (1998). Similarly, both anandamide (Terranova et al., 1995) and 2-AG (Stella et al., 1997) are also reported to inhibit LTP in CA1 but have no effect on basal EPSPs. In light of these diverse results, the mechanism by which CB1 agonists might inhibit LTP remains uncertain. $CB1^{-/-}$ mice also reportedly show increased CA1 LTP (Bohme et al., 2000), but the difference in LTP between wild-type and mutant mice appears to be insignificant by any conventional statistical test.

Since CB1 is undetectable in glutamatergic neurons in the hippocampus, these findings suggest that there may be a second cannabinoid receptor in the brain with a pharmacology very similar to CB1. Consistent with this hypothesis, anandamide has SR141716-sensitive effects in the cardiovascular system which are independent of either CB1 or CB2 (Wagner et al., 1999; Járai et al., 1999).

Cerebellum

High levels of CB1 expression in the cerebellum suggest that cannabinoids exert a powerful effect on this structure. Purkinje cells themselves contain no CB1 mRNA (Matsuda et al., 1993). However, intense labeling for CB1 mRNA is associated with the granule cells of the cerebellum (Matsuda et al., 1993). The granular layer of the cerebellum shows only low CB1 immunoreactivity, suggesting that CB1 is not abundant on granule cell somata or dendrites (Tsou et al., 1998). Granule cell axons form the glutamatergic parallel fiber projections onto Purkinje cells, and LTD at these synapses may mediate motor learning (Linden, 1994). The molecular layer of the cerebellum, where parallel fiber (PF) synapses onto Purkinje cells are located, shows moderate CB1 immunoreactivity (Tsou et al., 1998), implying that CB1 is selectively localized to granule cell axon terminals.

Some of the CB1 immunoreactivity in the molecular layer may also be associated with climbing fibers (CFs), the axons of the glutamatergic inputs to Purkinje cells from the inferior olive, since CF and PF synapses are intermingled in this layer. However, CB1 mRNA labeling is very weak and diffuse thoughout the medulla, where the inferior

olive is located (Matsuda et al., 1993). It is not clear, therefore, whether there is any CB1 present at CF synapses.

The most intense CB1 immunoreactivity in the cerebellum is associated with the "pinceau" and perisomatic synapses made by GABAergic basket cells and stellate cells onto Purkinje neurons (Tsou et al., 1998). This implies that cannabinoids regulate the release of GABA and glutamate onto Purkinje cells.

Two careful studies recently described the electrophysiology of CB1 activation in the cerebellum, based on whole-cell recordings from Purkinje cells in cerebellar slices. Either WIN55212-2 or CP-55940 depressed evoked EPSCs at PF synapses, and this depression was blocked by SR141716 (Lévénés et al., 1998; Takahashi and Linden, 2000). The effect of WIN55212-2 had a presynaptic locus, since it was accompanied by: (1) an increase in the paired-pulse ratio, (2) an increase in the coefficient of variation of evoked EPSCs, and (3) a decrease in the frequency of asynchronous, quantal EPSCs in Sr^{2+} (Lévénés et al., 1998). There was no change in the PF fiber volley, ruling out an effect of WIN55212-2 on action potential conduction (Takahashi and Linden, 2000). Together, these results suggest that CB1 activation causes a decrease in the local probability of release, p, at PF axon terminals.

WIN55212-2 also depressed evoked EPSCs at CF synapses, although to a lesser degree than at PF synapses, and this effect was blocked by SR141716 (Takahashi and Linden, 2000). This is perhaps surprising, as CB1 mRNA levels are quite low in the inferior olive, where CFs originate (Matsuda et al., 1993). Here, too, as at CA1 glutamatergic synapses, an uncloned cannabinoid receptor may be responsible for the effects of cannabinoid receptor agonists. The depression of CF EPSCs by WIN55212-2

was accompanied by an increase in the paired-pulse ratio, suggesting a decrease in *p* (Takahashi and Linden, 2000). Also, WIN55212-2 did not affect currents elicited in Purkinje cells by glutamate iontophoresis (Lévénés et al., 1998), again consistent with a presynaptic locus for the depression at both types of excitatory synapses.

Since PF and CF synapses are intermingled on Purkinje cell dendrites and produce similar miniature EPSCs, it is not possible to analyse the effects of WIN55212-2 separately on the two types of synapses using this measure. Both studies did examine the effects of WIN55212-2 on mEPSCs. Lévénés et al. (1998) reported a small decrease in mEPSC frequency, but did not report whether any of the mEPSCs recorded under their conditions were Ca^{2+}-dependent. Takahashi and Linden (2000) found no change in mEPSC frequency, and showed that all mEPSCs under their conditions were completely independent of Ca^{2+}. These results are compatible if a small fraction of the mEPSCs recorded by Lévénés et al. were in fact Ca^{2+}-dependent, and if those were the events that were sensitive to WIN552121-2. In any case, these data imply that WIN55212-2 probably has no effect on the Ca^{2+}-independent presynaptic release machinery in either CF or PF synapses. The most likely scenario seems to be that WIN55212-2 decreases *p* at both synapses by decreasing presynaptic Ca^{2+} entry. Neither study found any change in mEPSC amplitude, consistent with a presynaptic locus at both synapses.

Lévénés et al. (1998) also examined the regulation of synaptic plasticity by cannabinoids in the cerebellum. They reported that WIN55212-2 decreases LTD at PF-Purkinje cell synapses, and that this effect is sensitive to SR141716. This effect is probably a simple consequence of decreasing glutamate release from PF axons, since cerebellar LTD requires glutamate released from PFs to activate mGluRs (Linden, 1994).

This result provoked the first published statement of the idea that endocannabinoids might function as retrograde messengers:

> Finally, because synthesis of the two known potential endogenous cannabinoids, anandamide and 2-AG, is calcium dependent, it could occur in PCs [Purkinje cells] during the induction of LTD... Thus, endogenous cannabinoids might be produced by PCs during induction of LTD and then modulate this plasticity by a presynaptic effect (Lévénés et al., 1998).

However, these authors found no effect of SR141716 alone on LTD induction, implying that their stimulation protocols did not cause significant endocannabinoid synthesis under these experimental conditions.

As predicted by anatomical data, CB1 also regulates GABA release onto Purkinje cells. WIN55212-2 decreased the frequency and amplitude of spontaneous, action potential-dependent IPSCs in these cells, and these effects were blocked by SR141716 (Takahashi and Linden, 2000). WIN55212-2 had no effect on mIPSC amplitude, implying a presynaptic locus. Interestingly, a small but significant decrease in the frequency of Ca^{2+}-independent mIPSCs was also observed. These authors speculated that CB1 activation may inhibit not only Ca^{2+} entry at these synapses (as at PF and CF synapses) but also a subsequent, Ca^{2+}-independent step in vesicle release at GABAergic synapses. If so, this would be consistent with the finding that presynaptic inhibition can affect Ca^{2+}-dependent and -independent components of release differently at GABAergic versus glutamatergic synapses (Scanziani et al., 1992).

Functional conclusions

Taken together, data from the hippocampus and cerebellum suggest two general conclusions. First, a major function of endocannabinoids is likely to be inhibition of

neurotransmitter release. Anatomical and electrophysiological data imply that this presynaptic inhibition occurs locally at boutons, and is not a consequence of action potential conduction failures along the axon. Furthermore, inhibition of presynaptic Ca^{2+} channels appears to be a plausible general mechanism for this local decrease in *p*, although other mechanisms may also contribute. The subcellular location of endocannabinoid synthesis and release is unknown, but the biochemistry of these ligands suggests that they need not be released only from axon terminals, as classical neurotransmitters are. Thus endocannabinoids may function either as fast retrograde signals, or as autocrine/paracrine regulators of transmitter release, or all of these.

Second, whether cannabinoids tend to excite or inhibit any brain region will depend on which synapses express cannabinoid receptors. In the hippocampus, cannabinoids appear to increase excitability by decreasing GABA release. In the cerebellum, cannabinoids are likely to produce complex effects by inhibiting both GABA and glutamate release onto Purkinje cells.

The global behavioral consequences of these cellular actions are difficult to predict. By analogy with marijuana, endocannabinoids are sometimes thought to function as general CNS depressants, or are assumed to have vague euphoric (or anti-dysphoric) effects. The naming of the first endocannabinoid (anandamide = "ananda", the Sanskrit word for bliss, + "amide") reveals this prejudice. These preconceptions may also affect the design or interpretation of behavioral experiments: for example, $CB1^{-/-}$ mice are reported to show both impaired learning (Ledent et al., 1999) and enhanced learning (Reibaud et al., 1999). Because CB1 expression is restricted to different neuron types in different regions, understanding the role of endocannabinoids in any complex

CHAPTER 2: Methods

Slice preparation and basic electrophysiology

Transverse hippocampal slices (300 μm thick) were obtained from Sprague-Dawley rats (P16-30) and mice (see below) and maintained in artificial cerebrospinal fluid (ACSF) for at least 1 hr prior to recording. ACSF contained (in mM): NaCl 119, $NaHCO_3$ 26, glucose 10, KCl 3, $CaCl_2$ 2.5, $MgSO_4$ 2, NaH_2PO_4 1, NBQX disodium 0.005, CPP 0.002, and was equilibrated with 95% O_2 and 5% CO_2 at 20-22°C. Carbachol (5-10 μM) was added to the ACSF for those experiments where spontaneous IPSCs were examined; this increases sIPSC frequency and permits monitoring of DSI at higher temporal resolution (Pitler and Alger, 1992). Except where otherwise noted, recording electrodes were filled with a solution of (in mM): $CsCH_3SO_3$ 100, CsCl 60, QX-314 chloride 5, HEPES 10, EGTA 0.2, $MgCl_2$ 1, MgATP 1, and Na_3GTP 0.3 (pH 7.3, 275 mOsm). Synaptic currents were filtered at 2 kHz and collected at 5 kHz. When series resistance exceeded 40 MΩ or input resistance fell below 100 MΩ, experiments were terminated. Stimulus-evoked IPSCs (eIPSCs) were elicited using bipolar tungsten electrodes placed in or near CA1 stratum pyramidale.

DSI induction and analysis

DSI tests, generally performed every 120 sec, consisted of 30 stimuli at 0.33 Hz, with depolarization from –60 mV to 0 mV for 5 sec after the 13th stimulus. DSI is conventionally expressed as a percentage decrease in eIPSC amplitude (Morishita and

Alger, 1997). DSI was calculated using the mean of the three eIPSCs just before the depolarization ($amp_{baseline}$) and the three eIPSCs just after the depolarization (amp_{test}):

$$DSI\ (\%) = 100(1-(amp_{test}/amp_{baseline}))$$

It is thus possible to obtain small negative values for DSI as a result of statistical noise, especially when the measurement is based on a small number of trials, or in unitary connections which have a high variability in IPSC amplitude.

Pharmacology

For experiments involving extended pre-incubations (see Figures 5A, 6, 7, and 13A), slices were pre-incubated with the drug for 45-150 min, and recordings were performed in the presence of the same concentration. Drug-treated slices were interleaved with control slices from the same animal incubated for an equivalent period of time in the same concentration of the solvent (water, dilute NaOH, or DMSO) used to make the drug stock. Phosphate was omitted from the ACSF for the Sn PP IX experiments and their controls (Fig. 6). In these pre-incubation experiments, recordings were performed from one cell per slice, so that each cell was a relatively independent measure of average DSI. DSI was averaged across 4-5 trials per cell in the first 10 min after break-in. Overall, about 60% of cells have significant DSI, with DSI in these cells averaging about 50% in magnitude; thus, DSI averaged about 30% in control experiments.

For some experiments using acute applications of drugs (Figures 5B, 8, 9, and 14; also, HEPES wash-on in Fig. 6), it was desirable to begin with a baseline period showing

clear DSI. Therefore, in these experiments, cells were discarded immediately if they did not show DSI of at least 30% during the 10-min baseline period.

Drugs were purchased from Alexis (N-nitro-arginine), Biomol (2-AG, BN52021), Calbiochem (BPB, calyculin A, CaMKII peptide, catalase, ω-conotoxin GVIA, FK-506, indomethacin, NDGA, ODQ, Sn PP IX, staurosporine, trifluoperazine), ListBiolabs (BoTxA light chain, BoTxB light chain), RBI (carbachol, WIN55212-2), Sigma (ω-agatoxin TK, apamin, CPP, HEPES, TEA), and Tocris (AM251, AM404, forskolin, LY341495, (S)-MCPG, NBQX disodium). SR141716 was obtained from the National Institute on Drug Abuse.

Pyramidal cell pairs

For the experiments shown in Figure 2, we made 39 pairs of simultaneous recordings from CA1 pyramidal neurons (78 neurons); 44 of the 78 (56%) were able to induce DSI of their own IPSCs. This percentage is consistent with the finding that only a subpopulation of interneurons express CB1 (see Chapter 1). Of these 44 neurons, 26 were members of a pair where both neurons were able to produce DSI of their own IPSCs. This set of recordings was then analysed to determine under what conditions DSI might spread. The distance between neurons was defined as the distance between the tips of the two recording electrodes.

For analysis of these experiments, the amplitude threshold for IPSC detection was set at 30 pA, and thus the majority of events detected will be action potential-dependent (not miniatures). Events were detected and analyzed using Mini Analysis software (Synaptosoft); coincident events were detected using a routine custom-written in IgorPro.

Coincident sIPSCs were defined as events whose peak amplitude occurred within 7 ms of each other. A 7-ms window was chosen because longer windows did not substantially increase the frequency of calculated coincidence, whereas shorter windows did substantially decrease that frequency; also, average sIPSC rise time sometimes differed by 2-4 ms between the two cells, probably due to different series resistances. Since DSI of sIPSCs is a decrease in both frequency and amplitude of events, we express DSI here as a function of charge transfer normalized to time, i.e. the sum of the areas of all sIPSCs in a period of time divided by the number of seconds in that period. Thus, expressed as a percentage decrease,

$$\text{DSI (\%)} = 100(1-(\text{charge transfer}_{test}/\text{charge transfer}_{baseline}))$$

where the baseline period was the 20 sec immediately preceding the depolarization, and the test period was the 15 sec immediately following the depolarization.

Botulinum toxins

BoTxE, BoTxB, or BoTxA light chain (500 nM) were dissolved in the normal cesium-based electrode-filling solution along with 5 mM DTT. Recordings from both control and BoTx-filled cells were performed at 31°C to increase the rate of proteolysis. Cells which had DSI of less than 30% on the first test (1 min after break-in) were discarded immediately. For control experiments (Fig. 3B), recombinant SNAP-25 (gift of R. Scheller) was diluted to a concentration of 0.2 mg/ml in electrode-filling solution, along with 5 mM DTT and 0-500 nM BoTxE. After incubation for 60 min at 31°C, proteins were separated on a 12% polyacrylamide gel and stained with Coomassie Blue.

Preparation of recombinant BoTxE and SNAP-25 are described elsewhere (Chen et al., 1999).

Ca^{2+} uncaging

Recording electrodes were filled with a solution containing (in mM): $CsCH_3SO_3$ 100, TEA chloride 78, QX-314 chloride 5, HEPES 25, $MgCl_2$ 1, MgATP 2, Na_3GTP 0.3, nitrophenyl-EGTA (Molecular Probes) 5, CsOH, 4, $CaCl_2$ 2. Apamin (100 nM) was included in the ACSF. Internal TEA and external apamin were used to block Ca^{2+}-dependent K^+ conductances following uncaging. To uncage NP-EGTA, cells were exposed for 800 ms to UV light from a 100 W mercury burner (Olympus) passed through a 25% neutral density filter.

Glutamate iontophoresis

Borosilicate electrodes (70-100 MΩ) were filled with 1M Na^+ glutamate (pH 8-9). Electrodes were lowered into the slice under visual control and positioned approximately 20-80 μm away from the postsynaptic cell. Glutamate diffusion from the tip was controlled using a constant-current ionotophoresis instrument (WPI) with a backing current of approximately 20 nA. The position of the iontophoresis electrode and the magnitude of the ejection current were adjusted to produce a moderate, transient depression of evoked IPSCs. Large ejection currents (150-300 nA, 5-9 sec) were required to mimic the typical magnitude and time course of DSI. Once the ejection current amplitude and duration were optimized, they were fixed for the duration of the

experiment. The duration of the depolarizing step (1-5 sec) was then adjusted to produce DSI that closely mimicked the effect of the glutamate iontophoresis, and DSI tests (every 2 min) were interleaved with iontophoresis tests (every 2 min) continuously throughout the experiment.

Ca^{2+}-dependent miniature IPSCs

In experiments examining Ca^{2+}-dependent mIPSCs (Fig. 11), additional KCl (2.0-7.5 mM) was added to the ACSF at the beginning of the experiment until sIPSC frequency was at least 3 Hz. The ACSF in these experiments included high Ca^{2+} (7.5 mM total Ca^{2+}) and low Mg^{2+} (0.1 mM total Mg^{2+}) to maximize the probability of release, while high total divalents served to decrease action potential initiation. This permitted us, in DSI experiments (Fig. 11B, D), to record both action potential-dependent sIPSCs and, after addition of TTX, mIPSCs at a frequency of 3-10 Hz without changing external KCl concentrations during the course of the experiment. Phosphate was omitted from the ACSF to prevent formation of Ca^{2+} precipitates. In DSI experiments (Fig. 11B, D), cells showing DSI of eIPSCs measuring less than 30% on the first test (before addition of high external KCl) were discarded immediately. Miniature events were detected and measured using Mini Analysis software (Synaptosoft).

CB1-deficient mice

The generation of CB1-deficient mice is described elsewhere (Zimmer et al., 1999). $CB1^{+/+}$ (n=6), $CB1^{+/-}$ (n=2), and $CB1^{-/-}$ (n=5) mice were of both genders and

varied in age from 6 weeks to 8 months. Most of these animals had siblings in one of the other genetic groups of experimental animals. In all cases the experimenter was blind to genotype. The mouse was selected (according to a coin toss) and decapitated by a person other than the experimenter, in order to avoid possible behavioral indications of genotype.

Interneuron-pyramidal cell pairs

Interneurons were recorded in whole-cell current-clamp mode using electrodes filled with a solution of (in mM): K-gluconate 140, HEPES 10, EGTA 1, MgATP 4, and Na_3GTP 0.3 (pH 7.3, 275 mOsm). A constant hyperpolarizing current was used to maintain a resting potential of -60 to -70 mV. Single action potentials were elicited with 5-ms current injections sufficient to bring the cell just above threshold. Interneurons were selected for recording if their somata were <100 μm from stratum pyramidale, and do not represent a random sample of all CA1 interneurons, as we generally avoided somata in stratum lacunosum-moleculare, as well as very small or pyramidal-shaped somata. Most (77%) of the interneurons we recorded which were participating in synaptic connections had their somata in stratum radiatum. Three (2 GABA-$A_{fast\ I}$ and 1 GABA-A_{slow}) had somata in stratum oriens, and three (2 GABA-$A_{fast\ II}$ and 1 GABA-A_{slow}) had somata in stratum pyramidale. NBQX and CPP were added to the ACSF for all experiments, and so none of the connections we detected can be glutamatergic. All unitary PSCs were also observed to reverse near E_{Cl} (-18 mV), consistent with a GABA-A receptor-mediated response. Postsynaptic GABA-B receptor-mediated currents were

blocked by QX-314 and cesium in the electrode-filling solution used in pyramidal cell recordings.

Unitary IPSC rise time was measured from 20% to 80% of the peak IPSC amplitude. The falling phase of the IPSC was in all cases well-fit with a single exponential, and the decay time was expressed as τ, where current=(peak current)$e^{-t/\tau}$. The three types of connections did not differ in their average paired pulse ratios (GABA-$A_{fast\ I}$ 0.82±0.6; GABA-$A_{fast\ II}$ 0.81±0.6; GABA-A_{slow} 0.82±0.6). Paired-pulse ratios ($amp_{IPSC\ 2}/amp_{IPSC\ 1}$) were measured using an inter-pulse interval of 55 ms. For experiments testing the effects of ω-Aga-TK and ω-CTx-GVIA on unitary connections, uIPSCs were elicited continuously at 0.15-0.2 Hz, and the effects of each toxin were measured beginning 6 min after the initial application, when wash-in was complete. If application of the first antagonist (ω-CTx-GVIA or ω-Aga-TK) did not block the uIPSC completely, the other antagonist was then applied.

CHAPTER 3: Postsynaptic mechanisms of DSI

Introduction

Depolarization of a single hippocampal pyramidal neuron triggers a short-term suppression of GABAergic synaptic events recorded in that cell (Fig. 1). This phenomenon is termed "depolarization-induced suppression of inhibition", or DSI (Pitler and Alger, 1992). Postsynaptic activity initiates DSI, but DSI expression is likely presynaptic. This implies that a retrograde signal is traveling backwards across synapses to inhibit GABA release (Alger and Pitler, 1995). DSI is known to require postsynaptic Ca^{2+} (Pitler and Alger, 1992) and presynaptic G-proteins (Pitler and Alger, 1994), but the mechanism of DSI is not fully understood. It has previously been proposed that hippocampal DSI, like a related phenomenon in the cerebellum (Glitsch et al., 1996), involves retrograde signaling by glutamate (Morishita et al., 1998; Morishita and Alger, 1999).

In this study, we focus on elucidating the postsynaptic events that initiate DSI. We directly demonstrate the existence of a diffusible molecule which is released by pyramidal neurons and disinhibits a defined volume of tissue. We find that release of the retrograde signal is not blocked by botulinum toxins, specific inhibitors of membrane trafficking, suggesting that the retrograde messenger is not stored in postsynaptic vesicles. DSI can also be mimicked by flash photolysis of caged Ca^{2+} in the postsynaptic cell, implying that depolarization *per se* is not required, and that DSI does not involve an electrogenic transporter on the postsynaptic cell. Finally, we find that metabotropic glutamate receptors do not play a major role in DSI. Together, these results implicate a

retrograde messenger that is synthesized on demand when postsynaptic Ca^{2+} levels rise, and that exits the cell by diffusion or passive transport.

Results

DSI involves a diffusible signal

We began our investigation with a broad question about what sort of molecular mechanism we should imagine is involved in DSI. Previous work has suggested that retrograde signals may be either diffusible or, alternatively, tethered to the postsynaptic membrane. Integral membrane proteins in the postsynaptic cell may change synaptic strength by interacting directly, in a Ca^{2+}-dependent manner, with the extracellular domains of presynaptic proteins (Cash et al., 1996b; Tang et al., 1998; Fitzsimonds and Poo, 1998). Therefore, we began our search by asking whether the retrograde signal in DSI is able to diffuse through a volume of brain tissue; if so, then we ought to be able to observe DSI is neighboring cells which were not depolarized.

We recorded spontaneous inhibitory postsynaptic currents (sIPSCs) from pairs of CA1 pyramidal neurons 10 to 50 μm apart. Ionotropic glutamate receptor antagonists (NBQX and CPP) were present in the ACSF in all experiments to pharmacologically isolate GABAergic transmission. Depolarizing one of these two neurons (by stepping the membrane potential from -60 mV to 0 mV for 5 seconds) typically induces a depression of sIPSC frequency and amplitude lasting 10-40 seconds (Pitler and Alger, 1992). Figure $2A_1$ (cell 1) shows a representative example where depolarization suppressed sIPSCs. We found that, simultaneous with this DSI in the depolarized neuron, sIPSC frequency

and amplitude are often also depressed in the nondepolarized cell. In this example, cell 2 (Fig. $2A_2$) shows a depression of sIPSCs simultaneous with DSI in cell 1.

In total, we made 39 pairs of simultaneous recordings from CA1 pyramidal neurons (78 neurons). In these experiments, 44 of the 78 recorded neurons (56%) were able to induce DSI of their own IPSCs, signifying that these neurons were able to produce the retrograde signal and had presynaptic inputs sensitive to the signal. Of these 44 neurons, 26 were members of a pair where both neurons were able to produce DSI of their own IPSCs. This set of recordings was then analysed to determine under what conditions the retrograde signal might spread between neurons. Of these 26 neurons, 10 showed an average suppression of inhibition of at least 20% immediately after the other neuron in the pair was depolarized. We found that the degree of DSI propagation in these pairs is steeply dependent on the distance between the two neurons, with 9 of these 10 propagating pairs separated by 20 μm or less (Fig. 2B). At distances greater than ~20 μm, average DSI in the nondepolarized cell was close to zero (statistical noise can generate either small positive or negative values for DSI; see Methods, Chapter 2). The positive correlation between propagation and distance^{-1} was highly significant (r^2=0.34, DSI in nondepolarized cell versus distance^{-1}; $p<0.005$, ANOVA). These results imply that the signal generated by a single pyramidal cell can suppress GABA release from boutons within a sphere of tissue ~40 μm in diameter.

The most intuitive explanation for these results is that the retrograde signal in DSI can diffuse through the extracellular space. However, there is evidence that, in some cases, a retrograde messenger may locally initiate a regenerative signaling cascade in the presynaptic axon terminal which then propagates the depression through that axon to

other synapses (Vincent and Marty, 1993; Cash et al., 1996b). If hippocampal DSI shared this property, then the degree of propagation should depend on the degree to which the two postsynaptic neurons share some presynaptic inputs, as estimated by the percentage of sIPSCs in the two postsynaptic neurons that are coincident (the coupling index). Instead, we found that the degree of propagation is unrelated to the size of this coupling index (Fig. 2C; r^2=0.03, DSI in nondepolarized cell versus percent sIPSCs coincident, p=0.41, ANOVA). At this range (0-40 μm), the coupling index is not related to distance (r^2=0.01, percent sIPSCs coincident versus distance^{-1}, p=0.68, ANOVA), consistent with the wide arborization of hippocampal interneurons (Freund and Buzsáki, 1996). Therefore, since propagation is strongly dependent on distance and independent of shared inputs, it is unlikely that DSI is initiated via a cell adhesion molecule or other fixed transmembrane element signaling to the presynaptic cell, which would then propagate the signal throughout its axonal arborization. Rather, the retrograde signal is likely to be a molecule that diffuses through the extracellular space.

Release of the retrograde signal is non-vesicular

Next, we asked how this diffusible signal is able to exit from the postsynaptic cell. Previous work has indicated that DSI induction requires postsynaptic Ca^{2+} entry via voltage-dependent Ca^{2+} channels (Pitler and Alger, 1992; Lenz et al., 1998; Lenz and Alger, 1999). It has been proposed that DSI is mediated by glutamate or a related molecule which then acts on a presynaptic metabotropic glutamate receptor (Morishita et al., 1998; Morishita and Alger, 1999). Glutamate, or indeed any classical neurotransmitter, could be released via either of two Ca^{2+}-dependent mechanisms. First,

a small hydrophilic molecule such as glutamate could be released by Ca^{2+}-dependent vesicular fusion. Alternatively, such a molecule could be released when a depolarizing step reverses an electrogenic neurotransmitter transporter. Transporters of this class—which may pump in either direction depending on membrane voltage—include carriers for glutamate, GABA, glycine, taurine, dopamine, serotonin, and norepinephrine. Ca^{2+}-dependent kinases regulate some of these transporters (Vizi, 2000), which could explain the Ca^{2+}-dependence of DSI.

In order to investigate the role of vesicular fusion, we filled the postsynaptic cell via the recording electrode with botulinum toxin E light chain (BoTxE; 500 nM; gift of R. Scheller) while continuously monitoring DSI. BoTxE proteolytically cleaves members of the SNAP-25/23 family of SNARE proteins, which are required components of the minimal machinery necessary for all cellular membrane fusion (Weber et al., 1998). We found that the magnitude of DSI is as stable over one hour in BoTxE filled cells as in control cells (Fig. 3A; n=5 BoTxE cells, n=8 control cells; DSI magnitude normalized to initial DSI just after break-in not significantly different, t-test). This result argues against a role for vesicular fusion in releasing the retrograde signal. As a positive control, we incubated the BoTxE with recombinant SNAP-25 in the solution used for our electrophysiological recordings and monitored the efficacy of cleavage using SDS-PAGE separation of the fragments followed by Coomassie staining. The results of this experiment (Fig. 3B) show that the concentration of BoTxE used in our recordings was ten-fold greater than that sufficient to cleave virtually all the SNAP-25 in the sample within one hour. This demonstrates that the BoTxE is active, and that the composition of our electrode-filling solution did not inhibit substrate cleavage. As shown in Figure 3A,

DSI was also unaffected by BoTxB (List BioLabs), which cleaves VAMP2 (n=7 BoTxB cells, not significantly different from controls, t-test), or by BoTxA (List BioLabs), which cleaves SNAP-25 (n=6 BoTxA cells, not significantly different from controls, t-test).

Ca^{2+} is sufficient to trigger DSI

If DSI does not require vesicular fusion, the retrograde messenger could be released by reversal of an electrogenic transporter. In this case, DSI should require depolarization as an energy source for substrate efflux, and Ca^{2+} alone should not be sufficient. In order to elevate cytoplasmic Ca^{2+} while maintaining constant membrane voltage, we used a pulse of ultraviolet light to liberate Ca^{2+} from a photolabile chelator (nitrophenyl-EGTA; Molecular Probes) in the postsynaptic cell while monitoring sIPSCs. We found that the effect of depolarization (Fig. 4A) is indistinguishable from the effect of uncaging Ca^{2+} when the cell is not depolarized (Fig. 4B). Like DSI, Ca^{2+} uncaging depresses both sIPSC frequency and amplitude (Fig. 4C), and also transiently depresses evoked IPSCs (Fig. 4D). This depression is expressed at a presynaptic locus, since Ca^{2+} uncaging does not affect the amplitude of miniature IPSCs elicited by 150 mM sucrose in the presence of 1 μM TTX (measured 6 seconds after the flash, mIPSC amplitude is 97±4% of baseline amplitude, n=8; data not shown). In sum, this data indicates that Ca^{2+} is sufficient to initiate DSI and depolarization is not required. This is strong evidence that DSI does not involve an electrogenic transporter. As neither vesicular fusion nor voltage-dependent transport is required, the retrograde signal in DSI is unlikely to be a classical, hydrophilic neurotransmitter.

DSI does not require metabotropic glutamate receptors

Given our conclusion that glutamate is unlikely to find an exit from the postsynaptic cell during DSI, we then addressed the hypothesis, based on the work of other investigators (Morishita et al., 1998; Morishita and Alger, 1999), that DSI requires mGluRs. We pre-incubated slices in the novel, high-affinity, broad-spectrum mGluR antagonist LY341495 (50 μM) and performed recordings in the same concentration of the drug. We found that DSI is unaltered in LY341495-treated slices (Fig. 5A; n=10 LY341495 slices, n=10 control slices; average DSI not significantly different, t-test). We therefore reexamined the reported finding that DSI is attenuated by the broad-spectrum mGluR antagonist (S)-MCPG (Morishita et al., 1998; Morishita and Alger, 1999). As a within-cell control for the effectiveness of the antagonist, we elicited a DSI-like depression of eIPSCs by iontophoresing glutamate from a second electrode positioned near the recorded cell. In agreement with a previous report (Morishita et al., 1998), we found that (S)-MCPG (5 mM) significantly attenuates the depression of eIPSCs by glutamate (Fig. 5B; n=6; glutamate-induced depression significantly smaller in MCPG, $p<0.05$, paired t-test). However, (S)-MCPG had no effect on DSI measured in the same cells alternately with the glutamate-induced depression (Fig. 5B; DSI not significantly different in MCPG, paired t-test). In sum, our results are inconsistent with the hypothesis that mGluRs play a major role in DSI.

Discussion

In this study, we have investigated the postsynaptic mechanisms by which depolarization of a single pyramidal neuron causes reduction of GABA release onto that cell. Our results suggest that the retrograde signal in DSI has three general properties.

First, the retrograde messenger is likely to be a diffusible molecule. This is based on our observation that DSI also appears at synapses onto neurons that were not themselves depolarized. These "passive" recipients of DSI do not need to share many presynaptic inputs with the depolarized cell, suggesting that the signal does not propagate through the axons of presynaptic cells, but rather is able to move freely in the extracellular space. Since the coupling index we used (% of all sIPSCs that are coincident) is a only crude measure of shared presynaptic inputs, our results cannot eliminate a small role for the type of propagation through presynaptic axons that was proposed for cerebellar DSI (Vincent and Marty, 1993). However, we used essentially the same coupling index as Vincent and Marty, suggesting that if this measure were sensitive enough to detect a correlation under their conditions, then we ought to observe this, too. Also, it should be noted that Vincent and Marty found a strong negative correlation between the coupling index and distance (r^2=0.40), meaning that pairs of cells with a strong coupling index were generally close to each other. Thus, it is possible that the apparent requirement for presynaptic coupling merely reflects a requirement for short distances, as one would expect for a diffusible extracellular signal. By contrast, under our experimental conditions, the coupling index was not related to distance, and so these are truly independent measures. In sum, our results point to a small, diffusible molecule which can disinhibit a sphere of tissue ~40 μm in diameter.

Second, our results suggest that the retrograde signal in DSI is not stored in postsynaptic vesicles. This conclusion is based on the finding that DSI is not blocked by BoTxA, BoTxB, or BoTxE, which are specific inhibitors of vesicular trafficking (Schiavo et al., 2000). The strongest experiments of this type are probably those using BoTxE. Every cellular membrane fusion event is thought to require one member from each of three families of SNARE proteins (one VAMP, one syntaxin, and one SNAP) (Weber et al., 1998). Unlike the VAMP and syntaxin families, which each have many members, only three SNAP family members have been identified (Lin and Scheller, 2000). Of these, SNAP-25 is known to be cleaved by BoTxA (Binz et al., 1994), and murine/rat SNAP-23 is also an efficient substrate (Vaidyanathan et al., 1999). It is not known whether the recently cloned SNAP-29 is cleaved by BoTxE, but it contains a conserved BoTxE cleavage site (Steegmaier et al., 1998). Thus, it seems likely that BoTxE functions as a general inhibitor of membrane trafficking in rat neurons. However, our data cannot exclude the possibility that DSI depends on novel SNAP isoforms. We also cannot be certain that BoTx added through the recording electrode is reaching the appropriate intracellular targets. However, two previous studies using this technique showed that BoTxB inhibits processes thought to require vesicular fusion in the dendrites of pyramidal neurons—namely, LTP (Lledo et al., 1998) and stable glutamatergic transmission mediated by AMPA receptors (Lüscher et al., 1999). Thus, BoTx that enters cells in this manner appears to cleave postsynaptic SNAREs within minutes.

Third, we have shown that postsynaptic Ca^{2+} is sufficient to trigger a DSI-like phenomenon. Since uncaging-induced depression has a presynaptic locus, it is likely to

be identical to depolarization-induced depression. These results argue that the retrograde messenger is not primarily released by an electrogenic transporter.

Together, these three results place important constraints on the identity of the retrograde messenger. In principle, DSI could involve one of two possible scenarios: either (a) a preexisting molecule concentrated and trapped inside the cell is permitted to leave, or else (b) a new molecule is rapidly synthesized and exits by either passive transport or simple diffusion. Vesicular fusion and active transport are the only obvious ways that Ca^{2+}/depolarization could release a trapped molecule. As our data make these two mechanisms unlikely, we reason that scenario (b) is more plausible. These results will provide the framework for a pharmacological screen to identify the retrograde signal (see Chapter 4).

Finally, in agreement with these general conclusions, we do not find a major role for glutamate in DSI. Two broad-spectrum mGluR antagonists have no detectable effect on DSI under our experimental conditions. Although mGluRs are evidently not required for DSI, our results do not rule out the possibility that mGluRs might play a modulatory role. Indeed, recent experiments conducted by Alger and colleagues suggest that mGluR activation can enhance DSI in hippocampal slices (B.E. Alger, personal communication). Differences in experimental preparations could produce different levels of tonic mGluR activity, and hence could explain the variability in the effect of mGluR antagonists.

FIGURE 1: Examples of depolarization-induced suppression of inhibition

(A) A 5-second depolarizing step from -60 mV to 0 mV (indicated by the square step symbol) causes a transient decrease in eIPSC amplitude. Insets show raw traces before, during, and after DSI. IPSCs are inward currents due to chloride loading of the postsynaptic cell.

(B1) sIPSCs recorded in the presence of a low dose of carbachol (5 μM) are also depressed by the depolarizing voltage step. Note the decrease in both amplitude and frequency of sIPSCs.

(B2) sIPSPs recorded in current-clamp mode are similarly suppressed by a brief train of postsynaptic action potentials (20 action potentials at 20 Hz).

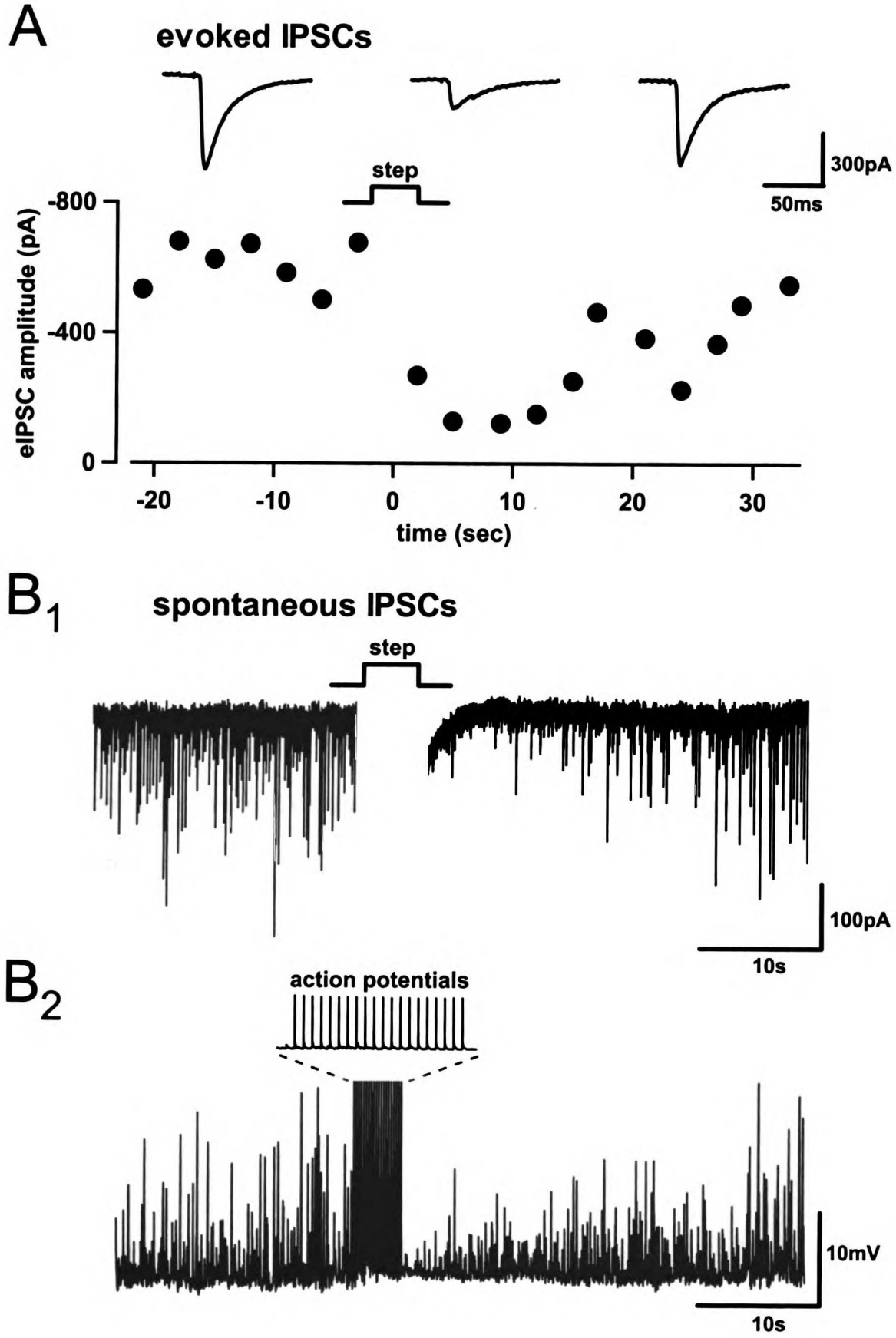
A
evoked IPSCs
300pA
50ms
step
-800
-400
0
eIPSC amplitude (pA)
-20
-10
0
10
20
30
time (sec)
B1
spontaneous IPSCs
step
100pA
10s
B2
action potentials
10mV
10s

FIGURE 2: DSI involves a diffusible retrograde messenger

(A1) Depolarizing one CA1 pyramidal neuron for 5 sec results in a transient suppression of sIPSCs (cell 1). The trace is blanked during the depolarizing step for clarity.

(A2) Meanwhile, a pyramidal cell 9 μm away (cell 2) also showed a suppression of sIPSCs, beginning about 1 sec after cell 1 was depolarized.

(B) In 13 pyramidal cell pairs, the suppression of sIPSCs in the nondepolarized cell was steeply related to its distance from the depolarized cell, with little propagation beyond 20 μm. Dotted line is a linear fit of DSI in nondepolarized cell versus distance^{-1}, graphed here with distance plotted on the x-axis.

(C) In these same pairs, the suppression of sIPSCs in the nondepolarized cell was not related to the degree of shared presynaptic input, assessed by the percent of sIPSCs in both cells during the baseline period which had a coincident event in the other cell. Dotted line is a linear fit of DSI in nondepolarized cell versus percent coincidence. Triangles are close pairs (<20 μm apart); squares are more distant pairs.

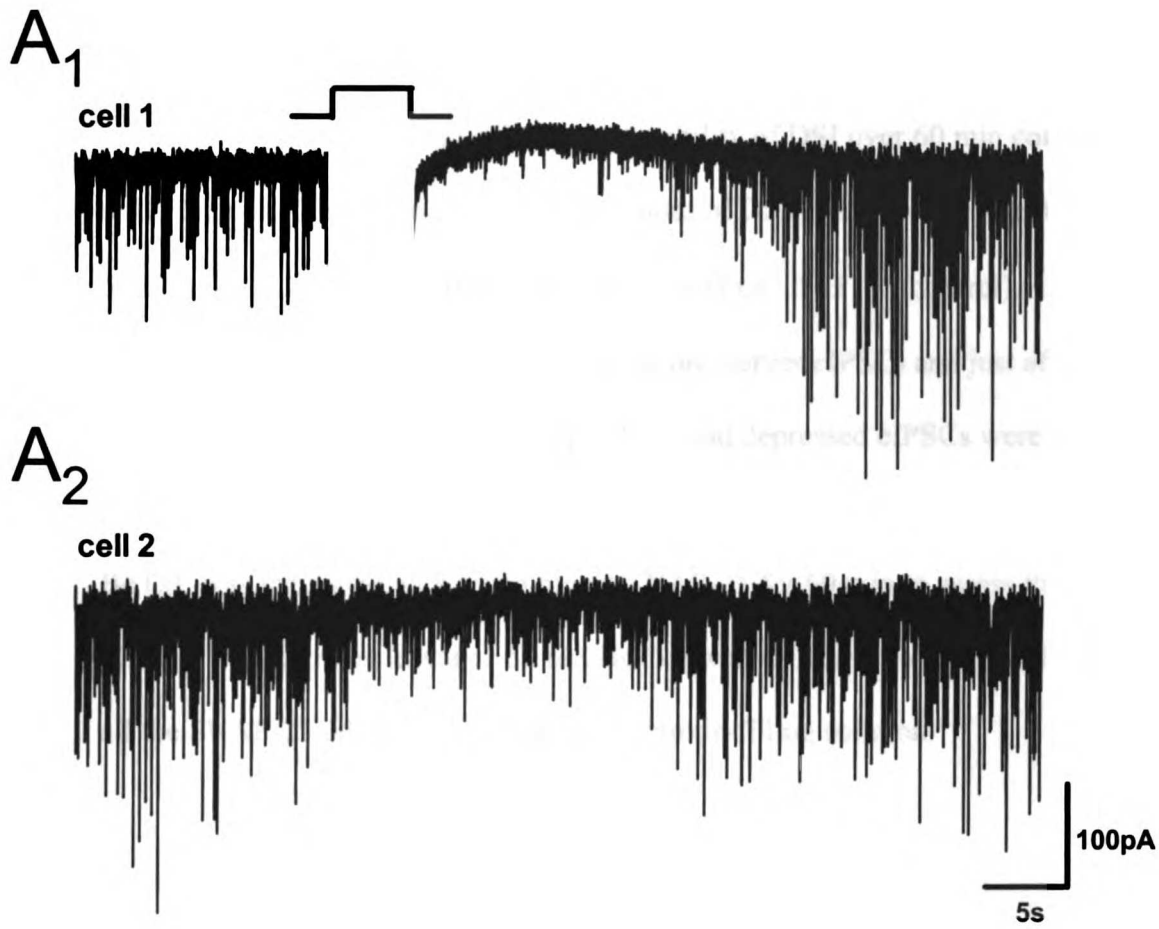
A1
cell 1
A2
cell 2
100pA
5s

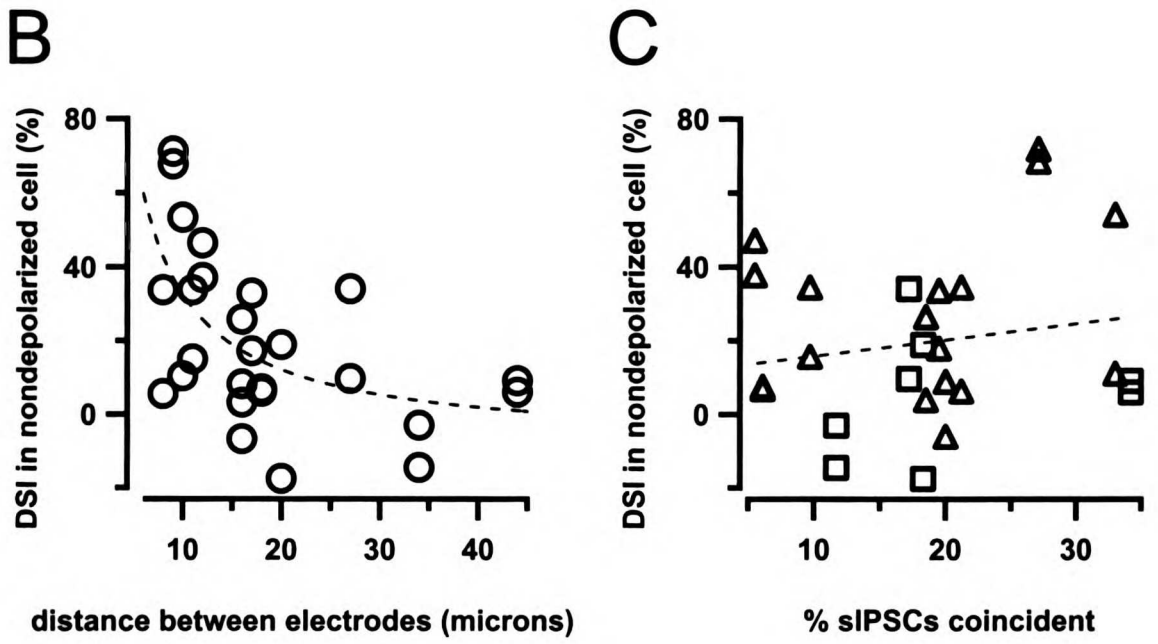
B
DSI in nondepolarized cell (%)
80
40
0
10
20
30
40
distance between electrodes (microns)
C
DSI in nondepolarized cell (%)
80
40
0
10
20
30
% sIPSCs coincident

FIGURE 3: DSI does not involve vesicular fusion in the postsynaptic cell

(A) Filling pyramidal neurons with BoTxE, BoTx B, or BoTxA (500 nM), plus the reducing agent DTT, had no effect on the stability of DSI over 60 min compared to DTT alone. The mean absolute magnitudes of DSI in these experiments were 52±3% (BoTxE), 45±3% (BoTxB), 60±2% (BoTxA), 59±7% (control). Insets show superimposed average eIPSCs just before (larger eIPSC) and just after (smaller eIPSC) the depolarizing step. Basal and depressed eIPSCs were similar just after break-in (left inset) compared to 60 min later (right inset).

(B) BoTxE was incubated with recombinant SNAP-25 for 60 min to assess the efficacy of substrate cleavage. 50 nM BoTxE was sufficient to completely cleave all the SNAP-25 diluted in a sample of electrode-filling solution.

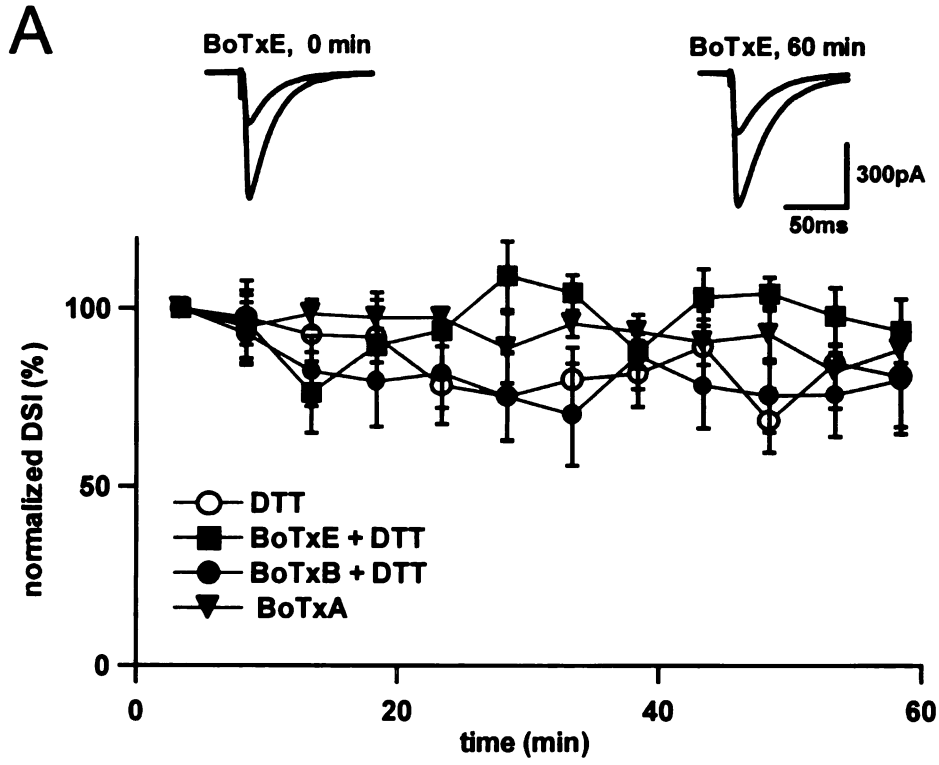
A
BoTxE, 0 min
BoTxE, 60 min
300pA
50ms
normalized DSI (%)
100
50
0
DTT
BoTxE + DTT
BoTxB + DTT
BoTxA
0
20
40
60
time (min)

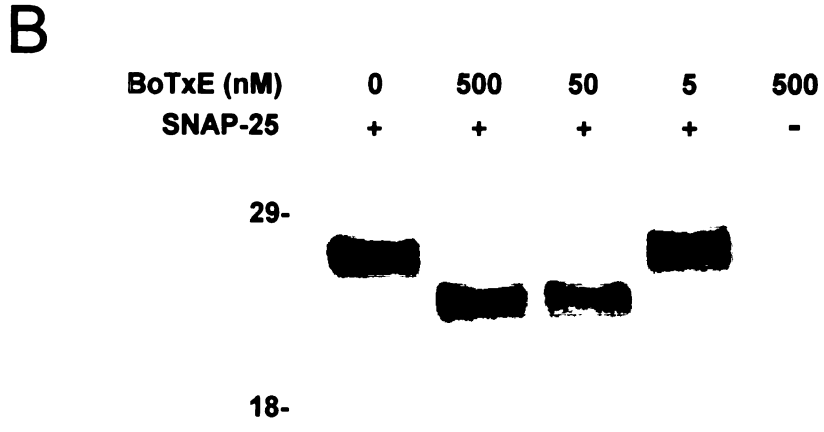
B
BoTxE (nM)
0
500
50
5
500
SNAP-25
+
+
+
+
-
29-
18-

FIGURE 4: Postsynaptic Ca^{2+} is sufficient to trigger DSI

(A) Depolarizing a pyramidal neuron results in a transient suppression of sIPSC frequency and amplitude.

(B) Flash-photolysis of caged Ca^{2+} inside a pyramidal neuron had similar effects on sIPSCs.

(C) Both sIPSC frequency and sIPSC amplitude were transiently depressed by Ca^{2+} uncaging.

(D) Representative raw traces showing eIPSC waveforms just before and just after Ca^{2+} was uncaged in the postsynaptic cell.

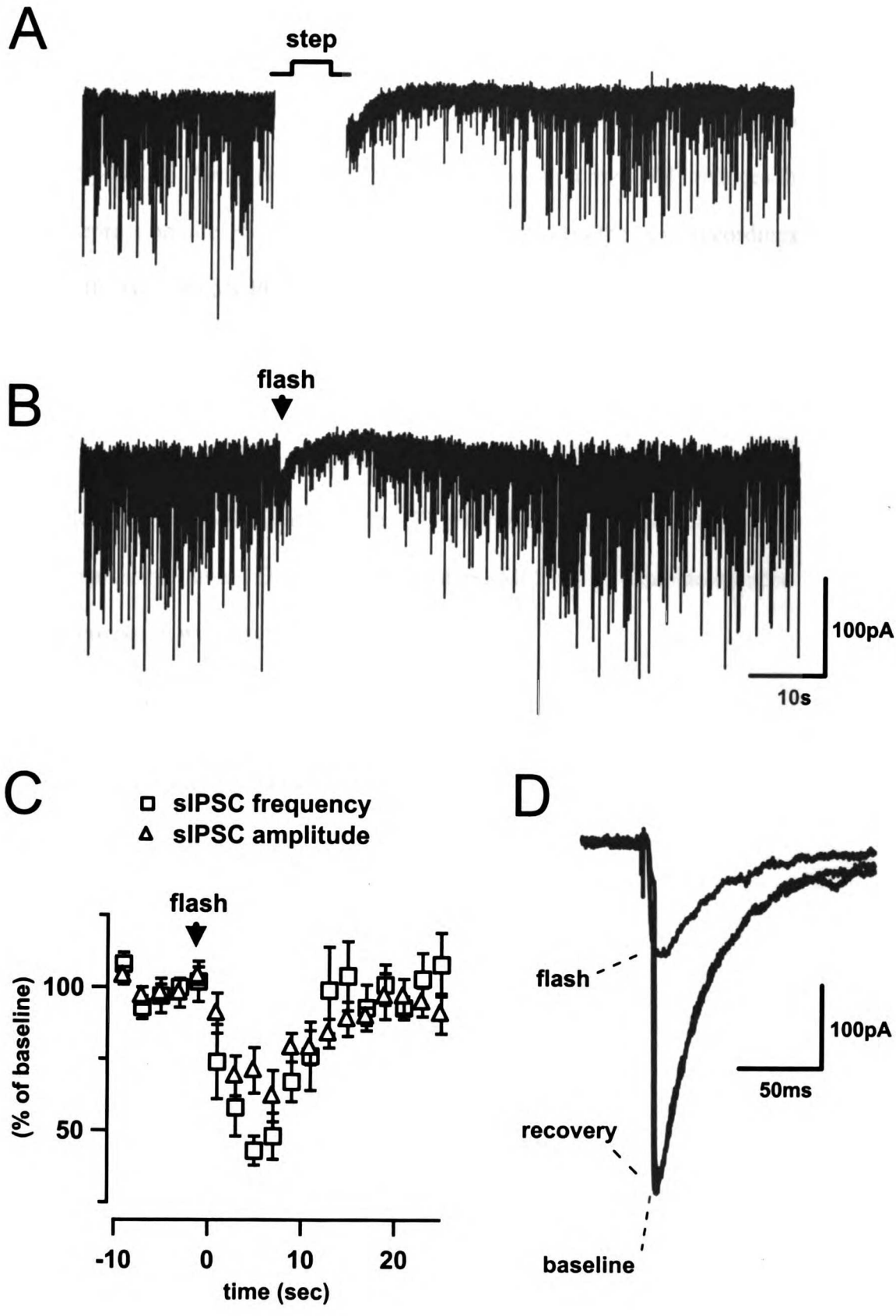
A
step
B
flash
100pA
10s
C
sIPSC frequency
sIPSC amplitude
flash
100
50
(% of baseline)
-10
0
10
20
time (sec)
D
flash
100pA
50ms
recovery
baseline

FIGURE 5: DSI does not require metabotropic glutamate receptors

(A) DSI is normal in slices pre-incubated and recorded in the broad-spectrum, high-affinity mGluR antagonist LY341495 (50 μM), compared to same-day controls.

(B1) (S)-MCPG (5 mM) does not affect DSI, although it reversibly reduces the depression of eIPSCs by iontophoresed glutamate in the same recordings.

(B2) Effects of (S)-MCPG in a representative experiment. Vertical bars represent eIPSC amplitude. Postsynaptic depolarizing steps were interleaved with glutamate iontophoresis, and the duration of depolarization and iontophoretic current were adjusted at the beginning of the experiment to produce similar depressions in eIPSC amplitude. (S)-MCPG attenuated glutamate-induced depression but not DSI. The effects of (S)-MCPG on glutamate-induced depression were reversible.

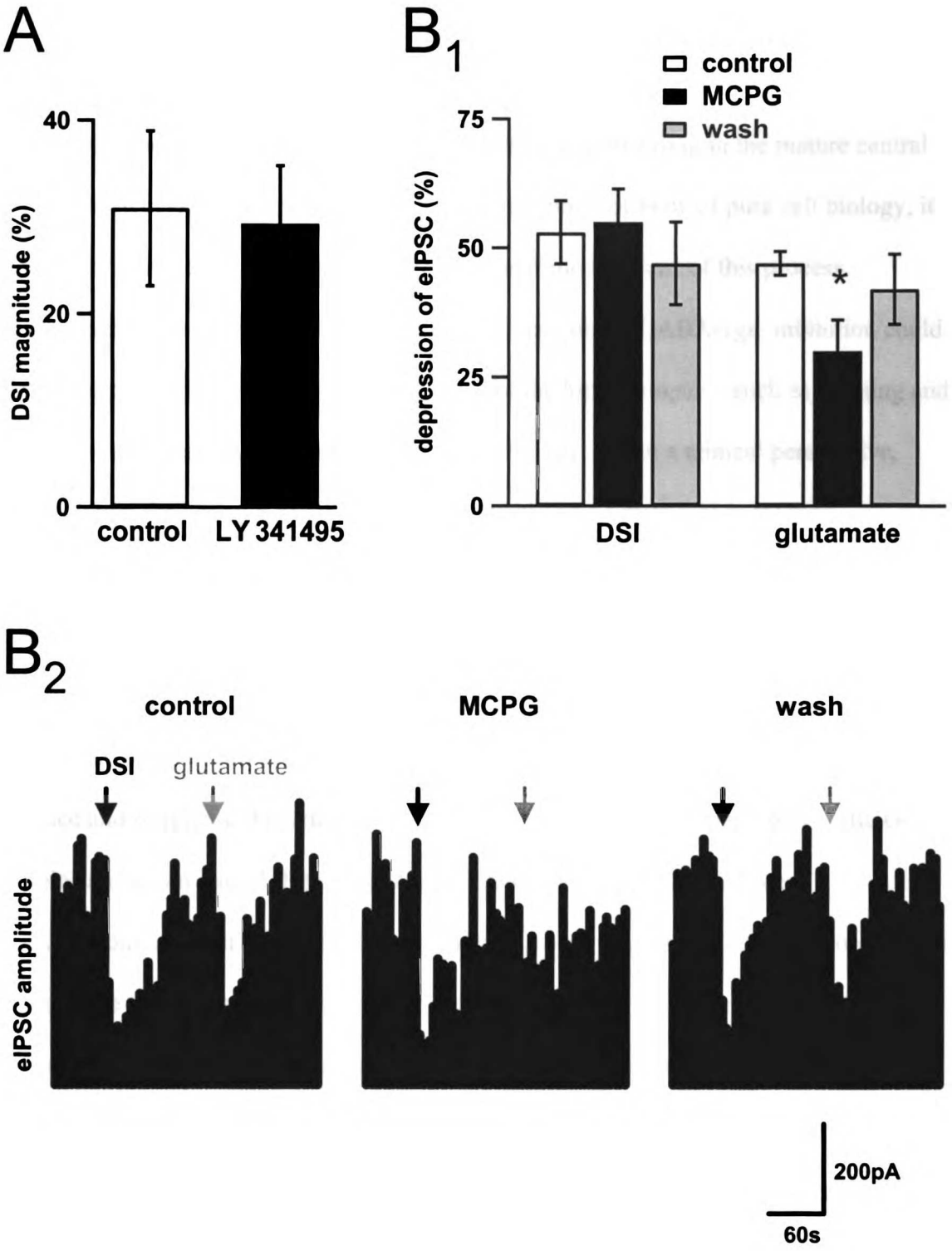
A
40
20
0
DSI magnitude (%)
control
LY 341495
B1
control
MCPG
wash
75
50
25
0
depression of eIPSC (%)
*
DSI
glutamate
B2
control
MCPG
wash
DSI
glutamate
eIPSC amplitude
200pA
60s

CHAPTER 4: Retrograde signaling by endocannabinoids

Introduction

Hippocampal depolarization-induced suppression of inhibition (DSI) may be the clearest and most compelling example of fast retrograde signaling in the mature central nervous system (Alger and Pitler, 1995). From the point of view of pure cell biology, it would therefore be of interest to identify molecular mechanisms of this process. Furthermore, activity-dependent regulation of hippocampal GABAergic inhibition could play an important role in the normal functions of the hippocampus—such as learning and memory—and possibly also in hippocampal pathology. From a clinical perspective, manipulating the strength of DSI could conceivably be a future tool in treating Alzheimer's disease or epilepsy. Here, again, naming the most important molecules in DSI—in particular, the retrograde signal itself—would be a prerequisite for further progress in this area.

The work of other investigators indicates that postsynaptic Ca^{2+} is required to produce and/or release this retrograde signal (Pitler and Alger, 1992). Presynaptic G-proteins are also required (Pitler and Alger, 1994). We have extended these investigations, and our findings (Chapter 3) have placed important constraints on the type of molecule that serves as the retrograde messenger in DSI. Specifically, the retrograde messenger is likely to be synthesized rapidly in response to a rise in cytoplasmic Ca^{2+}. Passive transport or simple diffusion probably mediate its release, and once outside the postsynaptic cell, this molecule is capable of diffusing at least ~20 μm through brain tissue.

In the experiments described in this section, we focus on identifying the primary retrograde messenger in DSI. We find that DSI is resistant to antagonists of common Ca^{2+}-dependent signaling pathways. However, DSI is almost completely blocked by antagonists of the brain-specific cannabinoid receptor-1 (CB1). Acute application of a CB1 antagonist blocks the effects of postsynaptic depolarization on IPSCs, whereas acute application of a CB1 agonist mimics and occludes DSI. A specific inhibitor of endocannabinoid uptake also mimics and occludes DSI. Furthermore, a CB1 agonist and DSI depress IPSCs by the same synaptic mechanism. Finally, DSI is completely absent in $CB1^{-/-}$ mice. These results argue that the retrograde signal in DSI is an endocannabinoid.

Results

DSI does not require common Ca^{2+}-dependent signaling pathways

We began by testing the role of common Ca^{2+}-dependent, vesicle-independent pathways in DSI. We pre-incubated slices in a variety of antagonists, and recorded (in the presence of the antagonist) from one CA1 pyramidal cell per slice to assess average DSI magnitude (Fig. 6). Recordings from control slices (incubated in the same concentration of the solvent used to dissolve the drug) were interleaved with drug-treated slices. We first focused on membrane-permeant messengers and their putative presynaptic targets. Many of these molecules have been the focus of efforts to find a retrograde signal in long-term potentiation (Williams, 1996). We find that DSI is not blocked by inhibitors of nitric oxide synthase (N-nitro-arginine, 1 mM); heme oxygenase

(Sn protoporphyrin IX, 2 μM); guanylyl cyclase, which is a common target for nitric oxide and carbon monoxide (ODQ, 10 μM); enzymes required for the synthesis of arachidonic acid or its metabolites (BPB, 50 μM; indomethacin, 25 μM ; NDGA, 50 μM); or the receptor for PAF (platelet-activating factor; BN52021, 200 μM). This suggests that DSI does not require nitric oxide, carbon monoxide, arachidonic acid, or PAF, although subtle modulatory effects would not necessarily be detected in this screen.

Next, we considered the possibility that DSI might be the consequence of Ca^{2+} clearance from the cytosol of the postsynaptic neuron. Ca^{2+} is removed from the cytosol by three major mechanisms: (1) pumping into mitochondria, (2) extrusion via the plasma membrane Na^{+}/Ca^{2+} exchanger, and (3) extrusion and sequestration by plasma membrane and endoplasmic reticulum Ca^{2+}-ATPases (Benham et al., 1992; Werth and Thayer, 1994; White and Reynolds, 1995). Mitochondrial Ca^{2+} loading produces H_2O_2 (Dugan et al., 1995; Reynolds and Hastings, 1995), which is membrane-permeant and can affect synaptic transmission (Pellmar et al., 1994). We find, however, that when we added catalase (which rapidly converts H_2O_2 to water and molecular oxygen) to the internal electrode-filling solution (4000 units/ml), DSI was unaffected even after 60 min of recording (Fig. 6). According to the second hypothesis, extrusion via the plasma membrane Na^{+}/Ca^{2+} exchanger could conceivably affect synaptic transmission by creating a local, transient decrease in extracellular $[Na^{+}]$. We prevented this pump from generating a net Na^{+} influx by replacing 120 mM Cs^{+} in the internal electrode-filling solution with 120 mM Na^{+}, which is equal to external $[Na^{+}]$. We find that DSI was not different in cells recorded using this internal solution compared to cells where 120 mM Cs^{+} had been replaced with 120 mM methylglucamine, an intert cation (compared at 30

min after break-in; Fig. 6). Finally, in the third scenario, Ca^{2+} pumping by plasma membrane Ca^{2+}-ATPases may be accompanied by alkalinization of the extracellular space (Trapp et al., 1996), which might affect neurotransmitter release. We tested this hypothesis by washing HEPES (10-20 mM; 20-35 min application) onto the slice during continuous monitoring of DSI, which should increase the pH-buffering capacity of the extracellular environment. DSI is not affected by this manipulation. In sum, these results suggest that Ca^{2+} sequestration or extrusion is unlikely to be a major component of DSI, although again small effects could have been missed in this initial screen, and Ca^{2+} clearance may have other effects which we have not considered. Finally, DSI also appears not to require the common Ca^{2+} sensor calmodulin (CaM), as DSI is unaffected by pre-incubation and recording in the CaM antagonist trifluoperazine (200 μM). DSI is also not affected after 30 min of recording when a CaM inhibitory peptide (CaM-binding domain of CaMKII; 400 μM) is included in the internal electrode-filling solution.

DSI requires cannabinoid receptors

In contrast to these negative results, DSI is virtually abolished by pre-incubating and recording from slices in AM251 (2 μM), a CB1 antagonist (Fig. 7A,B; n=14 AM251-treated slices and 17 DMSO controls; average DSI magnitudes significantly different at $p<0.005$, t-test). Similarly, SR141716 (2 μM), another CB1 antagonist, also blocks DSI (Fig. 7B; n=11 SR141716-treated slices and 10 DMSO controls; $p<0.005$, t-test). This effect is not due to some nonspecific action on postsynaptic Ca^{2+} channels, as AM251 antagonizes DSI elicited by flash photolysis of caged Ca^{2+} (Fig. 7C; n=16; average eIPSC depression significantly different from DMSO controls, $p<0.01$, t-test). These results

suggest that CB1 is required for DSI, and that an endogenous cannabinoid could be the retrograde messenger in this process.

We therefore used acute applications of a CB1 antagonist in order to investigate the mechanism by which this drug blocks DSI. In control experiments (Fig. 8A), we monitored DSI with step depolarizations every 2 min and found that the magnitude of DSI was relatively stable over 30 min (n=7). When SR141716 was applied after a 10-minute baseline period (Fig. 8B), the size of the baseline eIPSC was not affected (n=6). However, the ability of the depolarizing step to depress eIPSCs slowly diminished (average DSI at 30 min point normalized to baseline DSI was significantly less than in Fig. 8A; $p<0.005$, t-test). DSI is thus antagonized in the manner one would expect if CB1 were the target of the retrograde signal. Conversely, when the CB1 agonist WIN55212-2 is washed onto the slice (Fig. 8C; 800 nM), baseline eIPSC amplitude is depressed (n=5; $p<0.05$ vs. controls in Fig. 8A, t-test) and DSI is occluded (average DSI at 30 min point normalized to baseline DSI is significantly less than in Fig. 8A; $p<0.005$ vs. controls, t-test). Pre-incubation in AM251 blocks the depression of eIPSCs by WIN55212-2 (eIPSC amplitude 95±3 % of baseline 20 min after WIN55212-2 wash-in, n=6; data not shown; $p<0.05$ compared to slices without AM251, t-test), indicating that WIN55212-2 is probably acting on CB1.

Blocking endocannabinoid uptake occludes DSI

Next, we asked whether a natural ligand of CB1 could also mimic and occlude DSI. Exogenous 2-AG (30 μM) also depressed eIPSC amplitudes (Fig. 9A; n=6; depression is significant at $p<0.05$ vs. controls in Fig. 8A), though its effects were more

modest than those of WIN55212-2. A previous study reported that anandamide alone did not reproduce the effects of WIN55212-2 on synaptic transmission in spinal cord slices (Vaughan et al., 2000). These investigators were able to elicit a robust effect of anandamide, however, if it was applied in the presence of AM404, an antagonist of anandamide and 2-AG uptake (Beltramo et al., 1997; Piomelli et al., 1999). This suggests that in brain slices, natural CB1 ligands are rapidly removed from the extracellular space by endogenous uptake mechanisms. As a result, in our experiments, 2-AG may not have reached sufficient concentrations in the slice to fully activate CB1.

We therefore examined the effects of blocking this evidently powerful endocannabinoid uptake system. While continuously monitoring baseline eIPSCs and DSI, we washed AM404 (20 μM) onto the slice. AM404 depressed eIPSCs (Fig. 9B; n=6; $p<0.001$ vs. control data in Fig. 8A, t-test). The effects of AM404 resemble those of WIN55212-2 in that the DSI-resistant component of the eIPSC is not affected, and DSI is thus partially occluded (Fig. 9B; $p<0.05$ vs. control data in Fig. 8A). Pre-incubation of slices in SR141716 prevented the effects of AM404, indicating that the depression of eIPSCs by AM404 requires CB1 activation (Fig. 9C; n=5, $p<0.005$ vs. normalized eIPSC amplitudes in Fig. 9B, t-test). Since AM404 is not itself a CB1 agonist (Beltramo et al., 1997), the simplest explanation for these results is that AM404 is blocking the transporter required for terminating the effects of endocannabinoid release, and that when endocannabinoids are allowed to accumulate in the slice, they preclude any further DSI. Some of this progressive accumulation of endocannabinoids was due to the repeated activation of DSI, since, when we simply monitored IPSCs without depolarizing the postsynaptic cell, the effect of AM404 was smaller (eIPSC amplitude 71±5% of baseline,

n=6; data not shown; significantly smaller depression than data in Fig. 9B, $p<0.05$, t-test), though eIPSC depression by AM404 was still significant ($p<0.005$ vs. data in Fig. 8A). This suggests that hippocampal slices produce cannabinoids tonically, and that repetitive depolarization of a single pyramidal cell increases endocannabinoid production in a small region. Since SR141716 has no effect on baseline eIPSCs (Fig. 8B), tonic synthesis of endocannabinoids must be normally balanced by uptake, which keeps extracellular cannabinoid levels below that required for CB1 activation.

We also measured the kinetics of DSI decay after each depolarizing step, focusing on the period when AM404 had begun to enter the slice, but when DSI was not yet completely occluded. We found that the kinetics of DSI decay were not affected by AM404. Fig. 9D shows average eIPSC amplitude plotted versus time and fitted with a single exponential function, yielding a time constant of DSI decay τ=22.5 sec before AM404 wash-in, vs τ=21.8 sec during AM404 wash-in (a within-cell paired t-test comparison of τ was not significant, $p>0.7$). This suggests that the AM404-sensitive transporter does not clear the retrograde signal rapidly enough to affect DSI decay. The kinetics of DSI are therefore likely to reflect passive diffusion of cannabinoids away from the site of release, or else events inside the presynaptic terminal which terminate the effects of CB1 activation.

Cannabinoid receptor activation mimics DSI

If DSI is mediated by endogenous cannabinoids, DSI and WIN55212-2 must suppress GABA release by the same mechanism. We therefore looked in detail at the mechanisms of both effects. We find that the magnitude by which WIN55212-2

depresses eIPSCs varies from experiment to experiment; this is expected based on anatomical data showing that CB1 expression is limited to only a subset of interneurons (Marsicano and Lutz, 1999; Tsou et al., 1999; Katona et al., 1999). However, in those experiments where WIN55212-2 depressed eIPSCs by at least 40%, the amplitude ratio of two closely-spaced eIPSCs (the paired-pulse ratio, PPR) was significantly increased (Fig. 10A; $n=7$; $p<0.05$, paired t-test). Generally, a change in PPR is considered a hallmark of a presynaptic effect (Zucker, 1989), which is consistent with the localization of CB1 protein exclusively to the presynaptic side of GABAergic synapses in the hippocampus (Tsou et al., 1998; Tsou et al., 1999; Katona et al., 1999; Katona et al., 2000). Similar to the effects of WIN55212-2, DSI reversibly increases the paired-pulse ratio (Fig. 10B; $n=10$; $p<0.01$, paired t-test). Thus, both the CB1 agonist and DSI appear to act specifically on the presynaptic side of GABAergic synapses. Transmitter release can be suppressed either by inhibition of action potential propagation along the axon, or else by local events at the bouton which decrease Ca^{2+} influx or inhibit the vesicle release machinery. An increase in the paired-pulse ratio generally correlates with the latter scenario, a local decrease in the probability of release, p, of a vesicle from the axon terminal (Zucker, 1989; Dobrunz and Stevens, 1997).

A second method of distinguishing an effect on action potentials from a local effect at the bouton is to examine miniature IPSCs (mIPSCs) in the presence of TTX. A previous study (Hoffman and Lupica, 2000) found that WIN55212-2 did not affect mIPSCs recorded under normal (nondepolarizing) conditions. However, when KCl was added in order to depolarize presynaptic terminals and trigger presynaptic Ca^{2+} influx, these authors found that WIN55212-2 did decrease mIPSC frequency. Consistent with

this report, we also find that WIN55212-2 decreases the frequency of mIPSCs recorded in the presence of high external K^+ and Ca^{2+} (Fig. 11A,C; n=6, $p<0.005$, paired t-test). Adding the VDCC antagonist cadmium chloride to the bath further decreases mIPSC frequency (to 40 ± 12% of baseline values; $p<0.05$ vs. frequency in WIN55212-2, paired t-test; n=5), indicating that high K^+/Ca^{2+} produces some Ca^{2+}-dependent mIPSCs, and also that WIN55212-2 does not completely abolish all such Ca^{2+}-dependent events (Fig. 11A). This is not surprising, as CB1 is not expressed by all interneurons.

We then asked whether DSI, like WIN55212-2, affects Ca^{2+}-dependent mIPSCs. As a control, we first tested the effect of DSI on action potential-mediated events (sIPSCs) under these depolarizing conditions. Using the same high K^+/Ca^{2+} concentrations as before but without TTX, DSI significantly decreased sIPSC frequency (Fig. 11B; n=5; $p<0.001$, paired t-test) and sIPSC amplitude (to 87±6% of average baseline amplitude, data not shown; $p<0.05$, paired t-test). After adding TTX to the bath, depolarization decreased mIPSC frequency in the same cells (Fig. 11B,D; $p<0.005$, paired t-test). This effect on mIPSCs was comparable to the effect on sIPSCs (Fig. 11B). This result indicates that DSI, like WIN55212-2, acts locally at the presynaptic bouton. Consistent with a presynaptic locus, DSI does not affect mIPSC amplitude (100±3% of baseline mIPSC amplitude, n=5; data not shown). Thus DSI, like the CB1 agonist, appears to act locally at the presynaptic terminal to decrease *p*.

DSI is absent in CB1$^{-/-}$ mice

Given that CB1 is the only cloned cannabinoid receptor found in the brain (Matsuda et al., 1990; Munro et al., 1993), and that CB1 is strongly expressed by a subset

of hippocampal interneurons (Tsou et al., 1998; Tsou et al., 1999; Katona et al., 1999; Katona et al., 2000), it is certainly plausible that CB1 is the presynaptic target in DSI. However, endogenous cannabinoids have SR141716-sensitive actions in the cardiovascular system which are independent of either CB1 or CB2 (Wagner et al., 1999; Járai et al., 1999), suggesting that there might be an uncloned cannabinoid receptor which is sensitive to SR141716. Therefore, we used CB1-deficient mice (Zimmer et al., 1999) to determine whether hippocampal DSI is indeed mediated by CB1 activation.

The brains of $CB1^{-/-}$ mice appeared grossly normal, and hippocampi in transverse section were unremarkable. $CB1^{-/-}$ mice are reported to suffer increased mortality compared to wild-type littermates, but this difference develops gradually over adult life, and is probably the result of relatively subtle cardiovascular and immunological defects (Zimmer et al., 1999). We did not detect any major physical or behavioral defects in homozygotes during casual observations.

We began by investigating the effects of WIN55212-2 in $CB1^{-/-}$ mice (Fig. 12A). We monitored evoked inhibitory post-synaptic currents (eIPSCs) in whole-cell voltage-clamp recordings from hippocampal CA1 pyramidal cells. WIN55212-2 (800 nM) depressed eIPSCs by 21±6% in slices from $CB1^{+/+}$ and $CB1^{+/-}$ mice (n=10 +/+, 2 +/-, not significantly different from each other), compared to 0±4% in $CB1^{-/-}$ slices (n=7, $p<0.05$, t-test). This agrees with a previous study which showed that WIN55212-2 has no effect on eIPSCs recorded in dentate granule cells of $CB1^{-/-}$ mice (Hajos et al., 2000). Baclofen (3 μM) could still elicit a robust depression of eIPSCs in $CB1^{-/-}$ slices (average depression 69±9%; n=3; representative example in Fig. 12B), demonstrating that other components of presynaptic inhibition via G-proteins are still intact in these animals.

We then assessed DSI in these animals by recording from one CA1 pyramidal cell per slice, and averaging over 4-5 trials per cell during the first 10 min of recording. Using this method, average DSI magnitude in wild-type mice (32±4%, n=33) and heterozygotes (33±7%, n=9) is comparable to DSI measured in hippocampal slices from juvenile rats (Fig. 12C,D; compare with control experiments from rat slices in Figs. 5A, 6, and 7B). In $CB1^{-/-}$ mice, however, DSI is entirely absent (0.6±0.9%, n=25; $p<10^{-9}$, t-test; Fig. 12C,D). These data are strong evidence that CB1 is indeed an absolute requirement for hippocampal DSI, and is likely to be the direct presynaptic target of the retrograde signal.

Presynaptic inhibition by CB1 is likely to involve direct interaction of $G_{\beta\gamma}$ with VDCCs

Finally, having identified CB1 as the probable presynaptic target in DSI, we investigated the signaling pathway downstream from CB1. Work by other investigators has shown that, in hippocampal slices, WIN55212-2 suppresses a Ca^{2+}-dependent step in GABA release. Ca^{2+}-independent components of the release machinery are not affected. Also, the effects of WIN55212-2 can still be observed in the presence of a cocktail of K^+-channel antagonists, implying that presynaptic K^+ channels are not a CB1 target. It seems likely, therefore, that CB1 is inhibiting presynaptic voltage-dependent Ca^{2+} channels (VDCCs) (Hoffman and Lupica, 2000). We therefore asked how this inhibition of VDCCs is accomplished.

CB1 is likely to be acting via G-proteins in this context, as DSI is pertussis toxin-sensitive (Pitler and Alger, 1994). In principle, either of two mechanisms can account for inhibition of VDCCs by a G_i-coupled receptor such as CB1. First, $G_{\beta\gamma}$ can bind to and

inhibit VDCCs directly (Herlitze et al., 1996). This mechanism is sometimes called "membrane-delimited modulation" (Hille, 1992). CB1 activation inhibits VDCCs by this mechanism in a neural cell line (Mackie and Hille, 1992). A second possibility is that CB1 inhibits VDCCs indirectly, via inhibition of adenylate cyclase, leading to a downregulation of PKA (Howlett and Fleming, 1984). Potentiation of Ca^{2+} currents by PKA is well-known (Hille, 1992), and CB1 regulates K^+ channels by this pathway in cultured neurons (Mu et al., 2000).

We reasoned that if DSI is mediated by second messengers in the presynaptic bouton, then DSI should interact with pharmacological manipulations that affect kinases or phosphatases. However, we find that DSI is resistant to staurosporine (5 μM; n=5 treated, 5 control), a broad-spectrum inhibitor of serine/threonine kinases, as well as the phosphatase inhibitors FK506 (10 μM; n=6 treated, 5 control) and calyculin A (100 nM; n=6 treated, 5 control) (Fig. 13A). In agreement with other investigators (Morishita et al., 1998), we also find that DSI is unaffected by forskolin (50 μM), which activates adenylate cyclase and should interact with any process mediated by a change in cAMP levels (Fig. 13A). These results suggest that DSI probably does not require presynaptic PKA. Rather, DSI is likely to involve a direct action of $G_{\beta\gamma}$ on VDCCs by a fast, membrane-delimited pathway.

A previous study has qualitatively described a latency period before DSI onset (Pitler and Alger, 1994). We decided to examine the kinetics of DSI onset more precisely, in order to determine if they were consistent with direct inhibition of presynaptic VDCCs. Carbachol (5 μM) was added to the bath to increase the frequency of spontaneous IPSCs (sIPSCs) to 10-15 Hz (Pitler and Alger, 1992) to allow

visualization of DSI onset at higher temporal resolution, and very short depolarizing steps (100 ms) were used to elicit DSI. We observed that the depolarizing step was followed by a short delay before sIPSCs were depressed. On average, this delay lasted 1.2 seconds (Fig. 13B). This is comparable to the onset time (0.1-1.0 sec) of the membrane-delimited pathway in response to fast agonist applications (Hescheler and Schultz, 1993; Hille, 1994), and is consistent with the hypothesis that DSI also employs this mechanism.

Discussion

The experiments described in this chapter provide evidence that CB1 is required for DSI, and that endogenous cannabinoids can therefore function as rapid retrograde messengers in the nervous system. Five major results support these conclusions.

First, DSI is blocked by pre-incubation of hippocampal slices in either AM251 or SR141716. These drugs are specific antagonists of the CB1 receptor, and no other targets of these compounds have been reported (Pertwee, 1997). The small component of DSI that remains under these conditions could represent the action of a second retrograde signal, or else a postsynaptic depression of eIPSCs initiated by postsynaptic depolarization. Another possibility is that DSI is entirely dependent on CB1, and that these competitive antagonists are not completely blocking CB1 activation at these concentrations, possibly due to incomplete penetrance into the slice.

Second, acute applications of SR141716 have no effect on basal eIPSCs, but block the effects of postsynaptic depolarization on eIPSCs. This suggests that SR141716 blocks DSI by true antagonism—that is, by antagonizing the effects of the retrograde

signal. Conversely, the CB1 agonist WIN55212-2 acutely depresses basal eIPSCs while not affecting the size of the eIPSC immediately after postsynaptic depolarization. This suggests that WIN55212-2 blocks DSI by occlusion—that is, by tonically activating CB1 such that endocannabinoids have no additional effects. The action of WIN55212-2 is blocked by SR141716, implying that WIN55212-2 is indeed acting via CB1.

Third, AM404, a specific antagonist of the endocannabinoid transporter (Beltramo et al., 1997) reproduces the effects of WIN55212-2 on eIPSC and DSI. This suggests that cannabinoids produced endogenously by hippocampal neurons mimic and occlude DSI just as the synthetic agonist WIN55212-2 does. We cannot completely exclude the possibility that AM404 is acting by some other mechanism. However, these effects of AM404 on eIPSCs and DSI are entirely blocked by SR141716; this is good evidence that CB1 is involved in this process. Furthermore, AM404 is not itself a CB1 agonist (Beltramo et al., 1997), meaning that it must be working indirectly to activate the endocannabinoid system.

Fourth, WIN55212-2 and DSI depress eIPSCs by the same synaptic mechanism. We find that both WIN55212-2 and DSI increase the paired-pulse ratio, suggesting a local decrease in the probability of release at GABAergic boutons. This result disagrees with the results of a previous study, which found that PPR did not change with DSI (Alger et al., 1996). Several factors may explain this discrepancy. In contrast to Alger et al. (1996), we used a shorter inter-pulse interval (55 ms, versus 200 ms) to maximize interaction between the two eIPSCs. Also, we obtained a larger number of experiments, and we used a paired t-test to evaluate the significance of the PPR change. This is potentially an important factor, because basal PPR (before DSI) is highly variable in

hippocampal GABAergic transmission, possibly because different interneuron subtypes have different presynaptic release properties (Maccaferri et al., 2000). Thus a statistical comparison within cells (before vs. during DSI), rather than across cells, will have much better statistical resolution than an unpaired comparison. Finally, we note that under optimal conditions DSI might completely block transmission at the subset of terminals expressing CB1 and that, in these cases, a change in the paired-pulse ratio would not be expected.

We also find that, in agreement with a previous report (Hoffman and Lupica, 2000), WIN55212-2 decreases the frequency of Ca^{2+}-dependent mIPSCs. Similarly, we find that DSI also decreases Ca^{2+}-dependent mIPSC frequency. The latter result is not entirely consistent with the previous literature. One study has detected a small (12%) but statistically significant decrease in mIPSC frequency during DSI (Pitler and Alger, 1994). It is not clear what fraction of mIPSCs in the conditions of this study were Ca^{2+}-dependent. A second study by the same authors reported no change in either Ca^{2+}-independent or Ca^{2+}-dependent mIPSCs, and the reasons for this discrepancy were not discussed (Alger et al., 1996). We are uncertain of the reasons for this confusion, but we did note that the effect of DSI on Ca^{2+}-dependent mIPSCs is relatively small: mIPSC frequency decreased by only 23%. Also, the effect of DSI on action potential-dependent, sIPSCs before addition of TTX in the same cells was also small: sIPSC frequency decreased by only 25%, and sIPSC amplitude decreased by only 12%. In contrast, DSI had a much larger effect on eIPSC amplitude before additional KCl was added to the ACSF: initial average DSI in these cells was 60±4%. Although it is difficult to compare directly the magnitude of DSI using three different measures (eIPSC amplitude, sIPSC

frequency/amplitude, mIPSC frequency), it appears that elevating external [K^+] decreased the magnitude of DSI. Alger et al. (1996) used even higher external [K^+] than we did, which could also account for why DSI was not detectable in their experiments. We cannot say for certain why depolarization with high [K^+] decreases DSI, but two possibilities are plausible. For one, depolarization decreases the inhibition of VDCCs by G-proteins (Bean, 1989; Brody and Yue, 2000). Also, the mIPSCs elicited by high [K^+] are supported primarily (but not completely) by presynaptic Ca^{2+} entry through P/Q-type VDCCs, presumably because N-type VDCCs are partially inactivated in high [K^+]. We found in later experiments (Chapter 5) that DSI selectively affects interneurons that use only N-type VDCCs for GABA release; this implies that a disproportionately small fraction of mIPSCs in high [K^+] could be sensitive to DSI.

The fifth piece of evidence, and possibly the strongest single indication that endocannabinoids mediate DSI, is that DSI is completely absent in hippocampal slices from $CB1^{-/-}$ mice. We cannot exclude an indirect, developmental cause for this deficit, but this seems less likely, given that (1) $CB1^{-/-}$ mice show no obvious behavioral or neuroanatomical abnormalities, (2) GABAergic synaptic transmission is otherwise normal in $CB1^{-/-}$ mice, and (3) presynaptic depression of IPSCs by baclofen (which, like DSI, is probably mediated by direct inhibition of presynaptic VDCCs) was normal in these animals.

In sum, our results suggest that endocannabinoids function as rapid retrograde signals in the CNS. We propose a model whereby DSI is initiated when Ca^{2+} influx triggers the synthesis of endogenous cannabinoids in the postsynaptic cell. These lipids then exit the postsynaptic cell by diffusion or passive transport, and diffuse across the

synapse to bind CB1 on the presynaptic axon terminal. CB1 activation causes a down-regulation of presynaptic Ca^{2+} currents, probably via direct inhibition of VDCCs by $G_{\beta\gamma}$. As a result, GABA release is transiently inhibited.

This study represents the first description of a specific neurophysiological process mediated by endocannabinoids. It is fair to say that the basic conclusion of these experiments—that endocannabinoids function as retrograde synaptic signals—could have been predicted on the basis of CB1 anatomy and endocannabinoid biochemistry. Indeed, other investigators have speculated in the past that endocannabinoids might function as retrograde signals in the cerebellum (Lévénés et al., 1998) and at hippocampal GABAergic synapses (Egertová et al., 1998). In a sense, the major conclusions of this chapter are merely an experimental confirmation of these ideas—albeit, for us, an unexpected one.

However, although the results of these experiments could have been predicted in their general outline, they are still surprising in their particulars. Specifically, three experimental findings extend our understanding of endocannabinoids beyond the limits of previous anatomical and biochemical studies. First, our results suggest that endocannabinoids are synthesized and able to move out of cells and across synapses in less than approximately 1.2 seconds. This is still about 1000-fold slower than the kinetics of release for classical neurotransmitters. But these measurements are also much faster than the previously published upper limit of endocannabinoid synthesis (~2 minutes), which was based on biochemical techniques with poor temporal resolution (Stella et al., 1997). Second, we can now place spatial limits on endocannabinoid action. Since we can depolarize simple cells and use nearby cells as sensitive biosensors, we are

able to measure fairly precisely the limit of endocannabinoid diffusion. We find that endocannabinoids released by a single cell diffuse through a sphere of tissue about 40 μm in diameter before their concentrations fall to a level below that required to activate CB1. Again, this type of measurement was not possible given the poor spatial precision of previous biochemical experiments, which used KCl washes or electrical field stimulation to depolarize large amounts of tissue. Third and finally, our findings imply that uptake of endocannabinoids into cells by AM404-sensitive transporters is required if the rate of endocannabinoid hydrolysis by FAAH is to match the rate of synthesis. This in turn suggests that endocannabinoids may not be very membrane-permeant, and agrees with recent findings that AM404 increases the level of circulating anandamide in plasma (Giuffrida et al., 2000). It also suggests that blocking these transporters could be an effective way to potentiate the endocannabinoid system *in vivo*. Since there is only one brain cannabinoid receptor, exogenous agonists cannot provide the therapeutic benefits of Δ^9-THC without side effects such as drowsiness and confusion. However, if there were regional diversity in endocannabinoid transporter isoforms, it could be possible to selectively potentiate endocannabinoid function in specific regions of the CNS with specific transporter blockers (Piomelli et al., 2000; Christie and Vaughan, 2001). It might be possible to design such "SCRIs" (selective cannabinoid re-uptake inhibitors) that would avoid blocking hippocampal, cortical, and cerebellar transporters, for example. SCRIs would be expected to minimize cognitive and psychomotor side effects while supplying the potent analgesic and antiemetic benefits of cannabis.

FIGURE 6: DSI does not require common Ca^{2+}-dependent signaling pathways

Slices were pre-incubated in a variety of antagonists, and DSI was sampled in one pyramidal cell per slice (gray bars). DSI measurements in drug-treated slices were interleaved with measurements in slices pre-incubated in the same concentration of solvent used to dissolve the drug (white bars). Numbers in the right-hand column indicate the number of cells tested in each experimental group. None of these manipulations had any significant effect on DSI magnitude.

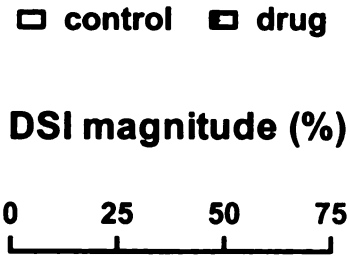

inhibitor	target	n (control/ treated)
N-nitro-arginine	nitric oxide synthase	5/6
Sn PP IX	heme oxygenase	5/7
ODQ	guanylyl cyclase	5/7
BPB+indo+NDGA	PLA_2, lipoxygenase, cyclooxygenase	8/6
BN52021	platelet activating factor receptor	4/6
catalase	H_2O_2	7/6
HEPES	protons	3/3
internal Na^+	Na^+-Ca^{2+} exchanger	3/3
trifluoperazine	calmodulin	5/5
CaMKII peptide	calmodulin	6/6

FIGURE 7: DSI is blocked by pre-incubation in CB1 antagonists

(A) In pyramidal neurons from slices pre-incubated in AM251 (2 μM), a 5-sec depolarizing step results in little or no suppression of eIPSCs, whereas interleaved solvent controls show a robust suppression. Insets show, for representative experiments, average IPSCs for the 10 sec before and 10 sec just after the depolarizing step.

(B) Summary data for the effect on DSI of AM251 and SR141716 (2 μM).

(C) Pre-incubation in AM251 also antagonizes the suppression of eIPSCs by flash photolysis of caged Ca^{2+} in the postsynaptic cell.

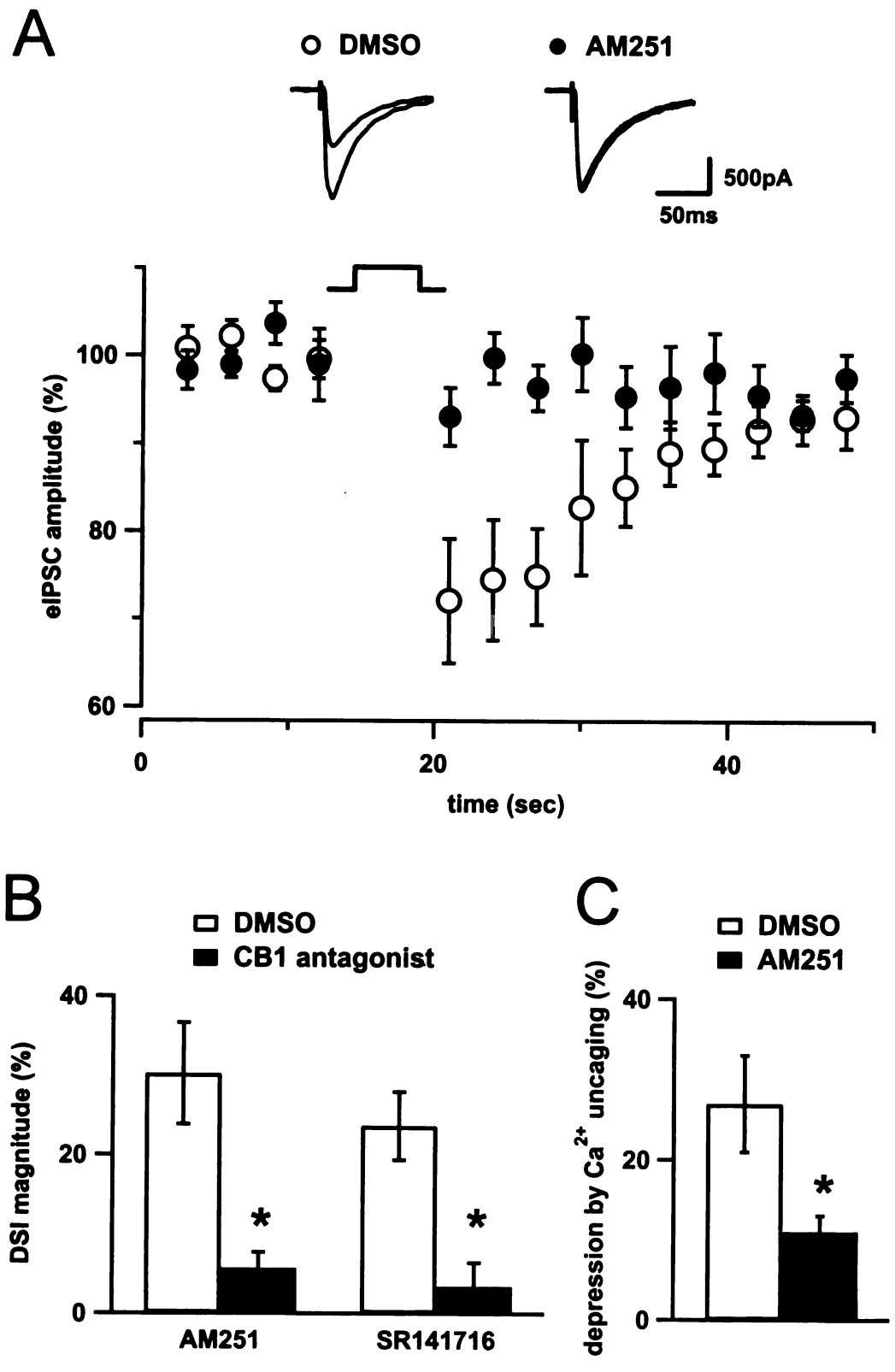
A
DMSO
AM251
500pA
50ms
eIPSC amplitude (%)
100
80
60
0
20
40
time (sec)
B
DMSO
CB1 antagonist
DSI magnitude (%)
40
20
0
*
*
AM251
SR141716
C
DMSO
AM251
depression by Ca2+ uncaging (%)
40
20
0
*

FIGURE 8: A CB1 antagonist and agonist diminish DSI by opposing mechanisms

(A) DSI is relatively stable over 30 min in control experiments. Black squares represent average eIPSC amplitudes (normalized to the 10-min baseline) just before the depolarizing step. White squares represent average eIPSC amplitudes (normalized to the same values as the black squares) just after the depolarizing step. DSI tests were performed continuously over the 30-min period. Insets show basal and depressed eIPSCs (superimposed) at the beginning and the end of representative experiments.

(B) SR141716 has no effect on basal eIPSCs, but blocks the ability of the depolarizing step to depress eIPSCs.

(C) The CB1 agonist WIN55212-2 depresses basal eIPSCs, but the DSI-insensitive component of the eIPSC is also insensitive to WIN55212-2, and DSI is occluded.

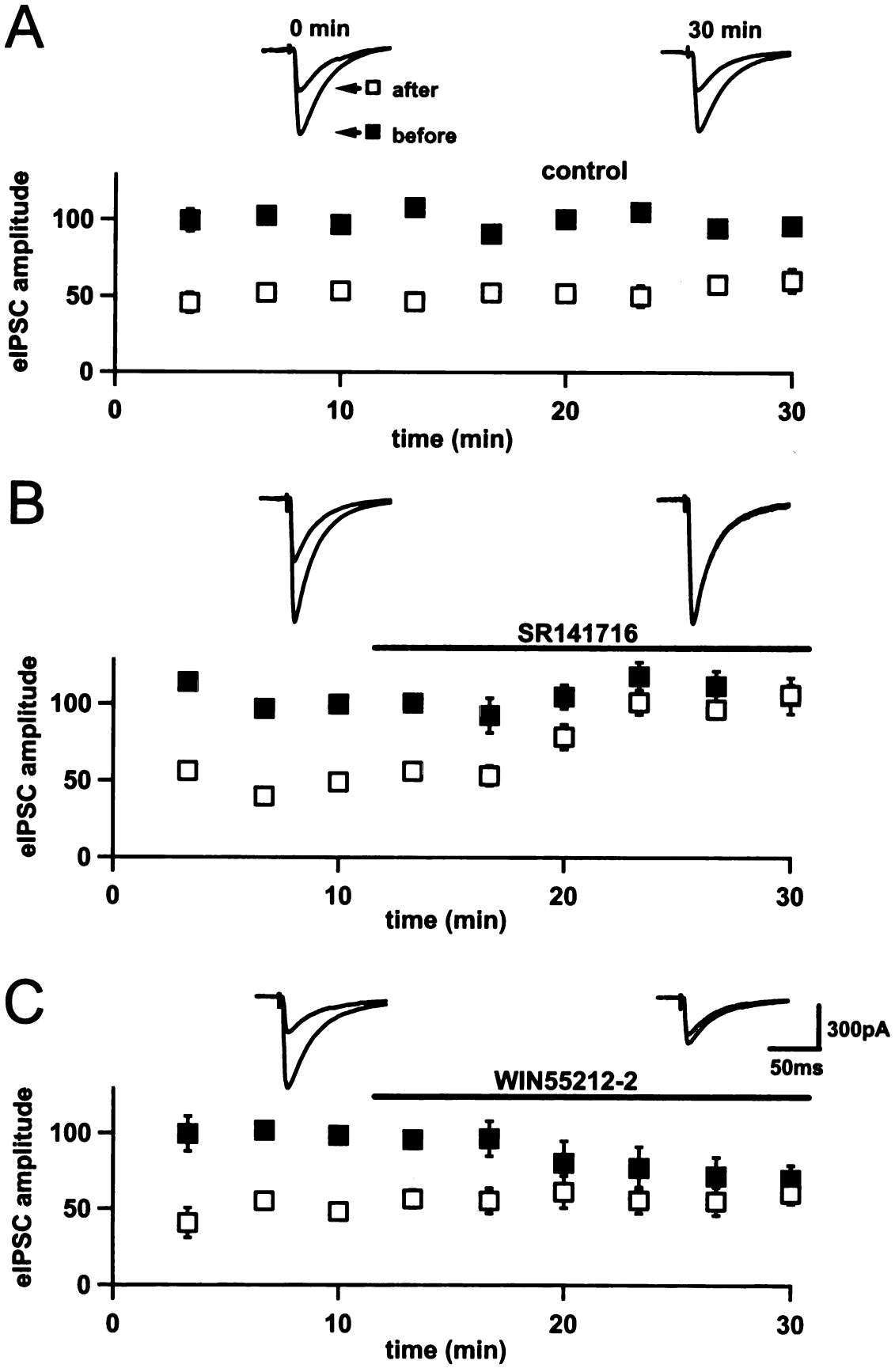
A
0 min
30 min
after
before
control
eIPSC amplitude
100
50
0
0
10
20
30
time (min)
B
SR141716
eIPSC amplitude
100
50
0
0
10
20
30
time (min)
C
300pA
50ms
WIN55212-2
eIPSC amplitude
100
50
0
0
10
20
30
time (min)

FIGURE 9: Blocking uptake of endogenous cannabinoids mimics and occludes DSI

(A) 2-AG has only a modest, although statistically significant, effect on eIPSCs, suggesting that uptake may be preventing complete penetration of 2-AG into the slice. Insets show average basal and depressed eIPSCs at 0 min and 30 min.

(B) AM404, an inhibitor of the anandamide/2-AG transporter, depresses eIPSCs and partially occludes DSI, implying that endocannabinoids produced by the slice can nearly saturate CB1 receptors if they are not transported into cells.

(C) Pre-incubation in SR141716 prevents the depression of eIPSCs by AM404.

(D) AM404 does not significantly affect the decay kinetics of DSI. Average normalized eIPSC amplitudes show the time course of DSI decay during baseline period (crosses), compared to the first 12 min of AM404 wash-in, during which DSI is being progressively occluded (dots). Lines are single-exponential fits to the data.

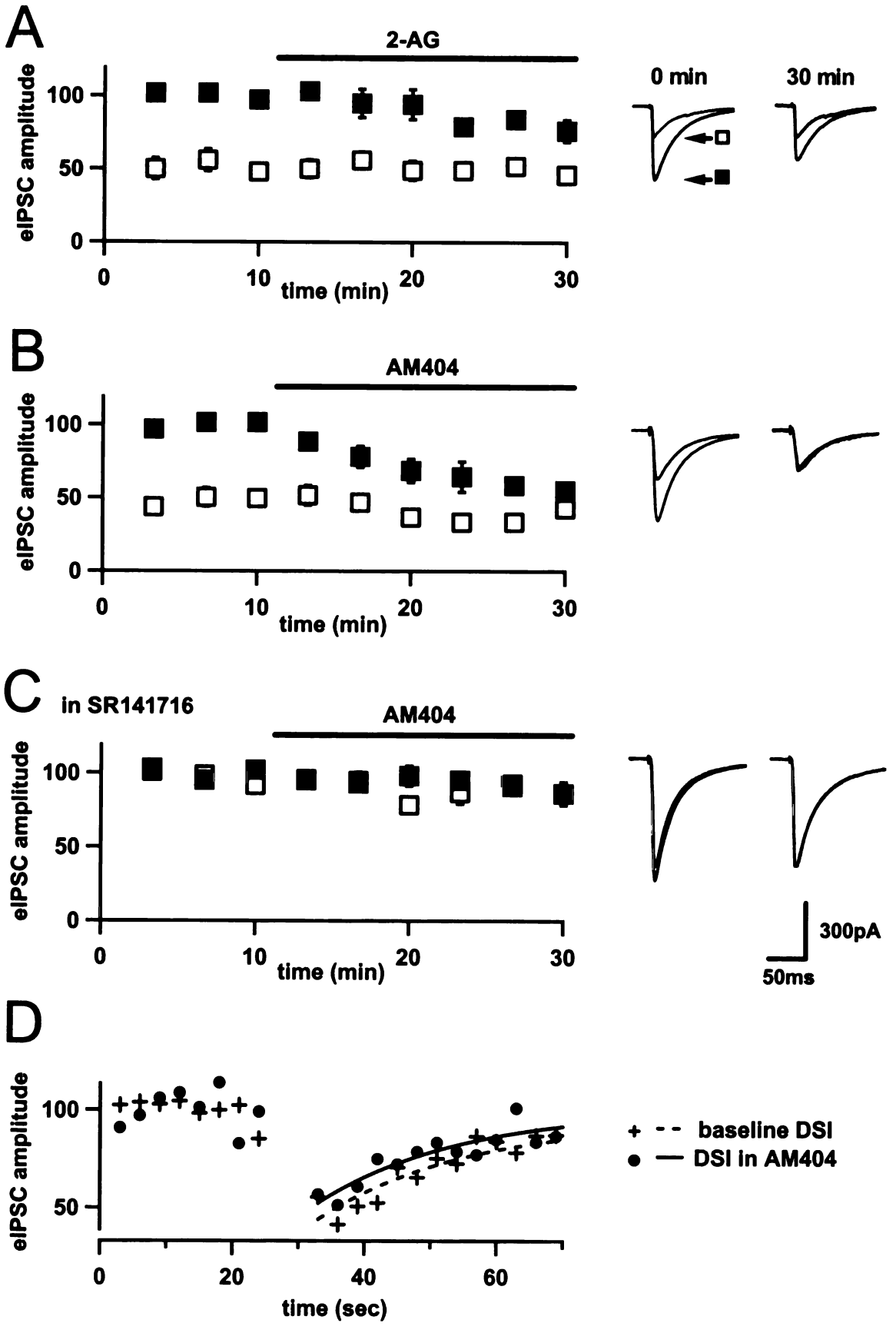
A
2-AG
0 min
30 min
eIPSC amplitude
100
50
0
0
10
20
30
time (min)
B
AM404
eIPSC amplitude
100
50
0
0
10
20
30
time (min)
C
in SR141716
AM404
eIPSC amplitude
100
50
0
0
10
20
30
time (min)
300pA
50ms
D
eIPSC amplitude
100
50
0
20
40
60
time (sec)
baseline DSI
DSI in AM404

FIGURE 10: Both WIN55212-2 and DSI cause an increase in the paired-pulse ratio

(A) In experiments where WIN55212-2 decreased eIPSC amplitude by at least 40%, the paired-pulse ratio ($amp_{IPSC\ 2}/amp_{IPSC\ 1}$) was increased. Insets (A2) show average eIPSCs during the baseline period and 20 min after WIN55212-2 wash-on.

(B) Similarly, in cells where postsynaptic depolarization decreased eIPSC amplitude by at least 30%, the paired-pulse ratio was also reversibly increased.

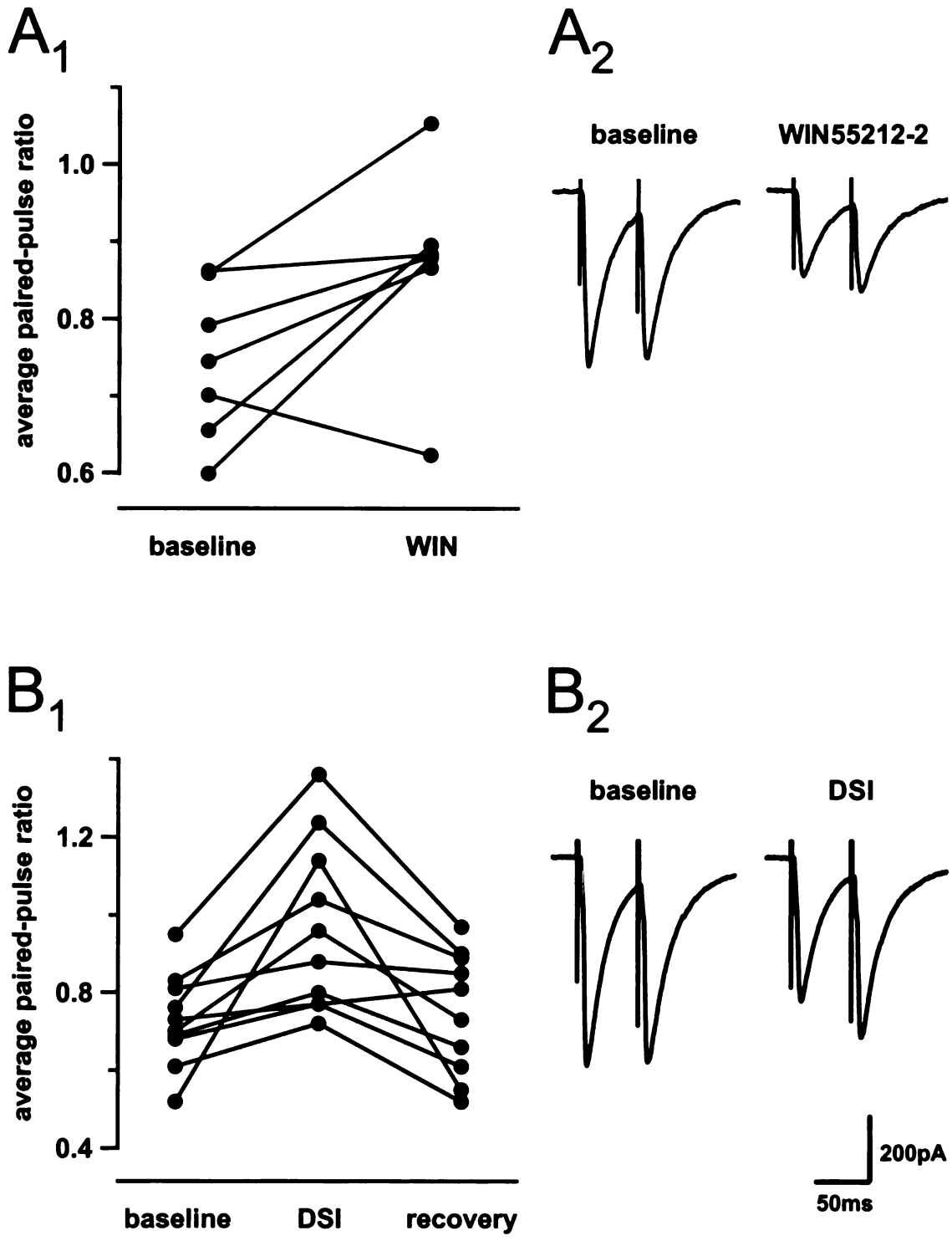
A1
average paired-pulse ratio
1.0
0.8
0.6
baseline
WIN
A2
baseline
WIN55212-2
B1
average paired-pulse ratio
1.2
0.8
0.4
baseline
DSI
recovery
B2
baseline
DSI
200pA
50ms

FIGURE 11: Both DSI and WIN55212-2 cause a decrease in the frequency of Ca^{2+}-dependent miniature IPSCs

(A) WIN55212-2 decreases the frequency of mIPSCs recorded in elevated external K^+ and Ca^{2+}. Subsequent addition of Cd^{2+} further decreases mIPSC frequency, suggesting that not all Ca^{2+}-dependent mIPSCs are sensitive to WIN55212-2. In sham experiments, where no drug was applied, there was no run-down in mIPSC frequency.

(B) DSI suppresses sIPSCs and mIPSCs to a similar degree. sIPSCs were elicited by washing on KCl (2.0-7.5 mM). DSI caused a moderate decrease in the frequency of these events (triangles). After addition of TTX, DSI caused a similar decrease in the frequency of mIPSCs (squares).

(C) Sample traces from a representative experiment showing the decrease in mIPSC frequency produced by WIN55212-2.

(D) Sample traces from a representative experiment showing the decrease in mIPSC frequency produced by DSI. Note that mIPSC amplitude is not affected by either manipulation.

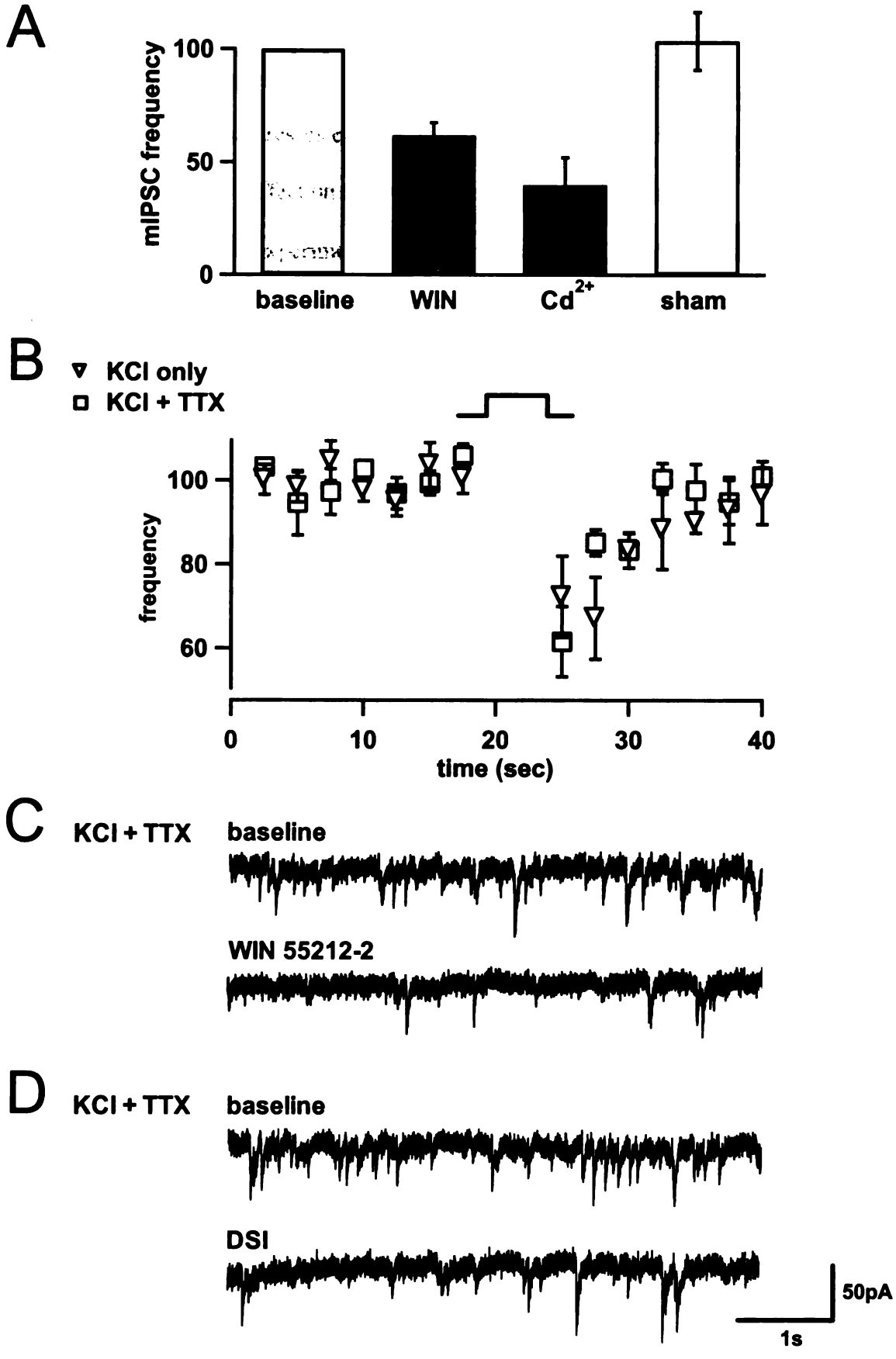
A
mIPSC frequency
100
50
0
baseline
WIN
Cd2+
sham
B
KCl only
KCl + TTX
frequency
100
80
60
0
10
20
30
40
time (sec)
C
KCl + TTX
baseline
WIN 55212-2
D
KCl + TTX
baseline
DSI
50pA
1s

FIGURE 12: Slices from $CB1^{-/-}$ mice are insensitive to WIN55212-2 and show no DSI

(A) WIN552121-2 depresses eIPSCs in CA1 pyramidal cells from $CB1^{+/+}$ and $CB1^{+/-}$ mice, but has no effect on eIPSCs in slices from $CB1^{-/-}$ mice.

(B) A representative experiment showing that baclofen (3 μM) elicits a robust depression of eIPSCs in $CB1^{-/-}$ mice, demonstrating that presynaptic inhibition by GABA-B receptors is intact in the mutant animals.

(C) DSI is normal in $CB1^{+/+}$ and $CB1^{+/-}$ mice, but completely absent in $CB1^{-/-}$ mice. DSI was measured during the first 10 sec after depolarization, averaged across 4-5 trials per sampled cell. DSI for each genotype is averaged across all cells tested. Insets show eIPSCs from representative experiments for each genotype, with basal and depressed eIPSCs overlaid.

(D) Average time course of eIPSC amplitudes after depolarization in $CB1^{+/+}$, $CB1^{+/-}$, and $CB1^{-/-}$ mice. Square step indicates 5-sec depolarization from -60 mV to 0 mV.

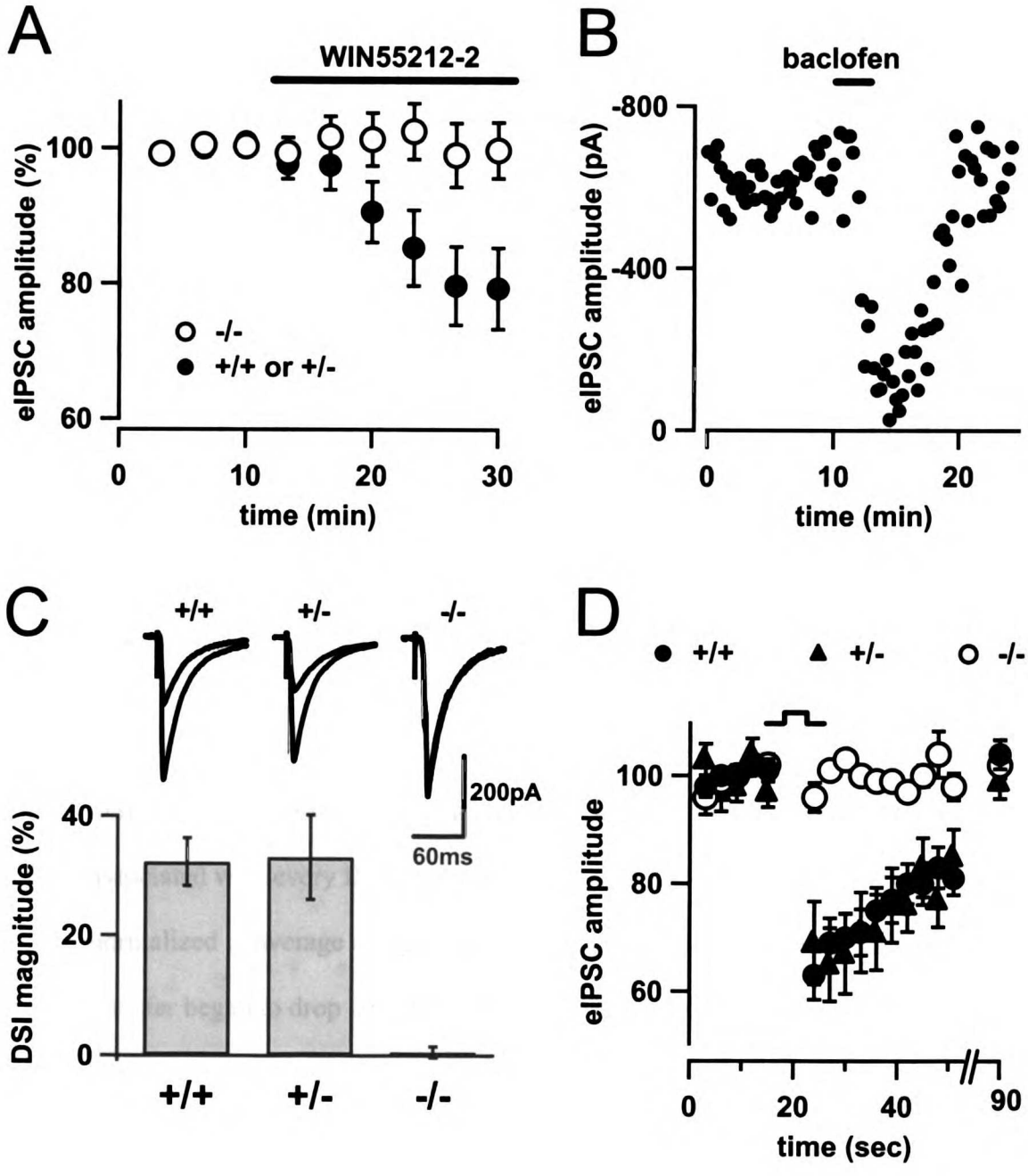
A
WIN55212-2
eIPSC amplitude (%)
100
80
60
-/-
+/+ or +/-
0
10
20
30
time (min)
B
baclofen
eIPSC amplitude (pA)
-800
-400
0
0
10
20
time (min)
C
+/+
+/-
-/-
200pA
60ms
DSI magnitude (%)
40
20
0
+/+
+/-
-/-
D
+/+
+/-
-/-
eIPSC amplitude
100
80
60
0
20
40
90
time (sec)

FIGURE 13: Presynaptic inhibition by endocannabinoids is likely to involve direct interaction of G-proteins with calcium channels

(A) DSI is not affected by staurosporine (5 μM), a broad spectrum kinase inhibitor, or the phosphatase inhibitors FK-506 (10 μM) or calyculin A (100 nM). DSI is also not affected by forskolin (10 μM), which activates adenylate cyclase. Slices were pre-incubated and recorded in either the drug or a solvent control, and DSI was sampled in one cell per slice.

(B) Kinetics of DSI onset are rapid. Spontaneous IPSCs elicited by carbachol (5 μM) are transiently suppressed following a 100-ms depolarization from -60 mV to 0 mV (arrow). Eight sweeps representing individual DSI trials from a single cell are overlaid to show the average time course of DSI (B1). The region surrounding the depolarizing step is displayed below on an expanded time scale (B2) to illustrate the short latency between the step and suppression of synaptic activity.

(C) Group data showing average kinetics of DSI onset. Spontaneous IPSCs from 37 DSI trials (4 cells) were detected and measured, and the total charge transfer associated with every IPSC was summed within 200-ms bins, and then normalized to average charge transfer during the baseline period. Overall, charge transfer began to drop about 1.2 sec after the start of the depolarizing step. Gray bar (in B2-C) indicates 100-ms depolarization.

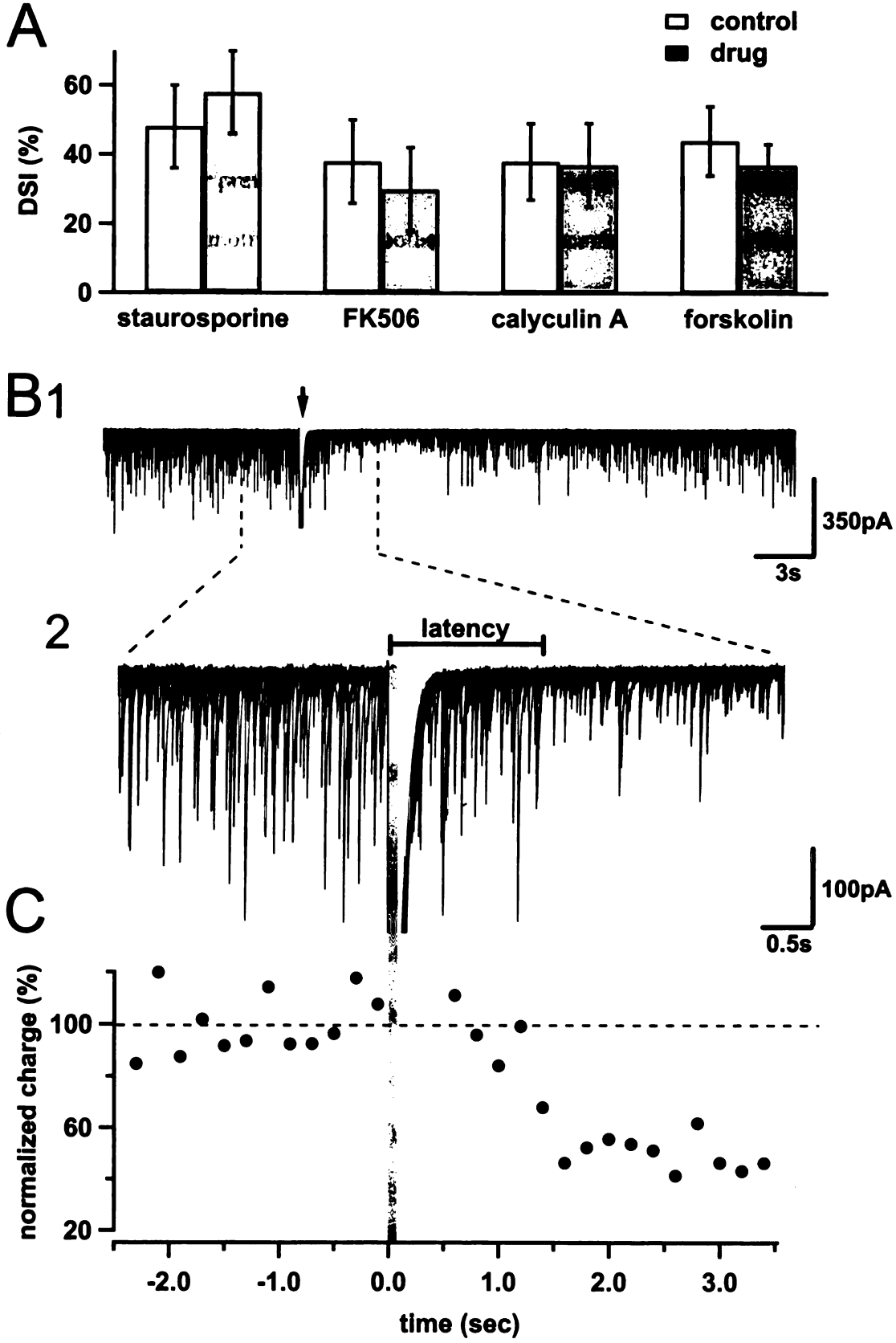
A
control
drug
DSI (%)
60
40
20
0
staurosporine
FK506
calyculin A
forskolin
B1
350pA
3s
2
latency
100pA
0.5s
C
normalized charge (%)
100
60
20
-2.0
-1.0
0.0
1.0
2.0
3.0
time (sec)

CHAPTER 5: Presynaptic specificity of retrograde signaling by endocannabinoids

Introduction

Results of our previous experiments (Chapters 3 and 4), together with other published data, have motivated the hypothesis that endocannabinoids function as retrograde messengers at hippocampal GABAergic synapses. According to this model, this process begins when postsynaptic depolarization opens voltage-dependent Ca^{2+} channels (Pitler and Alger, 1992; Lenz et al., 1998). Cytoplasmic Ca^{2+} then triggers the synthesis of endocannabinoids, possibly anandamide and/or 2-arachidonylglycerol (Di Marzo et al., 1998b; Piomelli et al., 1998), which exit the postsynaptic cell by an unknown mechanism, either simple diffusion or passive transport. Endocannabinoids then diffuse backwards across the synapse to activate CB1. Cannabinoid receptor activation then leads to a decrease in the probability of release of a vesicle of neurotransmitter from the axon terminal. This is likely to be due to inhibition of VDCCs (Hoffman and Lupica, 2000) by direct interaction with $G_{\beta\gamma}$.

In the hippocampus, CB1 is only expressed by GABAergic interneurons (Mailleux and Vanderhaeghen, 1992; Matsuda et al., 1993; Marsicano and Lutz, 1999; Tsou et al., 1998; Tsou et al., 1999; Katona et al., 1999; Egertová and Elphick, 2000; Hajos et al., 2000; Katona et al., 2000). Accordingly, hippocampal depolarization-induced suppression of inhibition (DSI), which we hypothesize is mediated by endocannabinoids, selectively affects GABAergic but not glutamatergic transmission (Pitler and Alger, 1992; Wagner and Alger, 1996). Together, these data suggest that the function of hippocampal endocannabinoids may be to regulate GABA release.

GABAergic interneurons in the hippocampus serve three important functions—regulating global excitability, coordinating oscillatory ensemble firing of pyramidal neurons, and controlling the threshold for induction of long-term synaptic plasticity. Several subtypes of hippcampal interneurons have been described on the basis of morphological, immunohistochemical, and physiological criteria; these different subtypes are thought to play distinct roles in these processes (Freund and Buzsáki, 1996; Buzsáki, 1997). CB1 expression appears to be limited to one subtype of interneurons, as hippocampal CB1 always co-localizes with cholecystokinin expression and never with parvalbumin expression (Tsou et al., 1999; Katona et al., 1999). However, since the functions of cholecystokinin and parvalbumin are still poorly understood, these molecules serve mainly as immunohistochemical markers, and do not say much about the functional role of this interneuron subclass (Freund and Buzsáki, 1996).

In the experiments described in this chapter, we focus on describing the physiological properties of endocannabinoid-sensitive GABA release. First, we find that an antagonist of N-type Ca^{2+} channels eliminates both DSI and the effects of WIN55212-2 on eIPSCs. Conversely, an antagonist of P/Q-type Ca^{2+} channels potentiates both DSI and the effects of WIN55212-2. We use paired recordings of single interneuron-pyramidal cell connections to determine whether this specificity reflects a highly selective inhibition of N-type over P/Q-type channels within boutons, or whether only N-type channels are present at CB1-positive synapses. Paired recordings show that DSI-sensitive synapses are distinguished by their fast synaptic kinetics and large synaptic conductance. Also, interneurons that make these connections have a significantly smaller after-hyperpolarization than DSI-insensitive interneurons, consistent with their likely

identification as basket cells. Finally, we find that these interneurons indeed use only N-type Ca^{2+} channels for transmitter release. These results suggest that endocannabinoids are specific inhibitors of a physiologically distinct class of interneurons displaying unusual presynaptic specialization. We suggest that the exclusive use of presynaptic N-type channels by these neurons could help explain why endocannabinoids are able to inhibit GABA release at these synapses so profoundly, and we hypothesize that the fast kinetics of these synapses means that endocannabinoids could function as regulators of fast "gamma"-band oscillations.

Results

Differential involvement of presynaptic VDCC subtypes in endocannabinoid signaling

GABA release from hippocampal interneurons is mediated by both N and P/Q subtypes of VDCCs in the presynaptic terminal (Doze et al., 1995). According to a previous report (Lenz et al., 1998), DSI is blocked by a specific antagonist of N-type channels, ω-conotoxin GVIA (ω-CTx-GVIA). This was interpreted as a postsynaptic requirement for N-type channels as the mediators of the depolarization-evoked, postsynaptic calcium spike which triggers DSI. We wondered whether DSI might require N-type VDCCs presynaptically.

We monitored eIPSC and DSI while washing ω-CTx-GVIA (250 nM) into the bath. ω-CTx-GVIA irreversibly depressed eIPSCs by 74±9% (Fig. 14A; n=4), and abolished DSI (Fig. 14A,C; DSI significantly decreased, $p<0.005$ vs. baseline DSI magnitudes, paired t-test). Surprisingly, ω-CTx-GVIA also blocked the depressant

effects of WIN55212-2 (Fig. 14A,D; significantly smaller effect of WIN55212-2 on eIPSCs than under control conditions, $p<0.05$, t-test; n=17 control experiments, control time course not shown). This result suggests that there may be a presynaptic requirement for N-type calcium channels in the regulation of GABAergic transmission by cannabinoids.

We then repeated these experiments using ω-agatoxin TK (ω-Aga-TK), a selective antagonist of P/Q-type calcium channels. ω-Aga-TK (250 nM) irreversibly depressed eIPSCs by 70±6% (Fig. 14B; n=5). In agreement with a previous report (Lenz et al., 1998), ω-Aga-TK actually increased the magnitude of DSI (Fig. 14B,C; significantly larger DSI vs. baseline DSI magnitudes, $p<0.005$, paired t-test). Previous investigators had considered this apparent potentiation of DSI to be an artifact; however, based on our results with ω-CTx-GVIA, we suspected that ω-Aga-TK might be acting presynaptically to remove a component of GABA release that is insensitive to DSI. Consistent with this hypothesis, eIPSCs in the presence of ω-Aga-TK were extremely sensitive to WIN55212-2 (Fig. 14B,D; significantly larger effect of WIN55212-2 than under control conditions, $p<0.05$, t-test).

Cannabinoid-sensitive and -insensitive interneurons have distinct synaptic properties

The differential involvement in DSI of two types of presynaptic VDCCs suggests two possible scenarios. One possibility is that CB1 is expressed on GABAergic terminals that use both N- and P/Q-type calcium channels for transmitter release, but that CB1 activation affects only the N-type channels in those terminals. It seems likely that there are at least some GABAergic terminals having both types of channels, since the

algebraic sum of the effects of ω-CTx-GVIA and ω-Aga-TK (144%) exceeds 100%, attributable to the supralinear relationship between calcium influx and neurotransmitter release (Dodge and Rahamimoff, 1967). Selective presynaptic inhibition of N-type versus P/Q-type channels by G-protein coupled receptors has been reported at excitatory synapses in the hippocampus, where these channel subtypes are colocalized in the same presynaptic boutons (Wu and Saggau, 1994). An alternative possibility is that CB1 is expressed on a subpopulation of terminals that use only N-type channels for transmitter release. Indeed, two studies of GABAergic connections among cultured hippocampal neurons (Ohno-Shosaku et al., 1994; Poncer et al., 1997) found that some interneurons use only N-type channels for transmitter release, whereas others use only P/Q-type channels.

In order to distinguish between these two hypotheses, we recorded from connected interneuron-pyramidal cell pairs in the CA1 region. Interneurons were recorded in whole-cell current-clamp mode, and presynaptic action potentials were elicited by brief (5 ms) current injections. We recorded from 343 interneuron/pyramidal cell pairs; we detected an interneuron-to-pyramidal cell synaptic connection in 30 of these. We found that unitary IPSCs (uIPSCs) recorded in these connections varied considerably in their kinetics, generating a bimodal histogram of uIPSC rise times (Fig. 15A,D). We termed these two groups GABA-A_{fast} and GABA-A_{slow}, following the convention established by a previous study (Pearce, 1993). GABA-A_{fast} inputs also had faster time constants of decay (19±1 ms) than GABA-A_{slow} inputs (40±4 ms). These kinetic differences cannot be explained by higher access resistance in GABA-A_{slow} recordings (R_{access}=13±1 MΩ for GABA-A_{slow}, compared to 16±2 MΩ for GABA-A_{fast}).

Also, cable filtering, which should produce a smooth distribution, seems unlikely to account for all of the kinetic differences we observed. In this respect, our data agrees with evidence that these two groups of synapses use different GABA-A receptors, which could account for the bimodal distribution, with few synapses showing intermediate kinetics (Pearce, 1993).

We also observed a bimodal distribution of connections in terms of their DSI susceptibility (Fig. 15B,D). One group of connections were strongly depressed by postsynaptic depolarization (average DSI 88±5%, n=7 connections). All of these connections had fast rise times (1.6±0.2 ms) and are termed here GABA-$A_{fast\ I}$. The other population of connections with fast kinetics, which we termed GABA-$A_{fast\ II}$ (average rise time 1.5±0.2 ms) were completely insensitive to DSI (average DSI -6±5%, n=8 connections). All GABA-A_{slow} connections were resistant to DSI (average DSI 1±2%, n=14 connections). GABA-$A_{fast\ I}$ inputs were also distinguished by their large uIPSC amplitudes compared to GABA-$A_{fast\ II}$ ($p<0.005$, t-test) and GABA-A_{slow} ($p<0.0005$, t-test) (Fig. 15C,D).

Cannabinoid-sensitive and -insensitive interneurons have distinct intrinsic properties

We also examined the intrinsic excitability profile of these interneurons. Consistent with previous work (Parra et al., 1998), we found a large diversity in excitability profiles which does not seem to map perfectly onto other physiological properties. Each of the three groups included several types of action potential waveforms (Fig. 16A1) and discharge patterns (Fig. 16A2). On average, however, interneurons forming GABA-$A_{fast\ II}$ connections were able to fire at a higher maximum initial rate than

the other types of connections, and showed significantly less accommodation (Fig. 16A2,B). We also noted that GABA-$A_{fast\ I}$ interneurons had significantly smaller after-hyperpolarizations (9±1 mV) than GABA-$A_{fast\ II}$ (17±2 mV; $p<0.05$, t-test) or GABA-A_{slow} (17±1 mV; $p<0.005$, t-test) interneurons (Fig. 16A1).

Cannabinoid-sensitive interneurons use only N-type Ca^{2+} channels for GABA release

In a subset of these connections where uIPSC amplitude was at least 10 pA and relatively stable, we were able to examine the involvement of different VDCC subtypes in GABA release. All GABA-$A_{fast\ I}$ synapses that we tested were completely blocked by ω-CTx-GVIA (Fig. 17A,D; 99±0.4% block; n=4). When ω-Aga-TK was washed in prior to ω-CTx-GVIA, it had no effect on the uIPSC (0±9%; n=2). Conversely, all GABA-$A_{fast\ II}$ synapses were completely blocked by ω-Aga-TK (Fig. 17B,D; 99±0.3% block; n=5) but insensitive to ω-CTx-GVIA (0±8%, n=3). Finally, all GABA-A_{slow} connections relied on both N- and P/Q-type channels in roughly equal proportions (Fig. 17C,D). When ω-CTx-GVIA was washed on first, it blocked these synapses by 71±3%, and subsequent addition of ω-Aga-TK blocked 96±4% of the remaining response (n=3). When ω-Aga-TK was washed on first, it blocked GABA-A_{slow} synapses by 68±7%, and subsequent addition of ω-CTx-GVIA blocked 97±1% of the remaining response (n=3). The magnitude of the depression caused by a given toxin was significantly different for each of the three groups (for all six comparisons $p<0.01$, t-tests).

Discussion

Anatomical studies have demonstrated that CB1 receptors are expressed by a subclass of hippocampal interneurons that arborize mainly in stratum pyramidale, and to a lesser extent in radiatum close to pyramidale (Tsou et al., 1998; Katona et al., 1999; Hajos et al., 2000; Katona et al., 2000). This is also the class of interneurons which release the neuromodulatory peptide cholecystokinin (CCK) (Tsou et al., 1999; Marsicano and Lutz, 1999). These interneurons have been classified as basket cells by morphological criteria; another class of basket cells (expressing the immunocytochemical marker parvalbumin) is CB1-negative. Consistent with the anatomical restriction of CB1 expression, prior investigators have also shown that individual GABAergic connections show marked differences in their sensitivity to DSI (Alger et al., 1996) and to WIN55212-2 (Hajos et al., 2000).

Using paired recordings in acute slices, we now have extended these investigations to demonstrate that the hippocampal endocannabinoid system targets a subclass of interneurons with distinctive physiological properties. First, these interneurons form powerful connections with their postsynaptic targets, generating uIPSCs that are on average four-fold greater than the cannabinoid-insensitive connections. Thus cannabinoid signaling is likely to play a more important role in hippocampal function than the relatively small number of CB1-immunopositive interneurons would suggest.

Second, cannabinoid-sensitive interneurons generated uIPSCs with fast kinetics. These connections, together with a group of cannabinoid-insensitive fast synapses, probably represent the group of furosemide-sensitive synapses termed GABA-A_{fast}

(Pearce, 1993). What might be the functional significance of the observation that DSI disproportionately affects fast synapses? It has been proposed that GABA-A_{fast} interneurons are responsible for controlling oscillations in the gamma band (40 Hz) (Banks et al., 2000). Gamma oscillations occur synchronously in multiple brain regions and have been proposed to be involved in binding simultaneous perceptions (Gray, 1994). Consistent with the idea that endocannabinoids regulate the gamma rhythm, WIN55212-2 decreases the power of gamma-range oscillations induced in hippocampal slices by kainate (Hajos et al., 2000).

Furthermore, GABA-A_{fast} synapses are known to be segregated onto the somata and proximal dendrites of pyramidal cells, whereas the population termed GABA-A_{slow} is located on distal dendrites (Pearce, 1993; Maccaferri et al., 2000). This is consistent with the morphological identification of CB1-immunopositive cells as basket cells, which arborize selectively in stratum pyramidale and proximal radiatum; basket cells also exhibit small after-hypolarizations (Sik et al., 1995), consistent with our data on the excitability profile of GABA-$A_{fast\ I}$ cells. It appears, therefore, that endocannabinoids regulate primarily somatic inhibition. This is likely to have important functional consequences, as somatic synapses account for most tonic, action potential-independent inhibition (Soltesz et al., 1995).

We have found that a third distinguishing mark of cannabinoid-sensitive connections is that they use exclusively N-type Ca^{2+} channels for vesicular release. This was never observed at cannabinoid-resistant synapses, and so it is tempting to speculate that these two unusual properties are somehow related. Both N- and P/Q-type channels are inhibited by $G\beta\gamma$; however, N-type channels are twice as sensitive to inhibition by

this mechanism (Zhang et al., 1996; Currie and Fox, 1997). Selective targeting of N-type VDCCs to these terminals might therefore explain why endocannabinoids are able to cause such a profound inhibition of GABA release at these synapses.

We found that cannabinoid-insensitive synapses fell into two broad categories. GABA-$A_{fast\ II}$ connections had fast kinetics, were capable of firing at significantly higher rates than the other two types of interneurons, and showed less accommodation in firing rate. A complete mapping of physiological properties onto morphological types has not been undertaken for hippocampal interneurons, and indeed may not be possible, given their diversity (Parra et al., 1998; Freund and Buzsáki, 1996). However, GABA-$A_{fast\ II}$ interneurons may include parvalbumin-positive/CCK-negative basket cells, axo-axonic cells, and bistratified/trilaminar cells (Freund and Buzsáki, 1996). All GABA-$A_{fast\ II}$ synapses we recorded used exclusively P/Q-type Ca^{2+} channels for neurotransmitter release. The reasons for this selectivity are unclear, but might relate to the high, sustained firing rates that these neurons are capable of. Bistratified/trilaminar cells, which are probably included in this group, exhibit high in vivo firing rates, sometimes >300 Hz (Sik et al., 1995). It might be advantageous for these cells to use only P/Q-type VDCCs at the presynaptic terminal because this VDCC subtype shows much less inactivation than N-type channels (Usowicz et al., 1992), and thus may permit sustained neurotransmitter release under depolarizing conditions of high firing rates. Consistent with this idea, P/Q-type channels support most of the miniature IPSCs elicited by strong depolarization (high external potassium) in the CA1 region (Doze et al., 1995); this might account for why miniature IPSCs recorded under these conditions are only modestly depressed by endocannabinoids (Chapter 4, Fig. 11). Also, reconstruction of

interneurons in hippocampal slice cultures that use only P/Q-type channels for neurotransmitter release has shown that the axonal varicosities of these neurons are consistently larger in size than those of other filled cells (Poncer et al., 1997), suggestive of boutons with large reserve pools of vesicles well-suited to repetitive release.

Finally, a second type of cannabinoid-insensitive synapse (GABA-A_{slow}) showed quite different properties, namely slow uIPSC rise and decay kinetics. Based on these kinetics, interneurons responsible for this type of synapse are likely to include O-LM cells, and possibly also S-LM cells displaced into stratum radiatum (Maccaferri et al., 2000; Freund and Buzsáki, 1996). We have shown that these interneurons use both N- and P/Q-type channels for neurotransmitter release, which seems to be typical of CNS neurons in general (Takahashi and Momiyama, 1993). GABA-A_{slow} synapses are likely to originate in the distal regions of the dendritic tree (Pearce, 1993), and it has been suggested that interneurons responsible for GABA-A_{slow} synapses are responsible for oscillations in the theta band (5-10 Hz) (Banks et al., 2000), which are prominent during exploratory behaviors (Gray, 1994). Endocannabinoids might therefore be predicted to suppress gamma oscillations selectively while preserving theta oscillations, thus altering the temporal output of the hippocampus.

In sum, endocannabinoid signaling appears to be a specific mechanism for rapidly turning off a distinct class of hippocampal interneurons. *In vivo* physiological and behavioral experiments, as well as a better understanding of interneuron classification and function, should help unravel the role of this system in the cognitive functions of the hippocampus.

FIGURE 14: Presynaptic N-type Ca^{2+} channels are required for endocannabinoid signaling

(A) DSI was monitored by comparing eIPSC amplitudes just before (filled symbols) and just after (open symbols) depolarizing steps. After a stable baseline period, the N-type VDCC antagonist ω-conotoxin GVIA (ω-CTx-GVIA) was washed onto the slice, causing a depression of basal IPSC ampltude and a complete block of DSI. Subsequent wash-in of WIN55212-2 had no effect, indicating that N-type VDCCs are required for presynaptic inhibition by cannabinoids.

(B) The same experiment as in (A) was performed using the P/Q-type VDCC antagonist ω-agatoxin TK (ω-Aga-TK). ω-Aga-TK also depressed basal IPSC amplitude, but increased DSI magnitude. Subsequent wash-in of WIN55212-2 blocked most of the remaining IPSC, indicating that the component of release mediated by N-type VDCCs is highly sensitive to cannabinoids.

(C) Summary data showing that in experiments where ω-CTx-GVIA was added (squares), DSI was blocked, whereas in experiments where ω-Aga-TK was added (triangles), DSI was increased.

(D) Summary data showing that after ω-CTx-GVIA addition, eIPSCs are not depressed by WIN55212-2. By contrast, after ω-Aga-TK addition, eIPSCs are depressed more strongly than in control conditions (control WIN55212-2 time course not shown).

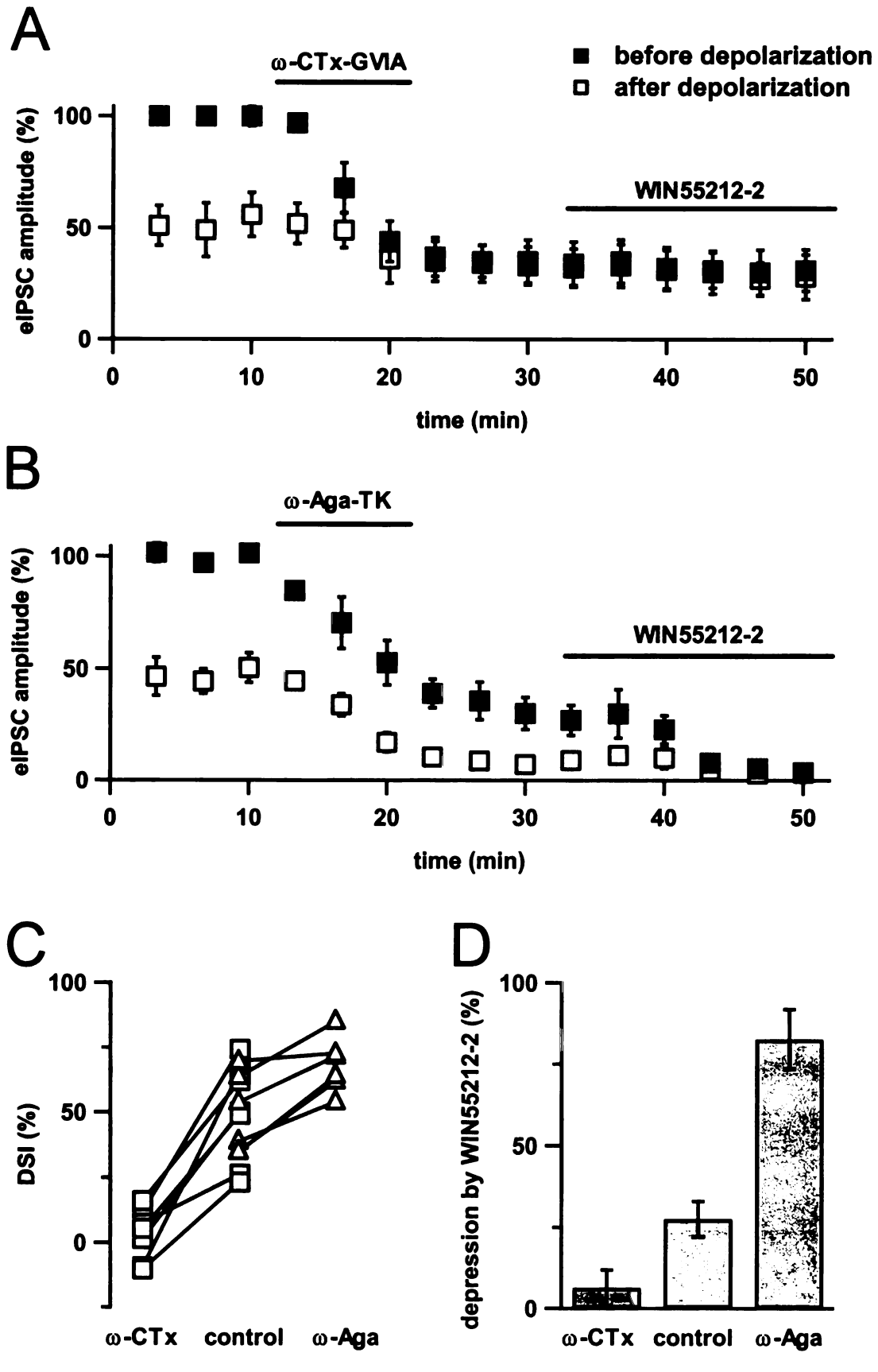
A
ω-CTx-GVIA
before depolarization
after depolarization
WIN55212-2
eIPSC amplitude (%)
100
50
0
0
10
20
30
40
50
time (min)
B
ω-Aga-TK
WIN55212-2
eIPSC amplitude (%)
100
50
0
0
10
20
30
40
50
time (min)
C
DSI (%)
100
50
0
ω-CTx
control
ω-Aga
D
depression by WIN55212-2 (%)
100
50
0
ω-CTx
control
ω-Aga

FIGURE 15: Endocannabinoids selectively affect an interneuron subtype with distinctive synaptic properties

(A) Recordings from connected interneuron-pyramidal cell pairs yielded 30 GABAergic connections. A histogram of uIPSC rise times produced a bimodal distribution, which we termed GABA-A_{fast} and GABA-A_{slow}. Dotted line is a fit to the sum of two gaussian functions, and events are classified (open and gray bars) according to which gaussian better describes them.

(B) A histogram of DSI magnitude shows that all connections were either very sensitive to DSI or else completely insensitive. All the DSI sensitive connections belonged to the fast kinetic group, and are referred to here as GABA-$A_{fast\ I}$, whereas the DSI-insensitive group included both fast synapses (termed here GABA-$A_{fast\ II}$) and all slow synapses (GABA-A_{slow}).

(C) Average uIPSC amplitude is significantly larger for GABA-$A_{fast\ I}$ connections compared to either of the other two groups.

(D) Raw traces from representative connections. Three overlaid raw sweeps acquired just before depolarization are displayed next to three overlaid raw sweeps acquired just after depolarization. Note the different vertical scaling for D1-3; horizontal scaling is the same for all three groups. GABA-$A_{fast\ I}$ connections (D1) show both failures and small-amplitude successes after depolarization, whereas connnections from the other two groups (GABA-$A_{fast\ II}$, D2, and GABA-A_{slow}, D3) are not affected by depolarization.

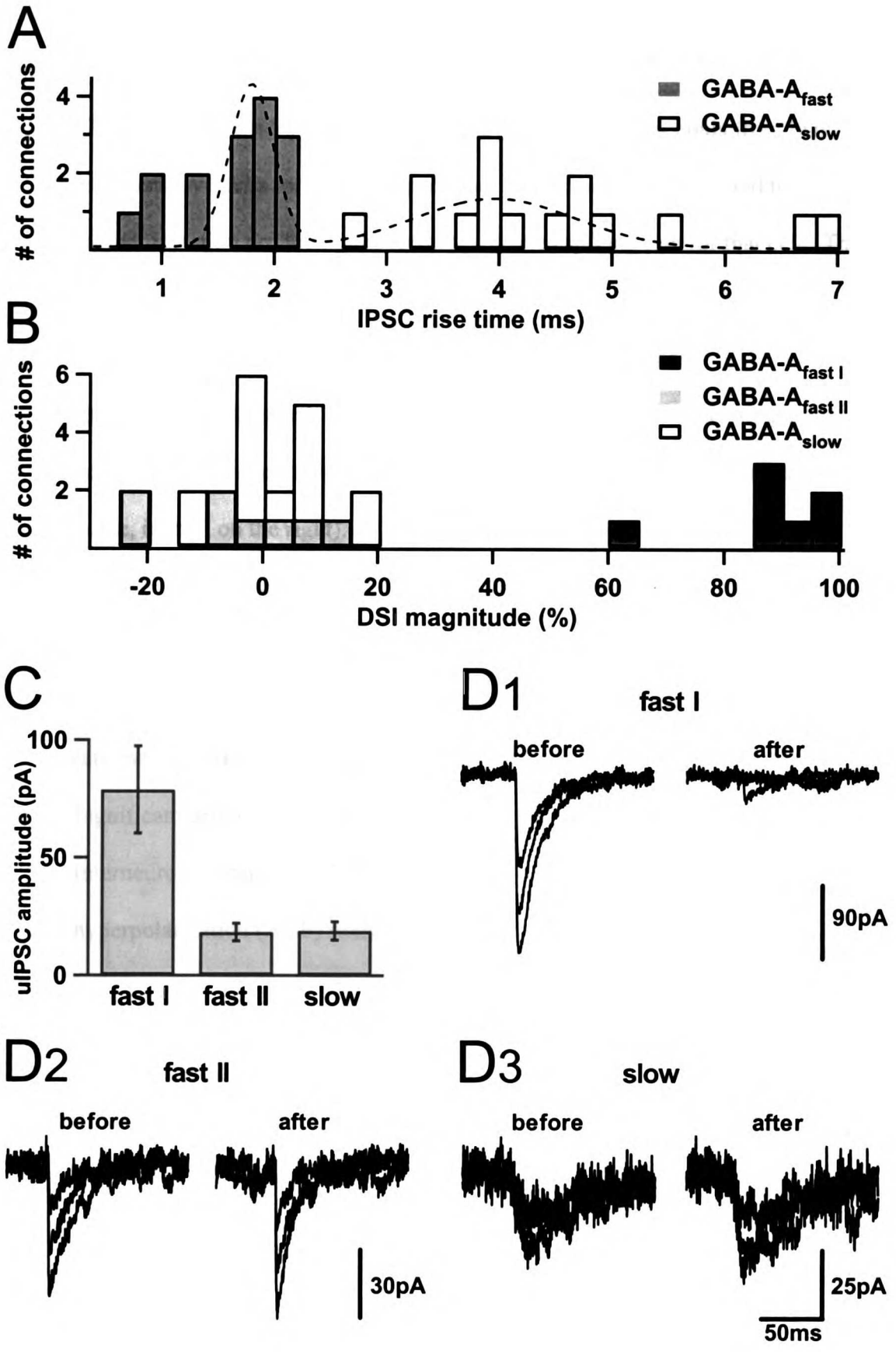
A
# of connections
GABA-A$_{fast}$
GABA-A$_{slow}$
IPSC rise time (ms)
B
# of connections
GABA-A$_{fast\ I}$
GABA-A$_{fast\ II}$
GABA-A$_{slow}$
DSI magnitude (%)
C
uIPSC amplitude (pA)
fast I
fast II
slow
D1
fast I
before
after
90pA
D2
fast II
before
after
30pA
D3
slow
before
after
25pA
50ms

FIGURE 16: Intrinsic excitability differs for cannabinoid-sensisitive and -insensitive interneurons

(A) The left side of the top panel (A1) shows single action potentials from two representative cells for each synapse type. These sweeps correspond to the current injection producing the lowest (nonzero) spiking rate for that cell. The right side of the panel (A2) shows trains of action potentials for the same six cells. These sweeps correspond to the current injection producing the maximal spiking rate for that cell. Note the different horizontal scaling for single action potentials and trains; vertical scaling and alignment is the same for all traces (see guide, in mV, on the right).

(B) Average inter-spike interval is shown for the first two, middle two, and last two spikes in a train 350 ms long where the interneuron is spiking at its maximal rate. Interneurons forming GABA-$A_{fast\ II}$ synapses are able to spike at a higher maximal rate than the other two groups of interneurons, and show less spike adaptation. Significant differences ($p<0.05$) are indicated by brackets.

(C) Interneurons forming GABA-$A_{fast\ I}$ synapses have a smaller after-hyperpolarization (AHP) immediately following the action potential.

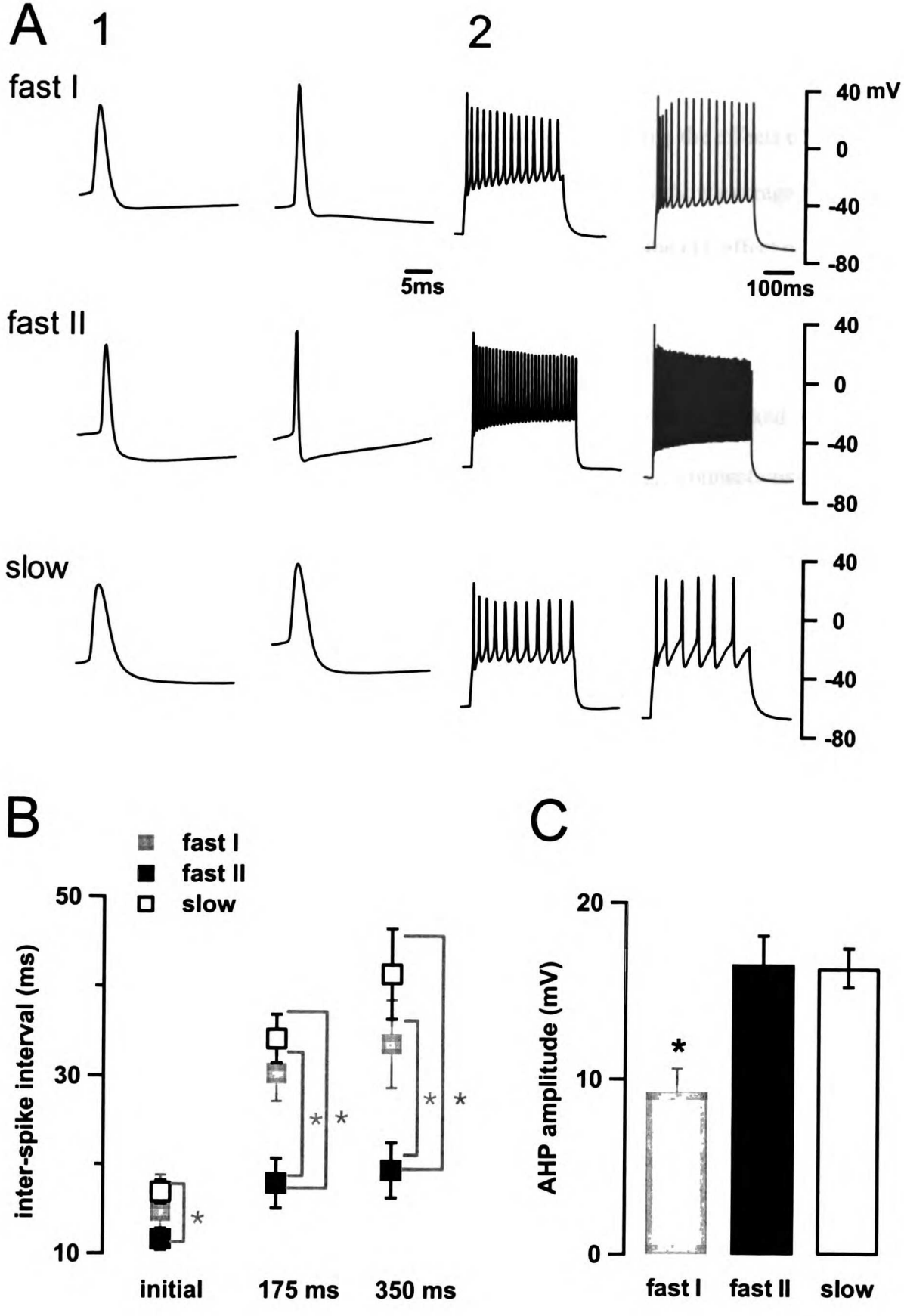
A
1
2
fast I
40 mV
0
-40
-80
5ms
100ms
fast II
40
0
-40
-80
slow
40
0
-40
-80
B
fast I
fast II
slow
50
30
10
inter-spike interval (ms)
*
*
*
*
*
initial
175 ms
350 ms
C
20
10
0
AHP amplitude (mV)
*
fast I
fast II
slow

FIGURE 17: Cannabinoid-sensitive and -insensitive interneurons use different Ca^{2+} channels for GABA release

(A-C) Representative experiments for each connection type showing the effects of specific VDCC antagonists on synaptic transmission. Insets show averaged traces (30-60 sweeps) for each experiment corresponding to baseline (1), effect of the first toxin (2), and effect of the second toxin (3). Note different vertical scaling in (A-C) insets; horizontal scaling is the same.

(D) Group data showing that GABA-$A_{fast\ I}$ connections are completely blocked by ω-CTx-GVIA, but resistant to ω-Aga-TK, whereas GABA-$A_{fast\ II}$ connections are completely blocked by ω-Aga-TK, but resistant to ω-CTx-GVIA. GABA-A_{slow} connections are blocked partially by both toxins, with the first toxin application eliminating about 70% of the IPSC.

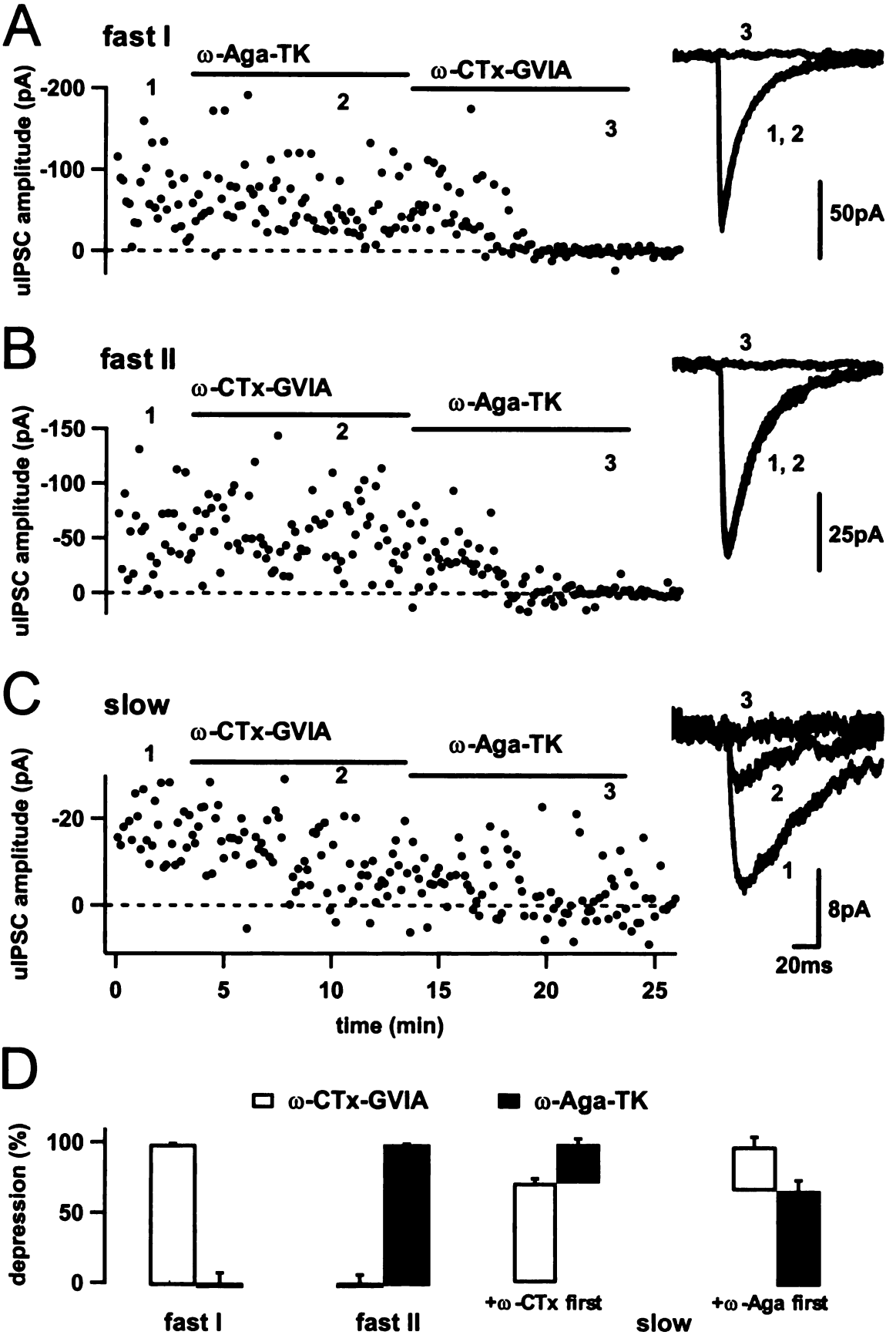
A
fast I
ω-Aga-TK
ω-CTx-GVIA
uIPSC amplitude (pA)
-200
-100
0
1
2
3
1, 2
50pA
B
fast II
ω-CTx-GVIA
ω-Aga-TK
-150
-100
-50
0
25pA
C
slow
ω-CTx-GVIA
ω-Aga-TK
-20
0
8pA
20ms
0
5
10
15
20
25
time (min)
D
ω-CTx-GVIA
ω-Aga-TK
depression (%)
100
50
0
fast I
fast II
+ω-CTx first
+ω-Aga first
slow

CHAPTER 6: General Conclusions

Implications for endocannabinoid signaling

The experiments described here provide strong evidence that endocannabinoids function as fast retrograde messengers at hippocampal GABAergic synapses. This represents the first account of a specific neurophysiological phenomenon mediated by endocannabinoids, and one of the most complete descriptions to date of fast retrograde signaling.

Using this experimental preparation, we have also been able to acquire data that extends our understanding of endocannabinoid biology beyond the limits of previous anatomical and biochemical studies. On the basis of these data, we propose that:

1. Endocannabinoids are synthesized within ≤ 1 second and their effects are terminated in about 20-40 seconds. This is about three orders of magnitude slower than the actions of classical neurotransmitters, but faster than certain actions of some classical neuromodulators, such as the monoamines.
2. Endocannabinoids are also intermediate between these classical extremes in terms of their spatial range, which extends over a radius of approximately 20 μm in brain tissue. This is more diffuse than the typical actions of neurotransmitters and more local than many classical neuromodulators.
3. Endocannabinoids—unlike, for example, the "atypical" neuronal messenger nitric oxide—are probably not completely membrane-permeant. Consistent with previous evidence in cultured neurons and *in vivo* (Beltramo et al., 1997), our results suggest that in brain tissue, transport across membranes is a

requirement for efficient hydrolysis of endocannabinoids by intracellular fatty acid amide hydrolase. Furthermore, we found that inhibition of endocannabinoid uptake was sufficient to completely saturate the effects of hippocampal endocannabinoids on GABA release. This implies that transport inhibition could be a useful therapeutic strategy for potentiating the endocannabinoid systems in select CNS regions.

Together, these results paint a picture of a novel class of signaling molecules, intermediate between fast, local neurotransmitters and slow, global neuromodulators. Much more work will be required to complete the picture, including biochemical and anatomical studies in addition to electrophysiology and behavior. In particular, it will be important to identify the enzymes which synthesize endocannabinoids, to identify which endocannabinoids are produced in the hippocampus and elsewhere by brief depolarizations, to describe the mode of endocannabinoid release, and to locate CB1 subcellularly in other brain regions.

Implications for hippocampal function and dysfunction

The results of this study throw into starker relief two obvious questions: How might endocannabinoids contribute to hippocampal function? And how might Δ^9-THC produce hippocampal dysfunction, as the impairments in memory associated with cannabis use would seem to imply?

There are at least two possible answers to the first question. First, endocannabinoids may regulate the induction of plasticity in the hippocampus. Decreasing GABAergic inhibition generally promotes the induction of LTP (Wigström

and Gustafsson, 1985), and endocannabinoids would therefore be expected to increase the magnitude of LTP. Consistent with this hypothesis, recent data obtained by Alger and colleagues shows that DSI lowers the threshold for LTP induction in CA1 (Alger, 2000). Another prediction of this hypothesis is that SR141716 ought to decrease LTP by blocking DSI. Data from one study appears to show that SR141716 inhibits an early phase of LTP, but it is not clear if this effect is significant, and in any case the effect disappears by 30 minutes post-tetanus (Paton et al., 1998). Although GABAergic inhibition was not blocked in this study, it is not clear whether the strength of GABAergic transmission was a limiting factor in LTP induction under their conditions. The pattern and strength of tetanic stimulation are likely to determine the amount of GABAergic inhibition recruited by the tetanus, and the degree to which this inhibition keeps the postsynaptic membrane voltage below the threshold for LTP induction. In the future, it will be important to see whether SR141716 can decrease LTP induced by a pattern of tetanic stimulation where GABA is clearly regulating the induction of LTP.

If CB1 does indeed normally regulate LTP induction in the hippocampus, then this suggests a possible mechanism for the impairments in memory and cognition caused by Δ^9-THC. It is likely that under normal conditions, endocannabinoids are produced by those individual pyramidal neurons which are firing at relatively high rates, in the range of 20 Hz (Morishita and Alger, 2001). Only these select, highly excited neurons (and also their very near neighbors) could then experience a decrease in their LTP induction threshold. Because DSI is spatially limited (Chapter 3) and brief, this threshold shift would have only limited effects. By contrast, marijuana floods the hippocampus with cannabinoids and ought to cause global, tonic disinhibition. This should promote LTP

and Gustafsson, 1985), and endocannabinoids would therefore be expected to increase the magnitude of LTP. Consistent with this hypothesis, recent data obtained by Alger and colleagues shows that DSI lowers the threshold for LTP induction in CA1 (Alger, 2000). Another prediction of this hypothesis is that SR141716 ought to decrease LTP by blocking DSI. Data from one study appears to show that SR141716 inhibits an early phase of LTP, but it is not clear if this effect is significant, and in any case the effect disappears by 30 minutes post-tetanus (Paton et al., 1998). Although GABAergic inhibition was not blocked in this study, it is not clear whether the strength of GABAergic transmission was a limiting factor in LTP induction under their conditions. The pattern and strength of tetanic stimulation are likely to determine the amount of GABAergic inhibition recruited by the tetanus, and the degree to which this inhibition keeps the postsynaptic membrane voltage below the threshold for LTP induction. In the future, it will be important to see whether SR141716 can decrease LTP induced by a pattern of tetanic stimulation where GABA is clearly regulating the induction of LTP.

If CB1 does indeed normally regulate LTP induction in the hippocampus, then this suggests a possible mechanism for the impairments in memory and cognition caused by Δ^9-THC. It is likely that under normal conditions, endocannabinoids are produced by those individual pyramidal neurons which are firing at relatively high rates, in the range of 20 Hz (Morishita and Alger, 2001). Only these select, highly excited neurons (and also their very near neighbors) could then experience a decrease in their LTP induction threshold. Because DSI is spatially limited (Chapter 3) and brief, this threshold shift would have only limited effects. By contrast, marijuana floods the hippocampus with cannabinoids and ought to cause global, tonic disinhibition. This should promote LTP

induction at all plastic synapses in the hippocampus, and cause a noisier, more random pattern of synaptic modification. Under these conditions, LTP would be the result not of a meaningful "coincidence detection", but rather the consequence of a fairly random fluctuation. Thus, memory should be impaired although plasticity is still occurring.

A second, equally plausible possibility is that endocannabinoids contribute to the proper regulation of synchronous oscillations in the hippocampus. Our results show that the population of synapses which is sensitive to endocannabinoids is a subset of those synapses which generate GABA-A_{fast} IPSCs. It has been previously suggested that GABA-A_{fast} synapses are responsible for orchestrating oscillations in the gamma band (Banks et al., 2000), raising the possibility that CB1 activation might selectively suppress gamma oscillations. Accordingly, WIN55212-2 decreases oscillations in the gamma range in hippocampal slices (Hajos et al., 2000). Endocannabinoids might therefore be important in down-regulating gamma oscillations *in vivo*, conceivably in order to accomplish some change in behavioral or attentive state, since gamma oscillations are proposed to mediate perceptual binding (Gray, 1994). It also seems reasonable to imagine that an activity-dependent decrease in hippocampal synchrony could be an important mechanism in avoiding epileptic seizures in the temporal lobe.

Again, this explanation for the possible importance of endocannabinoids may be reversed to account for cognitive impairment by marijuana. Whereas endocannabinoids may cause a moderate, local, brief escape from synchronous oscillations, marijuana would be more likely to caused a global suppression of gamma band oscillations in the hippocampus, and also perhaps in other brain regions. This may be relevant to one

commonly reported experience of marijuana users. In the words of one 60s-era college student describing his experiences while smoking marijuana,

> "When I walk someplace my experience of the distance covered is quite changed so that distances seem to get greater... Time passes very slowly; it's not just that things take longer, certain experiences seem outside of time, are timeless."
>
> —quoted in Snyder, 1971

On average, smoking marijuana tends to increase subjects' estimation of time intervals by about 2-fold (Snyder, 1971). It is possible that this sense of timelessness results from the suppression of synchronous oscillations in firing rates, either in the gamma band or otherwise, which would, in effect, turn off the brain's own metronome. Speculations like these are far from testable at the moment. One day, however, the development of finer pharmacological tools that alter endocannabinoid function in specific brain regions could have not only therapeutic value, but could also give us a window onto some of the mysterious properties of our own minds.

CHAPTER 7: Postscript

Two recent studies (Kreitzer and Regehr, 2001; Ohno-Shosaku et al., 2001) provide independent confirmation of the role of endocannabinoids in fast retrograde signaling. Both these studies were submitted for publication while a portion of this material in this thesis (Figs. 2-11) was under review, and all three manuscripts were published on March 29, 2001. All the results of these two independent studies are completely consistent with our findings, and are summarized here in brief.

Ohno-Shosaku et al. (2001) have investigated the mechanism of DSI in dissociated cultures of hippocampal neurons. They find that unitary GABAergic connections in culture are either extremely sensitive to WIN55212-2 (depressed on average by 98%) or else completely insensitive. This agrees in general with the results of a previous study which used minimal stimulation in acute hippocampal slices (Hajos et al., 2000). Both types of connections were equally sensitive to baclofen. They also show that WIN55212-2 causes a robust increase in the paired-pulse ratio in those connections that are depressed by WIN55212-2, in agreement with our results (Fig. 10). Next, these investigators find that individual unitary connections show a similar heterogeneity in their sensitivity to DSI, which is consistent with our results using paired recordings in acute slices (Fig. 15). They show that all DSI-sensitive connections are WIN55212-2-sensitive, but that there is also a small population of connections which are depressed by WIN55212-2 but not by DSI. This is intriguing, because it suggests that not all postsynaptic neurons are capable of producing cannabinoids. Next, they show that DSI in culture is completely blocked by either AM251 or SR141716, consistent with our results (Fig. 7, 8). Finally, they show that DSI is not affected by any mGluR antagonist

they have tested (MCPG, MPEP, CPPG, CGP), although all these antagonists were able to block the suppression of IPSCs by their corresponding mGluR agonists. Together, these results suggest that DSI in dissociated culture is basically similar to DSI in acute slices, and support the conclusion that endocannabinoids function as the primary retrograde messenger in DSI.

Kreitzer and Regehr (2001) have examined the mechanism of a novel DSI-like phenomenon at excitatory synapses in the cerebellum. In a phenomenon they call "depolarization-induced suppression of excitation" (DSE), they find that depolarization of a cerebellar Purkinje neuron causes a transient suppression of either parallel fiber (PF) or climbing fiber (CF) synapses onto that cell. PFs are more sensitive to DSE than CFs, consistent with the low level of CB mRNA in the inferior olive (Matsuda et al., 1993), where CFs originate. Like DSI, DSE is blocked by postsynaptic BAPTA, indicating a requirement for postsynaptic Ca^{2+}. And, evidently also like DSI, DSE at either PF or CF synapses is associated with an increase in the paired-pulse ratio, consistent with a decrease in the probability of release at the presynaptic bouton. Because CF boutons are large and densely clustered in a single plane, these investigators are able to image presynaptic Ca^{2+} during DSE. They find that DSE inhibits presynaptic Ca^{2+} influx, and that this inhibition is uniform across the entire CF arborization. This indicates that action potential propagation failures at branchpoints are unlikely to account for the presynaptic inhibition, and that a local effect on boutons is more plausible. Next, these investigators report that DSE at both PF and CF synapses is blocked by AM251, and mimicked and occluded by WIN55212-2. Finally, they show that the mGluR antagonist LY341495 has no effect on DSI, although in the same cells this drug is able to antagonize completely the

suppression of EPSCs by mGluR agonists. In sum, these results suggest that endocannabinoids released by depolarized Purkinje cells mediate presynaptic inhibition at both CF and PF synapses.

Particularly valuable is Kreitzer and Regehr's direct demonstration that endocannabinoids do indeed inhibit presynaptic Ca^{2+} influx. Results presented in this thesis (Figs. 10, 11) are consistent with the hypothesis that the same mechanism accounts for hippocampal DSI. The data reported by Kreitzer and Regehr complement nicely the findings of Hoffman and Lupica (2000), who had pinpointed the locus of WIN55212-induced inhibition at hippocampal GABAergic synapses to a Ca^{2+}-dependent step in presynaptic release, and had ruled out participation by presynaptic Na^+ or K^+ channels, but could not directly show that Ca^{2+} influx was decreasing (as opposed to a subsequent Ca^{2+} step). If we may assume that presynaptic inhibition by cannabinoids is mechanistically similar in the hippocampus and cerebellum, then all these results converge on presynaptic VDCCs as the direct target of $G_{\beta\gamma}$-mediated inhibition.

Recently, it was reported that the potent mGluR antagonist LY341495 has only a small effect on cerebellar DSI, reducing DSI by about 20% on average (Glitsch and Jack, 2001). These authors therefore suggested that glutamate may be only a modulator of cerebellar DSI, and that some other molecule is likely to be the primary retrograde signal. Given that depolarized Purkinje neurons do release endocannabinoids (Kreitzer and Regehr, 2001), and that GABAergic synapses onto Purkinje cells are depressed by WIN55212-2 (Takahashi and Linden, 2000) and are associated with some of the highest densities of CB1 in the brain (Tsou et al., 1998), it seems likely that endocannabinoids also mediate cerebellar DSI.

References

Alger, B. E. (2000). "Symposium: Retrograde signaling in the short-term regulation of synaptic transmission in cerebellum, hippocampus, and neocortex." Soc. Neurosci. Abstracts, 26: 678.

Alger, B. E., and Pitler, T. A. (1995). Retrograde signaling at GABAA-receptor synapses in the mammalian CNS. Trends Neurosci. 18, 333-40.

Alger, B. E., Pitler, T. A., Wagner, J. J., Martin, L. A., Morishita, W., Kirov, S. A., and Lenz, R. A. (1996). Retrograde signalling in depolarization-induced suppression of inhibition in rat hippocampal CA1 cells. J. Physiol. 496, 197-209.

Banks, M. I., White, J. A., and Pearce, R. A. (2000). Interactions between distinct GABA(A) circuits in hippocampus. Neuron 25, 449-57.

Barde, Y. A. (1989). Trophic factors and neuronal survival. Neuron 2, 1525-34.

Bean, B. P. (1989). Neurotransmitter inhibition of neuronal calcium currents by changes in channel voltage dependence. Nature 340, 153-6.

Beltramo, M., Stella, N., Calignano, A., Lin, S. Y., Makriyannis, A., and Piomelli, D. (1997). Functional role of high-affinity anandamide transport, as revealed by selective inhibition. Science 277, 1094-7.

Benham, C. D., Evans, M. L., and McBain, C. J. (1992). Ca2+ efflux mechanisms following depolarization evoked calcium transients in cultured rat sensory neurones. J. Physiol. 455, 567-83.

Binz, T., Blasi, J., Yamasaki, S., Baumeister, A., Link, E., Südhof, T. C., Jahn, R., and Niemann, H. (1994). Proteolysis of SNAP-25 by types E and A botulinal neurotoxins. J. Biol. Chem. 269, 1617-20.

Bisogno, T., Sepe, N., Melck, D., Maurelli, S., De Petrocellis, L., and Di Marzo, V. (1997). Biosynthesis, release and degradation of the novel endogenous cannabimimetic metabolite 2-arachidonoylglycerol in mouse neuroblastoma cells. Biochem. J. 322, 671-7.

Bliss, T. V., and Collingridge, G. L. (1993). A synaptic model of memory: long-term potentiation in the hippocampus. Nature 361, 31-9.

Bohme, G. A., Laville, M., Ledent, C., Parmentier, M., and Imperato, A. (2000). Enhanced long-term potentiation in mice lacking cannabinoid CB1 receptors. Neurosci. 95, 5-7.

Brody, D. L., and Yue, D. T. (2000). Relief of G-protein inhibition of calcium channels and short-term synaptic facilitation in cultured hippocampal neurons. J. Neurosci. 20, 889-98.

Buzsáki, G. (1997). Functions for interneuronal nets in the hippocampus. Can. J. Physiol. Pharmacol. 75, 508-15.

Calignano, A., La Rana, G., Beltramo, M., Makriyannis, A., and Piomelli, D. (1997). Potentiation of anandamide hypotension by the transport inhibitor, AM404. Eur. J. Pharm. 337, R1-2.

Cash, S., Dan, Y., Poo, M. M., and Zucker, R. (1996a). Postsynaptic elevation of calcium induces persistent depression of developing neuromuscular synapses. Neuron 16, 745-54.

Cash, S., Zucker, R. S., and Poo, M. M. (1996b). Spread of synaptic depression mediated by presynaptic cytoplasmic signaling. Science 272, 998-1001.

Chen, Y. A., Scales, S. J., Patel, S. M., Doung, Y. C., and Scheller, R. H. (1999). SNARE complex formation is triggered by Ca2+ and drives membrane fusion. Cell 97, 165-74.

Childers, S. R., and Breivogel, C. S. (1998). Cannabis and endogenous cannabinoid systems. Drug Alcohol Depend. 51, 173-87.

Christie, M. J., and Vaughan, C. W. (2001). Cannabinoids act backwards. Nature 410, 327-9.

Cravatt, B. F., Giang, D. K., Mayfield, S. P., Boger, D. L., Lerner, R. A., and Gilula, N. B. (1996). Molecular characterization of an enzyme that degrades neuromodulatory fatty-acid amides. Nature 384, 83-7.

Currie, K. P., and Fox, A. P. (1997). Comparison of N- and P/Q-type voltage-gated calcium channel current inhibition. J. Neurosci. 17, 4570-9.

Dan, Y., and Poo, M. M. (1992). Hebbian depression of isolated neuromuscular synapses in vitro. Science 256, 1570-3.

Davis, G. W., DiAntonio, A., Petersen, S. A., and Goodman, C. S. (1998). Postsynaptic PKA controls quantal size and reveals a retrograde signal that regulates presynaptic transmitter release in Drosophila. Neuron 20, 305-15.

Davis, G. W., and Goodman, C. S. (1998). Genetic analysis of synaptic development and plasticity: homeostatic regulation of synaptic efficacy. Curr. Opin. Neurobiol. 8, 149-56.

Davis, G. W., and Murphey, R. K. (1994a). Long-term regulation of short-term transmitter release properties: retrograde signaling and synaptic development. Trends Neurosci. 17, 9-13.

Davis, G. W., and Murphey, R. K. (1994b). Retrograde signaling and the development of transmitter release properties in the invertebrate nervous system. J. Neurobiol. 25, 740-56.

Deutsch, D. G., and Chin, S. A. (1993). Enzymatic synthesis and degradation of anandamide, a cannabinoid receptor agonist. Biochem. Pharmacol. 46, 791-6.

Devane, W. A., Dysarz, F. A. d., Johnson, M. R., Melvin, L. S., and Howlett, A. C. (1988). Determination and characterization of a cannabinoid receptor in rat brain. Mol. Pharm. 34, 605-13.

Di Marzo, V., Bisogno, T., Sugiura, T., Melck, D., and De Petrocellis, L. (1998a). The novel endogenous cannabinoid 2-arachidonoylglycerol is inactivated by neuronal- and basophil-like cells: connections with anandamide. Biochem. J. 331, 15-9.

Di Marzo, V., Fontana, A., Cadas, H., Schinelli, S., Cimino, G., Schwartz, J. C., and Piomelli, D. (1994). Formation and inactivation of endogenous cannabinoid anandamide in central neurons. Nature 372, 686-91.

Di Marzo, V., Melck, D., Bisogno, T., and De Petrocellis, L. (1998b). Endocannabinoids: endogenous cannabinoid receptor ligands with neuromodulatory action. Trends Neurosci. 21, 521-8.

Dobrunz, L. E., and Stevens, C. F. (1997). Heterogeneity of release probability, facilitation, and depletion at central synapses. Neuron 18, 995-1008.

Dodge, F. A., and Rahamimoff, R. (1967). Co-operative action of calcium ions in transmitter release at the neuromuscular junction. J. Physiol. 193, 419-32.

Doze, V. A., Cohen, G. A., and Madison, D. V. (1995). Calcium channel involvement in GABAB receptor-mediated inhibition of GABA release in area CA1 of the rat hippocampus. J. Neurophysiol. 74, 43-53.

Dugan, L. L., Sensi, S. L., Canzoniero, L. M., Handran, S. D., Rothman, S. M., Lin, T. S., Goldberg, M. P., and Choi, D. W. (1995). Mitochondrial production of reactive oxygen species in cortical neurons following exposure to N-methyl-D-aspartate. J. Neurosci. 15, 6377-88.

Egertová, M., and Elphick, M. R. (2000). Localisation of cannabinoid receptors in the rat brain using antibodies to the intracellular C-terminal tail of CB1. J. Comp. Neurol. 422, 159-71.

Egertová, M., Giang, D. K., Cravatt, B. F., and Elphick, M. R. (1998). A new perspective on cannabinoid signalling: complementary localization of fatty acid amide hydrolase and the CB1 receptor in rat brain. Proc. R. Soc. Lond. B 265, 2081-5.

Evans, D. M., Johnson, M. R., and Howlett, A. C. (1992). Ca(2+)-dependent release from rat brain of cannabinoid receptor binding activity. J. Neurochem. 58, 780-2.

Evans, D. M., Lake, J. T., Johnson, M. R., and Howlett, A. C. (1994). Endogenous cannabinoid receptor binding activity released from rat brain slices by depolarization. J. Pharm. Exp. Ther. 268, 1271-7.

Felder, C. C., Briley, E. M., Axelrod, J., Simpson, J. T., Mackie, K., and Devane, W. A. (1993). Anandamide, an endogenous cannabimimetic eicosanoid, binds to the cloned human cannabinoid receptor and stimulates receptor-mediated signal transduction. Proc. Natl. Acad. Sci. U.S.A. 90, 7656-60.

Fitzsimonds, R. M., and Poo, M. M. (1998). Retrograde signaling in the development and modification of synapses. Physiol. Rev. 78, 143-70.

Freund, T. F., and Buzsáki, G. (1996). Interneurons of the hippocampus. Hippocampus 6, 347-470.

Galiègue, S., Mary, S., Marchand, J., Dussossoy, D., Carrière, D., Carayon, P., Bouaboula, M., Shire, D., Le Fur, G., and Casellas, P. (1995). Expression of central and peripheral cannabinoid receptors in human immune tissues and leukocyte subpopulations. Eur. J. Biochem. 232, 54-61.

Gaoni, Y., and Mechoulam, R. (1964). Isolation, structure, and partial synthesis of an active constituent of hashish. J. Am. Chem. Soc. 86, 1646-47.

Gifford, A. N., and Ashby, C. R., Jr. (1996). Electrically evoked acetylcholine release from hippocampal slices is inhibited by the cannabinoid receptor agonist, WIN 55212-2, and is potentiated by the cannabinoid antagonist, SR 141716A. J. Pharm. Exp. Ther. 277, 1431-6.

Giuffrida, A., Rodriguez de Fonseca, F., Nava, F., Loubet-Lescoulié, P., and Piomelli, D. (2000). Elevated circulating levels of anandamide after administration of the transport inhibitor, AM404. Eur. J. Pharm. 408, 161-8.

Glitsch, M., Llano, I., and Marty, A. (1996). Glutamate as a candidate retrograde messenger at interneurone-Purkinje cell synapses of rat cerebellum. J. Physiol. 497, 531-7.

Glitsch, M. D., and Jack, J. J. B. (2001). Evidence that glutamate acting on presynaptic type-II metabotropic glutamate receptors alone does not fully account for the

phenomenon of depolarization-induced suppression of inhibition in cerebellar Purkinje cells. Pflugers Arch. 442, DOI 10.1007/s004240100559.

Goparaju, S. K., Ueda, N., Yamaguchi, H., and Yamamoto, S. (1998). Anandamide amidohydrolase reacting with 2-arachidonoylglycerol, another cannabinoid receptor ligand. FEBS Lett. 422, 69-73.

Gray, C. M. (1994). Synchronous oscillations in neuronal systems: mechanisms and functions. J. Comput. Neurosci. 1, 11-38.

Hajos, N., Katona, I., Naiem, S. S., Mackie, K., Ledent, C., Mody, I., and Freund, T. F. (2000). Cannabinoids inhibit hippocampal GABAergic transmission and network oscillations. Eur. J. Neurosci. 12, 3239-3249.

Herkenham, M., Lynn, A. B., Johnson, M. R., Melvin, L. S., de Costa, B. R., and Rice, K. C. (1991). Characterization and localization of cannabinoid receptors in rat brain: a quantitative in vitro autoradiographic study. J. Neurosci. 11, 563-83.

Herkenham, M., Lynn, A. B., Little, M. D., Johnson, M. R., Melvin, L. S., de Costa, B. R., and Rice, K. C. (1990). Cannabinoid receptor localization in brain. Proc. Natl. Acad. Sci. U.S.A. 87, 1932-6.

Herlitze, S., Garcia, D. E., Mackie, K., Hille, B., Scheuer, T., and Catterall, W. A. (1996). Modulation of Ca2+ channels by G-protein beta gamma subunits. Nature 380, 258-62.

Hescheler, J., and Schultz, G. (1993). G-proteins involved in the calcium channel signalling system. Curr. Opin. Neurobiol. 3, 360-7.

Hille, B. (1992). G protein-coupled mechanisms and nervous signaling. Neuron 9, 187-95.

Hille, B. (1994). Modulation of ion-channel function by G-protein-coupled receptors. Trends Neurosci. 17, 531-6.

Hoffman, A. F., and Lupica, C. R. (2000). Mechanisms of cannabinoid inhibition of GABA(A) synaptic transmission in the hippocampus. J. Neurosci. 20, 2470-9.

Howlett, A. C., and Fleming, R. M. (1984). Cannabinoid inhibition of adenylate cyclase: pharmacology of the response in neuroblastoma cell membranes. Mol. Pharm. 26, 532-8.

Hughes, J., Smith, T. W., Kosterlitz, H. W., Fothergill, L. A., Morgan, B. A., and Morris, H. R. (1975). Identification of two related pentapeptides from the brain with potent opiate agonist activity. Nature 258, 577-80.

Irving, A. J., Coutts, A. A., Harvey, J., Rae, M. G., Mackie, K., Bewick, G. S., and Pertwee, R. G. (2000). Functional expression of cell surface cannabinoid CB(1) receptors on presynaptic inhibitory terminals in cultured rat hippocampal neurons. Neurosci. 98, 253-62.

Járai, Z., Wagner, J. A., Varga, K., Lake, K. D., Compton, D. R., Martin, B. R., Zimmer, A. M., Bonner, T. I., Buckley, N. E., Mezey, E., Razdan, R. K., Zimmer, A., and Kunos, G. (1999). Cannabinoid-induced mesenteric vasodilation through an endothelial site distinct from CB1 or CB2 receptors. Proc. Natl. Acad. Sci. U.S.A. 96, 14136-41.

Johnson, M. R., and Melvin, L. S. (1886). "The discovery of non-classical cannabinoid analgesics." Cannabinoids as therapeutic agents, R. Mechoulam, ed., (CRC Press: Boca Raton, FL), 121-145.

Kanai, N., Lu, R., Satriano, J. A., Bao, Y., Wolkoff, A. W., and Schuster, V. L. (1995). Identification and characterization of a prostaglandin transporter. Science 268, 866-9.

Katona, I., Sperlágh, B., Maglóczky, Z., Sántha, E., Köfalvi, A., Czirják, S., Mackie, K., Vizi, E. S., and Freund, T. F. (2000). GABAergic interneurons are the targets of cannabinoid actions in the human hippocampus. Neurosci. 100, 797-804.

Katona, I., Sperlágh, B., Sík, A., Käfalvi, A., Vizi, E. S., Mackie, K., and Freund, T. F. (1999). Presynaptically located CB1 cannabinoid receptors regulate GABA release from axon terminals of specific hippocampal interneurons. J. Neurosci. 19, 4544-58.

Kim, D. J., and Thayer, S. A. (2000). Activation of CB1 cannabinoid receptors inhibits neurotransmitter release from identified synaptic sites in rat hippocampal cultures. Brain Res. 852, 398-405.

Kreitzer, A. C., and Regehr, W. G. (2001). Retrograde inhibition of presynaptic calcium influx by endogenous cannabinoids at excitatory synapses onto Purkinje cells. Neuron 29, 717-27.

Lawrence, D. K., and Gill, E. W. (1975). The effects of delta1-tetrahydrocannabinol and other cannabinoids on spin-labeled liposomes and their relationship to mechanisms of general anesthesia. Mol. Pharm. 11, 595-602.

Ledent, C., Valverde, O., Cossu, G., Petitet, F., Aubert, J. F., Beslot, F., Böhme, G. A., Imperato, A., Pedrazzini, T., Roques, B. P., Vassart, G., Fratta, W., and Parmentier, M. (1999). Unresponsiveness to cannabinoids and reduced addictive effects of opiates in CB1 receptor knockout mice. Science 283, 401-4.

Lenz, R. A., and Alger, B. E. (1999). Calcium dependence of depolarization-induced suppression of inhibition in rat hippocampal CA1 pyramidal neurons. J. Physiol. 521 Pt 1, 147-57.

Lenz, R. A., Wagner, J. J., and Alger, B. E. (1998). N- and L-type calcium channel involvement in depolarization-induced suppression of inhibition in rat hippocampal CA1 cells. J. Physiol. 512, 61-73.

Lévénés, C., Daniel, H., Soubrié, P., and Crépel, F. (1998). Cannabinoids decrease excitatory synaptic transmission and impair long-term depression in rat cerebellar Purkinje cells. J. Physiol. 510, 867-79.

Lin, R. C., and Scheller, R. H. (2000). Mechanisms of synaptic vesicle exocytosis. Annu. Rev. Cell Dev. Biol. 16, 19-49.

Linden, D. J. (1994). Long-term synaptic depression in the mammalian brain. Neuron 12, 457-72.

Llano, I., Leresche, N., and Marty, A. (1991). Calcium entry increases the sensitivity of cerebellar Purkinje cells to applied GABA and decreases inhibitory synaptic currents. Neuron 6, 565-74.

Lledo, P. M., Zhang, X., Südhof, T. C., Malenka, R. C., and Nicoll, R. A. (1998). Postsynaptic membrane fusion and long-term potentiation. Science 279, 399-403.

Lo, Y. J., and Poo, M. M. (1991). Activity-dependent synaptic competition in vitro: heterosynaptic suppression of developing synapses. Science 254, 1019-22.

Lüscher, C., Xia, H., Beattie, E. C., Carroll, R. C., von Zastrow, M., Malenka, R. C., and Nicoll, R. A. (1999). Role of AMPA receptor cycling in synaptic transmission and plasticity. Neuron 24, 649-58.

Maccaferri, G., Roberts, J. D., Szucs, P., Cottingham, C. A., and Somogyi, P. (2000). Cell surface domain specific postsynaptic currents evoked by identified GABAergic neurones in rat hippocampus in vitro. J. Physiol. 524 Pt 1, 91-116.

Mackie, K., and Hille, B. (1992). Cannabinoids inhibit N-type calcium channels in neuroblastoma-glioma cells. Proc. Natl. Acad. Sci. U.S.A. 89, 3825-9.

Mailleux, P., and Vanderhaeghen, J. J. (1992). Distribution of neuronal cannabinoid receptor in the adult rat brain: a comparative receptor binding radioautography and in situ hybridization histochemistry. Neurosci. 48, 655-68.

Marsicano, G., and Lutz, B. (1999). Expression of the cannabinoid receptor CB1 in distinct neuronal subpopulations in the adult mouse forebrain. Eur. J. Neurosci. 11, 4213-25.

Martin, B. R. (1986). Cellular effects of cannabinoids. Pharmacol. Rev. 38, 45-74.

Matsuda, L. A., Bonner, T. I., and Lolait, S. J. (1993). Localization of cannabinoid receptor mRNA in rat brain. J. Comp. Neurol. 327, 535-50.

Matsuda, L. A., Lolait, S. J., Brownstein, M. J., Young, A. C., and Bonner, T. I. (1990). Structure of a cannabinoid receptor and functional expression of the cloned cDNA. Nature 346, 561-4.

Maurelli, S., Bisogno, T., De Petrocellis, L., Di Luccia, A., Marino, G., and Di Marzo, V. (1995). Two novel classes of neuroactive fatty acid amides are substrates for mouse neuroblastoma 'anandamide amidohydrolase'. FEBS Lett. 377, 82-6.

Mechoulam, R., Ben-Shabat, S., Hanu*s, L., Ligumsky, M., Kaminski, N. E., Schatz, A. R., Gopher, A., Almog, S., Martin, B. R., Compton, D. R., and et al. (1995).

Identification of an endogenous 2-monoglyceride, present in canine gut, that binds to cannabinoid receptors. Biochem. Pharmacol. 50, 83-90.

Misner, D. L., and Sullivan, J. M. (1999). Mechanism of cannabinoid effects on long-term potentiation and depression in hippocampal CA1 neurons. J. Neurosci. 19, 6795-805.

Morishita, W., and Alger, B. E. (1997). Sr2+ supports depolarization-induced suppression of inhibition and provides new evidence for a presynaptic expression mechanism in rat hippocampal slices. J. Physiol. 505, 307-17.

Morishita, W., and Alger, B. E. (1999). Evidence for endogenous excitatory amino acids as mediators in DSI of GABA(A)ergic transmission in hippocampal CA1. J. Neurophysiol. 82, 2556-64.

Morishita, W., and Alger, B. E. (2000). Differential effects of the group II mGluR agonist, DCG-IV, on depolarization-induced suppression of inhibition in hippocampal CA1 and CA3 neurons. Hippocampus 10, 261-268.

Morishita, W., and Alger, B. E. (2001). Direct depolarization and antidromic action potentials transiently suppress dendritic IPSPs in hippocampal CA1 pyramidal cells. J. Neurophysiol. 85, 480-4.

Morishita, W., Kirov, S. A., and Alger, B. E. (1998). Evidence for metabotropic glutamate receptor activation in the induction of depolarization-induced suppression of inhibition in hippocampal CA1. J. Neurosci. 18, 4870-82.

Mu, J., Zhuang, S. Y., Hampson, R. E., and Deadwyler, S. A. (2000). Protein kinase-dependent phosphorylation and cannabinoid receptor modulation of potassium A current (IA) in cultured rat hippocampal neurons. Pflugers Arch. 439, 541-6.

Munro, S., Thomas, K. L., and Abu-Shaar, M. (1993). Molecular characterization of a peripheral receptor for cannabinoids. Nature 365, 61-5.

Nicoll, R. A., and Malenka, R. C. (1999). Expression mechanisms underlying NMDA receptor-dependent long-term potentiation. Ann. N.Y. Acad. Sci. 868, 515-25.

Ohno-Shosaku, T., Hirata, K., Sawada, S., and Yamamoto, C. (1994). Contributions of multiple calcium channel types to GABAergic transmission in rat cultured hippocampal neurons. Neurosci. Lett. 181, 145-8.

Ohno-Shosaku, T., Maejima, T., and Kano, M. (2001). Endogenous cannabinoids mediate retrograde sinals from depolarized postsynaptic neurons to presynaptic terminals. Neuron 29, 729-38.

Ohno-Shosaku, T., Sawada, S., and Yamamoto, C. (1998). Properties of depolarization-induced suppression of inhibitory transmission in cultured rat hippocampal neurons. Pflugers Arch. 435, 273-9.

Pan, X., Ikeda, S. R., and Lewis, D. L. (1996). Rat brain cannabinoid receptor modulates N-type Ca2+ channels in a neuronal expression system. Mol. Pharm. 49, 707-14.

Parra, P., Gulyás, A. I., and Miles, R. (1998). How many subtypes of inhibitory cells in the hippocampus? Neuron 20, 983-93.

Paton, G. S., Pertwee, R. G., and Davies, S. N. (1998). Correlation between cannabinoid mediated effects on paired pulse depression and induction of long term potentiation in the rat hippocampal slice. Neuropharmacology 37, 1123-30.

Pearce, R. A. (1993). Physiological evidence for two distinct GABAA responses in rat hippocampus. Neuron 10, 189-200.

Pellmar, T. C., Gilman, S. C., Keyser, D. O., Lee, K. H., Lepinski, D. L., Livengood, D., and Myers, L. S., Jr. (1994). Reactive oxygen species on neural transmission. Ann. N.Y. Acad. Sci. 738, 121-9.

Pert, C. B., and Snyder, S. H. (1973). Opiate receptor: demonstration in nervous tissue. Science 179, 1011-4.

Pertwee, R. G. (1997). Pharmacology of cannabinoid CB1 and CB2 receptors. Pharmacol. Ther. 74, 129-80.

Piomelli, D., Beltramo, M., Giuffrida, A., and Stella, N. (1998). Endogenous cannabinoid signaling. Neurobiol. Disease 5, 462-73.

Piomelli, D., Beltramo, M., Glasnapp, S., Lin, S. Y., Goutopoulos, A., Xie, X. Q., and Makriyannis, A. (1999). Structural determinants for recognition and translocation by the anandamide transporter. Proc. Natl. Acad. Sci. U.S.A. 96, 5802-7.

Piomelli, D., Giuffrida, A., Calignano, A., and Rodríguez de Fonseca, F. (2000). The endocannabinoid system as a target for therapeutic drugs. Trends Pharmacol. Sci. 21, 218-24.

Pitler, T. A., and Alger, B. E. (1992). Postsynaptic spike firing reduces synaptic GABAA responses in hippocampal pyramidal cells. J. Neurosci. 12, 4122-32.

Pitler, T. A., and Alger, B. E. (1994). Depolarization-induced suppression of GABAergic inhibition in rat hippocampal pyramidal cells: G protein involvement in a presynaptic mechanism. Neuron 13, 1447-55.

Poncer, J. C., McKinney, R. A., Gähwiler, B. H., and Thompson, S. M. (1997). Either N- or P-type calcium channels mediate GABA release at distinct hippocampal inhibitory synapses. Neuron 18, 463-72.

Ramon y Cajal, S. (1937). Recollections of My Life. Craigie, E.H., translator. (M.I.T. Press: Cambridge, MA).

Reibaud, M., Obinu, M. C., Ledent, C., Parmentier, M., Böhme, G. A., and Imperato, A. (1999). Enhancement of memory in cannabinoid CB1 receptor knock-out mice. Eur. J. Pharmacol. 379, R1-2.

Reynolds, I. J., and Hastings, T. G. (1995). Glutamate induces the production of reactive oxygen species in cultured forebrain neurons following NMDA receptor activation. J. Neurosci. 15, 3318-27.

Scanziani, M., Capogna, M., Gähwiler, B. H., and Thompson, S. M. (1992). Presynaptic inhibition of miniature excitatory synaptic currents by baclofen and adenosine in the hippocampus. Neuron 9, 919-27.

Schaffer, J. E., and Lodish, H. F. (1994). Expression cloning and characterization of a novel adipocyte long chain fatty acid transport protein. Cell 79, 427-36.

Schiavo, G., Matteoli, M., and Montecucco, C. (2000). Neurotoxins affecting neuroexocytosis. Physiol. Rev. 80, 717-66.

Schotzinger, R., Yin, X., and Landis, S. (1994). Target determination of neurotransmitter phenotype in sympathetic neurons. J. Neurobiol. 25, 620-39.

Shen, M., Piser, T. M., Seybold, V. S., and Thayer, S. A. (1996). Cannabinoid receptor agonists inhibit glutamatergic synaptic transmission in rat hippocampal cultures. J. Neurosci. 16, 4322-34.

Shen, M., and Thayer, S. A. (1998). The cannabinoid agonist Win55,212-2 inhibits calcium channels by receptor-mediated and direct pathways in cultured rat hippocampal neurons. Brain Res. 783, 77-84.

Sik, A., Penttonen, M., Ylinen, A., and Buzsáki, G. (1995). Hippocampal CA1 interneurons: an in vivo intracellular labeling study. J. Neurosci. 15, 6651-65.

Sim, L. J., Selley, D. E., Xiao, R., and Childers, S. R. (1996). Differences in G-protein activation by mu- and delta-opioid, and cannabinoid, receptors in rat striatum. Eur. J. Pharmacol. 307, 97-105.

Snyder, S. H. (1971). Uses of Marijuana. (Oxford University Press: New York).

Soltesz, I., Smetters, D. K., and Mody, I. (1995). Tonic inhibition originates from synapses close to the soma. Neuron 14, 1273-83.

Steegmaier, M., Yang, B., Yoo, J. S., Huang, B., Shen, M., Yu, S., Luo, Y., and Scheller, R. H. (1998). Three novel proteins of the syntaxin/SNAP-25 family. J. Biol. Chem. 273, 34171-9.

Stella, N., Schweitzer, P., and Piomelli, D. (1997). A second endogenous cannabinoid that modulates long-term potentiation. Nature 388, 773-8.

Sugiura, T., Kondo, S., Sukagawa, A., Nakane, S., Shinoda, A., Itoh, K., Yamashita, A., and Waku, K. (1995). 2-Arachidonoylglycerol: a possible endogenous cannabinoid receptor ligand in brain. Biochem. Biophys. Res. Comm. 215, 89-97.

Sugiura, T., Kondo, S., Sukagawa, A., Tonegawa, T., Nakane, S., Yamashita, A., Ishima, Y., and Waku, K. (1996). Transacylase-mediated and phosphodiesterase-mediated synthesis of N-arachidonoylethanolamine, an endogenous cannabinoid-receptor

ligand, in rat brain microsomes. Comparison with synthesis from free arachidonic acid and ethanolamine. Eur. J. Biochem. 240, 53-62.

Sullivan, J. M. (1999). Mechanisms of cannabinoid-receptor-mediated inhibition of synaptic transmission in cultured hippocampal pyramidal neurons. J. Neurophysiol. 82, 1286-94.

Takahashi, K. A., and Linden, D. J. (2000). Cannabinoid receptor modulation of synapses received by cerebellar Purkinje cells. J. Neurophysiol. 83, 1167-80.

Takahashi, T., and Momiyama, A. (1993). Different types of calcium channels mediate central synaptic transmission. Nature 366, 156-8.

Tang, L., Hung, C. P., and Schuman, E. M. (1998). A role for the cadherin family of cell adhesion molecules in hippocampal long-term potentiation. Neuron 20, 1165-75.

Terranova, J. P., Michaud, J. C., Le Fur, G., and Soubrié, P. (1995). Inhibition of long-term potentiation in rat hippocampal slices by anandamide and WIN55212-2: reversal by SR141716 A, a selective antagonist of CB1 cannabinoid receptors. Naunyn Schmiedebergs Arch. Pharmacol. 352, 576-9.

Tessier-Lavigne, M., and Goodman, C. S. (1996). The molecular biology of axon guidance. Science 274, 1123-33.

Thomas, E. A., Cravatt, B. F., Danielson, P. E., Gilula, N. B., and Sutcliffe, J. G. (1997). Fatty acid amide hydrolase, the degradative enzyme for anandamide and oleamide, has selective distribution in neurons within the rat central nervous system. J. Neurosci. Res. 50, 1047-52.

Tóth, K., and McBain, C. J. (2000). Target-specific expression of pre- and postsynaptic mechanisms. J. Physiol. 525 Pt 1, 41-51.

Trapp, S., Lückermann, M., Kaila, K., and Ballanyi, K. (1996). Acidosis of hippocampal neurones mediated by a plasmalemmal Ca2+/H+ pump. Neuroreport 7, 2000-4.

Tsou, K., Brown, S., Sañudo-Peña, M. C., Mackie, K., and Walker, J. M. (1998). Immunohistochemical distribution of cannabinoid CB1 receptors in the rat central nervous system. Neurosci. 83, 393-411.

Tsou, K., Mackie, K., Sañudo-Peña, M. C., and Walker, J. M. (1999). Cannabinoid CB1 receptors are localized primarily on cholecystokinin-containing GABAergic interneurons in the rat hippocampal formation. Neurosci. 93, 969-75.

Twitchell, W., Brown, S., and Mackie, K. (1997). Cannabinoids inhibit N- and P/Q-type calcium channels in cultured rat hippocampal neurons. J. Neurophysiol. 78, 43-50.

Usowicz, M. M., Sugimori, M., Cherksey, B., and Llinás, R. (1992). P-type calcium channels in the somata and dendrites of adult cerebellar Purkinje cells. Neuron 9, 1185-99.

Vaidyanathan, V. V., Yoshino, K., Jahnz, M., Dörries, C., Bade, S., Nauenburg, S., Niemann, H., and Binz, T. (1999). Proteolysis of SNAP-25 isoforms by botulinum neurotoxin types A, C, and E: domains and amino acid residues controlling the formation of enzyme-substrate complexes and cleavage. J. Neurochem. 72, 327-37.

Vaughan, C. W., Connor, M., Bagley, E. E., and Christie, M. J. (2000). Actions of cannabinoids on membrane properties and synaptic transmission in rat periaqueductal gray neurons in vitro. Mol. Pharm. 57, 288-95.

Vincent, P., and Marty, A. (1993). Neighboring cerebellar Purkinje cells communicate via retrograde inhibition of common presynaptic interneurons. Neuron 11, 885-93.

Vizi, E. S. (2000). Role of high-affinity receptors and membrane transporters in nonsynaptic communication and drug action in the central nervous system. Pharmacol. Rev. 52, 63-89.

Vogel, Z., Barg, J., Levy, R., Saya, D., Heldman, E., and Mechoulam, R. (1993). Anandamide, a brain endogenous compound, interacts specifically with cannabinoid receptors and inhibits adenylate cyclase. J. Neurochem. 61, 352-5.

Wagner, J. A., Varga, K., Járai, Z., and Kunos, G. (1999). Mesenteric vasodilation mediated by endothelial anandamide receptors. Hypertension 33, 429-34.

Wagner, J. J., and Alger, B. E. (1996). Increased neuronal excitability during depolarization-induced suppression of inhibition in rat hippocampus. J. Physiol. 495, 107-12.

Walter, L., Martilanova, A., and Stella, N. (2000). "CB1 cannabinoid receptors modulate proliferation of microglial cells." Soc. Neurosci. Abstracts, 26: 733.6.

Weber, T., Zemelman, B. V., McNew, J. A., Westermann, B., Gmachl, M., Parlati, F., Söllner, T. H., and Rothman, J. E. (1998). SNAREpins: minimal machinery for membrane fusion. Cell 92, 759-72.

Werth, J. L., and Thayer, S. A. (1994). Mitochondria buffer physiological calcium loads in cultured rat dorsal root ganglion neurons. J. Neurosci. 14, 348-56.

White, R. J., and Reynolds, I. J. (1995). Mitochondria and Na+/Ca2+ exchange buffer glutamate-induced calcium loads in cultured cortical neurons. J. Neurosci. 15, 1318-28.

Wigström, H., and Gustafsson, B. (1985). Facilitation of hippocampal long-lasting potentiation by GABA antagonists. Acta Physiol. Scand. 125, 159-72.

Williams, J. H. (1996). Retrograde messengers and long-term potentiation: a progress report. J. Lipid Mediat. Cell Signal. 14, 331-9.

Wu, L. G., and Saggau, P. (1994). Adenosine inhibits evoked synaptic transmission primarily by reducing presynaptic calcium influx in area CA1 of hippocampus. Neuron 12, 1139-48.

Zhang, J. F., Ellinor, P. T., Aldrich, R. W., and Tsien, R. W. (1996). Multiple structural elements in voltage-dependent Ca2+ channels support their inhibition by G proteins. Neuron 17, 991-1003.

Zilberter, Y. (2000). Dendritic release of glutamate suppresses synaptic inhibition of pyramidal neurons in rat neocortex. J. Physiol. 528, 489-96.

Zilberter, Y., Kaiser, K. M., and Sakmann, B. (1999). Dendritic GABA release depresses excitatory transmission between layer 2/3 pyramidal and bitufted neurons in rat neocortex. Neuron 24, 979-88.

Zimmer, A., Zimmer, A. M., Hohmann, A. G., Herkenham, M., and Bonner, T. I. (1999). Increased mortality, hypoactivity, and hypoalgesia in cannabinoid CB1 receptor knockout mice. Proc. Natl. Acad. Sci. U.S.A. 96, 5780-5.

Zucker, R. S. (1989). Short-term synaptic plasticity. Annu. Rev. Neurosci. 12, 13-31.